Robust Control of Systems Subject to Input Nonlinearities with Application to High Performance Helicopters

Thesis Submitted for the degree of
Doctor of Philosophy
at the University of Leicester

by

Matthew Christopher Turner BEng (Surrey)
Department of Engineering
University of Leicester

July 2000

ProQuest LLC
789 East Eisenhower Parkway
P.O. Box 1346
Ann Arbor, MI 48106-1346

Abstract

This thesis addresses some of the issues associated with linear systems subject to nonlinearities at their input, and considers robust control of high performance helicopters. In particular, the problems of substitution and saturation nonlinearities are discussed. In the case of the former, a new procedure based on ideas from optimal control is developed to help facilitate dynamic transfer between two linear controllers. For the latter, a generalisation of an existing scheme is made which allows asymptotic set-point tracking for all states belonging to a given subset of the state space. The closely related problem of limited authority control is considered and promising results are demonstrated on the Westland Lynx helicopter in a pilotted simulation. The thesis culminates with a discussion of the design and implementation of an $\mathcal{H}^\infty$ controller for the Bell 205 helicopter. The results show that in flight, the helicopter attained good handling qualities ratings, even though the fidelity of some of the mathematical models was relatively low.

Acknowledgements

First and foremost I would like to thank my supervisor, Dr. Daniel Walker for his guidance over the past few years. I have not only benefited from his judicious comments, but have also found his relaxed approach and straight-talking easy to work with. Also, the comments of my co-supervisor, Prof. Ian Postlethwaite, are much appreciated, particularly regarding the constrained input aspect of the work.

The members of the 'helicopter group', who worked concurrently with me, deserve special thanks: Xiao-Dong Sun, Ioannis Konstantopoulos, Alex Smerlas and Emmanuel Prempain. All provided coding templates for the various trials and were ready to discuss various project-associated issues. In conjunction with the Bell 205 trials I would like to thank Jeremy Howitt and Mike Strange from DERA, Bedford (particularly with regard to modelling issues), and Bill Gubbels from the NRC Flight Research Lab, Ottawa. The participation of test pilots Mike Haider and Robert Erdos was also much appreciated. The Westland trials could not have been conducted without the help of Adrian Alford who assisted with coding and supplied specifications for the limited authority system, as well as ensuring the trials went smoothly.

I have also enjoyed the company of everyone in the control group at Leicester. Thanks go particularly to Guido Herrmann for meticulously reviewing Chapter 4, and for being an instant reference for abstruse nonlinear control concepts. Additionally, I'm indebted to Mark Tucker for his patient explanations during the first couple of months of my PhD. I've also been fortunate enough to inherit some LaTeX style files from Chris Edwards and Fu Wah Poon.

Finally, I would not have completed this thesis without the support of my family and friends, to whom I am grateful.

Matthew Turner

July 2000

Contents

Mathematical notation

$\mathbb{R}^n$	n-dimensional Euclidean space.
$\mathbb{R}^{n\times m}$	The set of real n by m matrices.
$\mathbb{R}, \mathbb{I}, \mathcal{C}$	The fields of real, imaginary and complex number respectively.
$\mathbb{R}_+$	The positive real scalars (including 0).
$\mathcal{C}^-, \mathcal{C}^+, \mathcal{C}^0$	The open left-half, right half complex plane and the imaginary axis, respectively.
sup	Supremum (i.e. least upper bound)
inf	Infinmum (i.e. greatest lower bound)
I	Identity matrix of appropriate dimensions
I_n	$n \times n$ Identity matrix
$0_{n\times m}$	$n \times m$ matrix with all elements being zero
0_n	$n \times n$ matrix with all elements being zero
$\det(A)$	Determinant of the matrix A
$A > 0$	Matrix A is positive definite
$A \geq 0$	Matrix A is positive semi-definite
$A < 0$	Matrix A is negative definite
$A \leq 0$	Matrix A is negative semi-definite
$A > B$	Matrix $A - B$ is positive definite
A^{-1}	Inverse of the matrix A
A'	Transpose of the matrix A
A^*	Complex conjugate transpose of the matrix A
$\mathbf{spec}(A)$	The Spectrum or set of eigenvalues of the matrix A
A_{ij}	the (i,j) element of the matrix A
j	$\sqrt{-1}$; sometimes an index, as in x_{ij}
$\Re e(z)$	Real part of the complex number z
$\Im(z)$	Imaginary part of the complex number z
$\sigma(A)$	Singular values of the matrix A
$\bar{\sigma}(A)$	Maximum singular value of the matrix A
$\underline{\sigma}(A)$	Minimum singular value of the matrix A
s	Laplace operator
$\dot{x}\,(t)$	$:= \frac{dx(t)}{dt}$
$\left[\begin{array}{c\|c} A & B \\ \hline C & D \end{array}\right]$	short hand for the state-space realisation $C(sI - A)^{-1}B + D$
$\diamond\diamond$	End of proof

Chapter 1

Overview

Systems which require feedback control to enable them to perform adequately are common place in engineering and have been studied for many years. Despite the effective methodologies available for many systems, however, the ever tighter specifications on performance can compromise the utility of these traditional methods.

Among the problems associated with design for high-performance systems is the fact that no mathematical model is a true representation of the system it is said to describe; also the unavoidable presence of nonlinearities, in a variety of forms, at the system's inputs.

This thesis considers the concepts of *robust control* - the control of uncertain systems - and the control of plants with nonlinearities present at their inputs. The latter part of the thesis demonstrates the application of these ideas to military helicopters where high performance is a neccesity.

1.1 Structure of Thesis

Chapter 2: Concepts from Robust and Input-Nonlinearity Control. Fundamental ideas from both robust control and input-nonlinearity control are briefly reviewed. Uncertainty descriptions, the Small Gain Theorem and $\mathcal{H}^\infty$ -optimal control are discussed from the robust control perspective. Constrained input and anti-windup control approaches, together with a selection of stability results, are presented for the input-nonlinearity case.

Chapter 3: Linear Quadratic Bumpless Transfer. A new method of bumpless transfer is proposed which uses the machinery of linear quadratic optimal control to provide formulae for a feedback gain to enable 'graceful degradation' of performance during switching. The method, in contrast to some others available in the literature, is applicable to general linear controller types; formulae are given for both continuous and discrete time cases.

Chapter 4: Nonlinear Tracking for Multivariable Constrained Input Linear Systems. A significant enhancement to a method already existing in the literature is made. The results show how the addition of a nonlinear element in an otherwise linear state-feedback enables asymptotic set-point tracking to be achieved, without the size of the guaranteed domain of attraction being reduced. It is suggested that this nonlinear parameter can be chosen to enhance performance and examples which support this are given.

Chapter 5: The Helicopter Control Problem. An introduction to the characteristics of high performance helicopters is given, and the difficulty of the control problem is described. The descriptions can be considered fairly generic, although they are specifically aimed at the case-studies which follow.

Chapter 6: Limited Authority Control of Helicopters. The design and implementation of a control system with only partial authority over the actuator deflections is described, in the context of the Westland Mk7 Lynx helicopter. The relevant intricacies in the configuration are pointed out and the design of both the $\mathcal{H}^\infty$ controller and its accompanying anti-windup compensator are described. The effectiveness of the scheme is demonstrated with results of a piloted simulation exercise conducted at *GKN Westland Helicopters.*

Chapter 7: Robust Control of the Bell 205. The design of a robust $\mathcal{H}^\infty$ controller for a modified Bell 205 helicopter is decribed. Departing from recent efforts, the controller has a decoupled structure to take account of the poor off-axis response predicted by the models available. Together with desk-top analysis, results from a recent flight trial are given, which lend support to the suitability of the adopted design approach.

Chapter 8: Conclusion. The main contributions of the thesis are stated together with directions for continuing research and some closing comments.

Chapter 2

Concepts from Robust and Input-nonlinearity Control

This chapter aims to review some of the core ideas of the theory on which this dissertation is based. As many of these ideas will be used extensively in subsequent chapters, the aim is to give a fairly thorough treatment. The quantity of results available for both these topics prohibits an exhaustive review, although references containing more detail will be pointed out as the chapter progresses.

2.1 Robust Control

2.1.1 Overview

The concept of robust control is one which has occupied the minds of researchers and practitioners for some years, with significant progress being made in the last two decades. Historically, the *robustness* properties of control systems were given in terms of classical measures such as gain and phase margins; unfortunately these concepts are single-loop criteria and do not always give useful information about multivariable systems. The study of robustness began again with renewed vigour around the beginning of the 1980's, after the fragility of linear-quadratic-gaussian (LQG) control systems, and such like, was beginning to be appreciated. This led to several developments in control theory which attempted to take account of uncertainty, which inevitably exists in any mathematical model, *a priori*.

The type of robust control theory employed in this thesis is $\mathcal{H}^\infty$ -optimal control, which is one of the more popular of the modern control techniques. A more detailed discussion of the theory of $\mathcal{H}^\infty$ optimal control will be given later, but its more salient features are mentioned here briefly. $\mathcal{H}^\infty$ control was originally formulated by [98] and this paper spawned a considerable amount of related research. It was not until several years after, however, that the mathematical machinery was in place to solve the problem completely and efficiently. The modern formulae for solving the problem were first proposed in [22], with a more detailed treatment given in [13].

These two papers established that the general output feedback $\mathcal{H}^\infty$ optimal controller could be constructed from plant data, along with the solution of two de-coupled Riccati equations. The proofs relied on Hankel-Toeplitz operators and drew upon results in [21] for some of the ideas. Since then alternative proofs based on game-theoretic ideas, see [27], J-spectral factorisation, [26], J-lossless coprime factorisation, see [25], for example, have been given. The problem has also been solved from the point of view of linear matrix inequalities (LMI's) in [19], which have recently become more numerically tractable.

The above is a much abridged account of the emergence of robust control techniques and many more thorough descriptions already exist in the literature (see [27] and [65], for example). The literature in the field of $\mathcal{H}^\infty$ optimal control is now vast, and for a more comprehensive introduction the interested reader should consult [27] or [99].

2.1.2 Uncertainty Descriptions

'Robustness' implies that a system can tolerate a level of uncertainty being present, without behaving in an undesirable manner. It is difficult to quantify the phrase 'undesirable manner' though and thus robustness is generally taken to mean that the system can tolerate a certain level of uncertainty without becoming unstable.[1] Of course there are many types of uncertainty, and robustness to one type does not necessarily imply robustness to another (and vice versa). Some of the more common types are now briefly reviewed.

To aid the exposition the following notation is introduced.

$\mathbf{S}_o := (I - \mathbf{GK})^{-1}$ - Output Sensitivity
$\mathbf{S}_i := (I - \mathbf{KG})^{-1}$ - Input Sensitivity
$\mathbf{T}_o := \mathbf{S}_o\mathbf{GK}$ - Output Co-sensitivity
$\mathbf{T}_i := \mathbf{S}_i\mathbf{KG}$ - Input Co-sensitivity

Additive and Multiplicative Uncertainty

These types of uncertainty may correspond to actual physical uncertainties in the system, or may represent an abstract but meaningful level of 'lumped' uncertainty, and can be modelled or bounded if enough information is available. They can capture quite well unmodelled dynamics and nonlinearities, as well as uncertainties in the plant data; they are however mathematically inconvenient for capturing unstable uncertainties. Results derived for these uncertainty types are based on the Small Gain Theorem (described later), and hence require them to be stable,

[1] Note however that the concept of *robust performance* exists and is often associated with the structured singular value, μ.

which can restrict the class of uncertainty they represent. Common variants of this type of uncertainty are shown in Figures 2.1 - 2.4.

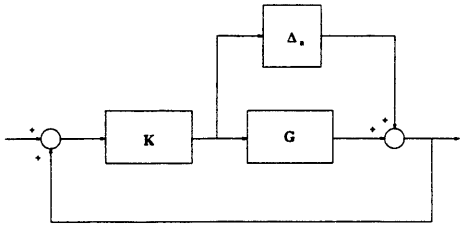

Figure 2.1: System with Additive Uncertainty

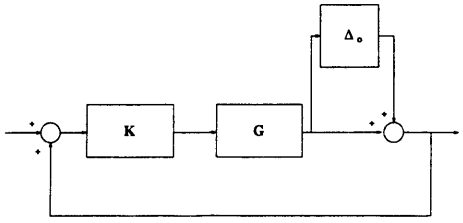

Figure 2.2: System with Ouput Multiplicative Uncertainty

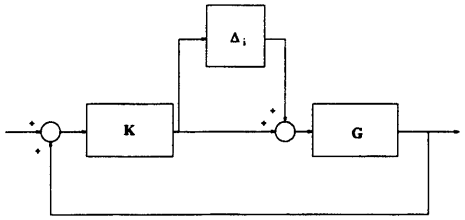

Figure 2.3: System with Input Multiplicative Uncertainty

Relationships exist between these forms of uncertainty. Some of the more common and useful, assuming the uncertainties in question can be represented as linear systems, are

$$\mathbf{\Delta}_a = \mathbf{\Delta}_o\mathbf{G} = \mathbf{G}\mathbf{\Delta}_i \tag{2.1}$$

$$\mathbf{\Delta}_o = (\mathbf{I} - \mathbf{G}\mathbf{\Delta}_f)^{-1} \tag{2.2}$$

Note that from the last equation that, given a stable $\mathbf{\Delta}_f$, the stability of $\mathbf{\Delta}_o$ is not implied (and vice versa), so care must be taken when interpreting one form of uncertainty as another. Other relations can also be derived. The reader is encouraged to consult [27] for more details.

Coprime Factor Uncertainty

Figure 2.5 shows the model of a feedback system with perturbations to the left coprime factors of the nominal plant, $\mathbf{G} = \mathbf{M}^{-1}\mathbf{N}$. The perturbed plant thus becomes $\mathbf{G}_\mathbf{\Delta} = (\mathbf{M} +$

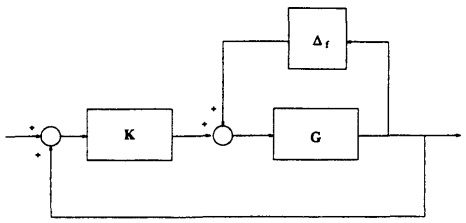

Figure 2.4: System with Ouput Feedback Multiplicative Uncertainty

$\mathbf{\Delta_M})^{-1}(\mathbf{N}+\mathbf{\Delta_N})$ This type of uncertainty is often not, in itself, open to simple interpretation from a physical point of view, but it can be shown that it is a quite generic uncertainty description: not only is it related to many forms of additive and multiplicative uncertainty, but it is also related to robustness in the *gap metric* - see, for example, [85] for more details. This description of uncertainty overcomes some of the difficulties of the previously mentioned forms as although $\mathbf{\Delta_M}$ and $\mathbf{\Delta_N}$ have to be taken as stable, this actually allows the perturbed plant to have a different number of unstable poles to the nominal model.

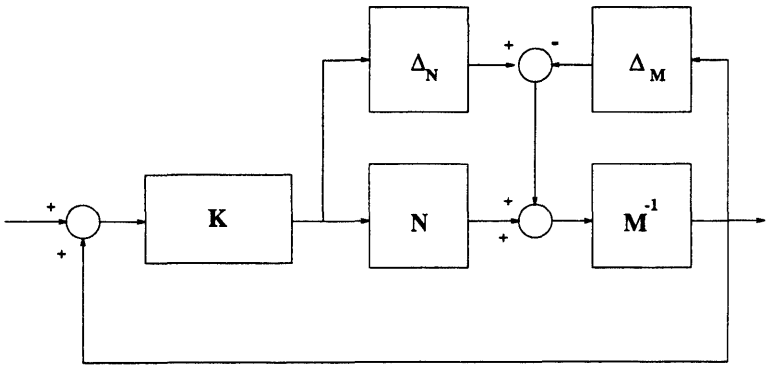

Figure 2.5: System with Coprime Factor Uncertainty

Parametric (structured) Uncertainty

This type of uncertainty arises from the variation of parameters within a known structure, and manifests itself as perturbations to the plant's state-space matrices, or transfer function representation. This model of uncertainty is probably the most narrow introduced, and can be related to the additive and multiplicative uncertainty already described. It can, however, be a fairly accurate description of uncertainty, providing the uncertainty due to unmodelled dynamics is minimal and the given structure is itself reasonably accurate.

If the plant is given by the state space data

$$\mathbf{G} \sim \left[\begin{array}{c|c} A & B \\ \hline C & D \end{array}\right] \tag{2.3}$$

then the perturbed plant $\mathbf{G}_\Delta$ is given by

$$\mathbf{G}_\Delta \sim \left[\begin{array}{c|c} A+\Delta_A & B+\Delta_B \\ \hline C+\Delta_C & D+\Delta_D \end{array}\right] \tag{2.4}$$

where the terms Δ_A, Δ_B, Δ_C and Δ_D are the perturbations of the nominal data. This type of uncertainty is taken to be described by additive and multiplicative uncertainty in this thesis (see [99], pages 261-266 for details regarding 'pulling out the Δ's').

2.1.3 The Small Gain Theorem

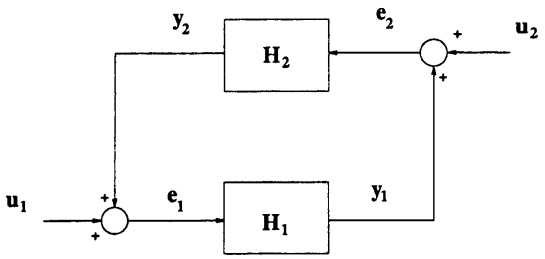

Figure 2.6: Small Gain Interconnection

The Small Gain Theorem is one of the more important results in modern control theory and has applications throughout the entire field of control. It imparts information about the stability of feedback inter-connections and it is the cornerstone on which many of the robustness tests are built. The Small Gain Theorem has many forms, of varying complexity, but those introduced here are adequate for the applications considered in this thesis.

Before beginning a detailed exploration of the theorem, let us briefly mention the important details surrounding it. The Small Gain Theorem offers a *sufficient* condition to guarantee the stability of the inter-connection in Figure 2.6, in terms of the gains of the two subsystems. Although the precise mathematical details will change for each exposure, this idea remains the same in all versions.

Two variants of the Small Gain Theorem, which are applicable to linear systems with uncertainties of the additive, multipilicative and coprime factor types listed above, are considered. It is important to realise that these versions allow the consideration of possibly *nonlinear* uncertainty blocks, which is not the case in some purely linear versions. Attention is then focused on a "linear" version of the theorem, where it is possible and useful to obtain stronger conditions.

The $\mathcal{L}_p$ Induced Norm Small Gain Theorem

The $\mathcal{L}_p$ norm of a vector-valued signal $x(t)$, denoted $\|x\|_p$, is defined as

$$\|x\|_p = \left\{ \int_0^\infty \|x(t)\|^p dt \right\}^{\frac{1}{p}} \tag{2.5}$$

The $\mathcal{L}_p$ induced norm of a stable, causal operator H is defined as

$$\|H\|_{i,p} := \sup_{0 \neq x \in \mathcal{L}_p} \frac{\|H(x)\|_p}{\|x\|_p} \tag{2.6}$$

This notation follows [60] and allows one to distinguish easily the induced norm of a nonlinear operator and its incremental gain (if it exists).

The space $\mathcal{L}_p$ is the space of all signals which have a finite $\mathcal{L}_p$ norm; the space $\mathcal{L}_{p,e}$ is the space of all signals whose norm is finite if the upper limit of the integral is taken as some finite time. Equivalently this can be expressed as

Definition 2.1 *The space $\mathcal{L}_{p,e}$ is defined as*

$$\mathcal{L}_{p,e} = \{P_T x(t) \in \mathcal{L}_p \; \forall T < \infty\} \tag{2.7}$$

where P_T denotes the truncation operator:

$$P_T x(t) = \begin{cases} x(t) & \forall t \leq T \\ 0 & \forall t > T \end{cases} \tag{2.8}$$

Before proceeding further it is convenient to define:-

Definition 2.2 (Finite Gain Stability) *A causal operator $H(.)$ is* finite gain stable *if*

$$\|H(x)\|_p \leq \gamma \|x\|_p + \beta \quad \forall x \in \mathcal{L}_{p,e} \tag{2.9}$$

for some $\gamma, \beta \in \mathbb{R}_+$.

The induced norm version of the Small Gain Theorem used in this thesis is essentially taken from [41].

Theorem 2.1 (Small Gain Theorem (Induced Norm)) *Consider the feedback system in Figure 2.6 where H_1 and H_2 are two nonlinear operators such that:*

$$H_1 : \mathcal{L}_{p,e} \mapsto \mathcal{L}_{p,e} \tag{2.10}$$

$$H_2 : \mathcal{L}_{p,e} \mapsto \mathcal{L}_{p,e} \tag{2.11}$$

Further suppose both operators are finite-gain $\mathcal{L}_p$ stable, that is

$$\|y_1\|_p \leq \gamma_1 \|e_1\|_p + \beta_1, \quad \forall e_1 \in \mathcal{L}_{p,e} \tag{2.12}$$

$$\|y_2\|_p \leq \gamma_2 \|e_2\|_p + \beta_2, \quad \forall e_2 \in \mathcal{L}_{p,e} \tag{2.13}$$

where

$$\|H_1\|_{i,p} := \gamma_1, \quad \|H_2\|_{i,p} := \gamma_2 \tag{2.14}$$

Suppose further that the closed loop is well defined in the sense that unique outputs exist for every set of inputs.

Then if

$$\gamma_1 \gamma_2 < 1 \tag{2.15}$$

then $\forall u_1, u_2 \in \mathcal{L}_{p,e}$ we have

$$\|e_1\|_p \leq \frac{1}{1-\gamma_1\gamma_2}(\|u_1\|_p + \gamma_2\|u_2\|_p + \beta_2 + \gamma_2\beta_1) \tag{2.16}$$

$$\|e_2\|_p \leq \frac{1}{1-\gamma_1\gamma_2}(\|u_2\|_p + \gamma_1\|u_1\|_p + \beta_1 + \gamma_1\beta_2) \tag{2.17}$$

That is, the interconnection is finite gain $\mathcal{L}_p$ stable

This version of the theorem is fairly comprehensive and encompasses many of the situations encountered practically; it will be adequate throughout most of the thesis. As will be seen this provides a convenient tool by which to analyse the robustness properties of systems. For more detail on the induced norm version of the Small Gain Theorem the reader is referred to the book [41] for example.

The Incremental Small Gain Theorem

Definition 2.3 *The incremental gain of a stable, causal operator* $H : \mathcal{L}_{p,e} \mapsto \mathcal{L}_{p,e}$ *is the quantity (if it exists):*

$$\|H\|_{\Delta,p} := \sup_{w,\tilde{w}(\neq w)\in\mathcal{L}_{p,e}} \frac{\|H(w) - H(\tilde{w})\|_p}{\|w - \tilde{w}\|_p} \tag{2.18}$$

This definition follows [60], but is well known.

Definition 2.4 (Incremental stability) *A causal operator* $H(.)$ *is* incrementally stable *if*

$$\|H(x) - H(\tilde{x})\|_p \leq \gamma\|x - \tilde{x}\|_p + \beta \quad \forall x, \tilde{x}(\neq x) \in \mathcal{L}_{p,e} \tag{2.19}$$

for some $\gamma, \beta \in \mathbb{R}_+$.

The next theorem is the Incremental version of the Small Gain Theorem, which is slightly stronger than the induced norm equivalent.

Theorem 2.2 *Consider the feedback connection in Figure 2.6, where* H_1 *and* H_2 *are two nonlinear operators such that:*

$$H_1 : \mathcal{L}_{p,e} \mapsto \mathcal{L}_{p,e} \tag{2.20}$$

$$H_2 : \mathcal{L}_{p,e} \mapsto \mathcal{L}_{p,e} \tag{2.21}$$

Further, suppose that both operators are incrementally stable, that is

$$\|y_1 - \tilde{y}_1\|_p \leq \gamma_1\|e_1 - \tilde{e}_1\|_p + \beta_1, \quad \forall e_1, \tilde{e}_1(\neq e_1) \in \mathcal{L}_{p,e} \tag{2.22}$$

$$\|y_2 - \tilde{y}_2\|_p \leq \gamma_2\|e_2 - \tilde{e}_2\|_p + \beta_2, \quad \forall e_2, \tilde{e}_2(\neq e_2) \in \mathcal{L}_{p,e} \tag{2.23}$$

where

$$\|H_1\|_{\Delta,p} := \gamma_1, \quad \|H_2\|_{\Delta,p} := \gamma_2 \tag{2.24}$$

then $\forall u_1, \tilde{u}_1(\neq u_1), u_2, \tilde{u}_2(\neq u_2) \in \mathcal{L}_{p,e}$ *if* $\gamma_1\gamma_2 < 1$ *we have*

$$\|e_1 - \tilde{e}_1\|_p \leq \frac{1}{1-\gamma_1\gamma_2}(\|u_1 - \tilde{u}_1\|_p + \gamma_2\|u_2 - \tilde{u}_2\|_p + \beta_2 + \gamma_2\beta_1) \tag{2.25}$$

$$\|e_2 - \tilde{e}_2\|_p \leq \frac{1}{1-\gamma_1\gamma_2}(\|u_2 - \tilde{u}_2\|_p + \gamma_1\|u_1 - \tilde{u}_1\|_p + \beta_1 + \gamma_1\beta_2) \tag{2.26}$$

That is, the interconnection is incrementally $\mathcal{L}_p$ stable.

Note that this theorem is also fairly comprehensive and is slightly stronger than the induced norm version: in the induced norm case, the assumption that the closed loop is well defined needs to be made; this can be dropped in the incremental gain case, as the finite incremental gain of the two operators guarantees existence and uniqueness of solutions. This is due to the incremental gain version of the small gain theorem being based on the *Contraction Mapping Theorem*, which guarantees existence and uniqueness [2]; Limebeer explores this relation in [27]. This version of the theorem also provides a useful tool for robustness analysis; in fact it is a mathematically stronger result, although as noted by various researchers (e.g. [60]) it is sometimes too strong to use.

Linear Small Gain Theorem

The "linear" version of the Small Gain Theorem is the strongest available for general use, although it can only be applied under the assumption that both operators in the feedback connection are linear. However this restriction does allow stronger conditions for stability to be given. The following is taken from [99], with some slight generalisations

Theorem 2.3 (Linear Small Gain Theorem) *1. Consider the feedback connection in Figure 2.6, where H_1 and H_2 are transfer function matrices $\mathbf{H}_1, \mathbf{H}_2 \in \mathcal{RH}^\infty$. Then the feedback loop is finite-gain $\mathcal{L}_p$ stable if*

$$\gamma_1\gamma_2 < 1 \tag{2.27}$$

where γ_1 (resp. γ_2) denotes the induced $\mathcal{L}_p$ norm (or $\mathcal{L}_p$ incremental gain) of $\mathbf{H}_1$ (resp. $\mathbf{H}_2$) [3] for any $p \in \{1, 2, \ldots, \infty\}$.

[2] In fact, if both operators are linear the induced norm version of the Small Gain Theorem also ensures well-posedness - see later

[3] For linear systems the induced $\mathcal{L}_p$ norm and the $\mathcal{L}_p$ incremental gain are identical. To see this note that $\|G\|_{\Delta,p} := \sup_{x,\tilde{x}(\neq x)} \frac{\|G(x)-G(\tilde{x})\|_p}{\|x-\tilde{x}\|_p} = \sup_{x,\tilde{x}\neq x} \frac{\|G(x-\tilde{x})\|_p}{\|x-\tilde{x}\|_p}$, by linearity of G. Defining $x - \tilde{x} := y$, then yields precisely the definition of the induced norm.

2. *In the particular case of the $\mathcal{L}_2$ induced norm or incremental gain with $\mathbf{H}_1 \in \mathcal{RH}^\infty$, then the system is well posed and internally stable for all $\mathbf{H}_2 \in \mathcal{RH}^\infty$ with*

   - $\|\mathbf{H}_2\|_{i/\Delta,2} \leq \gamma^{-1}$ *if and only if* $\|\mathbf{H}_1\|_{i/\Delta,2} < \gamma$
   - $\|\mathbf{H}_1\|_{i/\Delta,2} < \gamma^{-1}$ *if and only if* $\|\mathbf{H}_2\|_{i/\Delta,2} \leq \gamma$

The first part of the theorem is just a specialisation of the nonlinear incremental and induced norm versions to the linear case. Note that in the special case that H_1 and H_2 are linear, the induced norm and incremental gain are identical. The second part gives necessary conditions which are proved in [99] and are based on frequency domain criteria. This proof relies on the fact that the following is true

$$\mathbf{H}_{i,2} = \mathbf{H}_{\Delta,2} = \|H\|_\infty \tag{2.28}$$

where $\|(.)\|_\infty$ denotes the $\mathcal{H}^\infty$ norm of a stable transfer function matrix. This has a frequency domain interpretation; it is in fact, by *Plancharel's Theorem* [4], equivalent to the $\mathcal{L}_2$ induced norm in the frequency domain (although it is not trivial to prove this). This conveniently overlaps with the next topic.

2.1.4 $\mathcal{H}^\infty$ Optimal Control

$\mathcal{H}^\infty$ -control will now be introduced briefly and put into context with the Small Gain Theorem and its relation to robust stability of uncertain, or perturbed systems. Many more texts give a thorough treatment of this relationship and rigorously derive the synthesis equations for various $\mathcal{H}^\infty$ optimal controllers. The reader is referred [99] or [27] for a more exhaustive analysis.

The essence of the Small Gain Theorem is that provided the two elements in a feedback loop have a gain (defined in terms of $\|(.)\|_{i,p}$ or $\|(.)\|_{\Delta,p}$) less than unity, the interconnection will be stable. To use the small gain theorem to give information about practical systems it is often necessary to calculate these norms. Generally this is difficult, but due to the aforementioned frequency domain interpretation of the $\mathcal{L}_2$ induced norm - that is the $\mathcal{H}^\infty$ norm - for this special case it can be calculated. The objective of $\mathcal{H}^\infty$ control is to therefore guarantee small gain stability to uncertainty measured in the $\mathcal{L}_2$ induced norm (or incremental $\mathcal{L}_2$ induced norm).

The previous section discussed the use of the Small Gain Theorem in feedback system stability analysis. Often a general control system can be arranged as this type of small gain inter-connection, with one operator taking the part of the nominal (linear) system, and the

[4] Plancharel's Theorem, states that $\langle f(t), g(t)\rangle = \langle f(j\omega), g(j\omega)\rangle$. $\langle ., .\rangle$ denotes inner product.

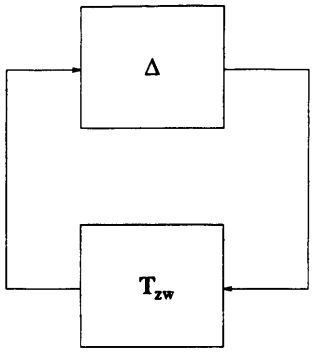

Figure 2.7: Small Gain interconnection for uncertain System

other operator as a perturbation to this nominal representation. With this in mind, most perturbed systems can be represented as Figure 2.7, where $\mathbf{T}_{zw} \in \mathcal{RH}^\infty$ represents the nominal closed-loop transfer function, and Δ represents a finite-gain $\mathcal{L}_p$ stable (or incrementally stable) perturbation.

Recall from the prior discussion that the feedback connection will be internally stable (providing the inter-connection is well defined if we use the induced $\mathcal{L}_p$ norm version) provided that

$$\gamma_1\gamma_2 < 1 \tag{2.29}$$

where $\gamma_i, \quad i = 1,2$ is either the $\mathcal{L}_p$ induced norm or $\mathcal{L}_p$ incremental gain of $\mathbf{T}_{zw}$ and Δ. Obviously this is equivalent to

$$\gamma_2 < \frac{1}{\gamma_1} \tag{2.30}$$

If we now consider the case of the $\mathcal{L}_2$ induced norm or incremental gain, it follows that the smaller the $\mathcal{H}^\infty$ norm of $\mathbf{T}_{zw}$ is, then the greater the amount of uncertainty, in the $\mathcal{L}_2$ induced norm or incremental gain sense, which can be tolerated by the system.

The $\mathcal{H}^\infty$ optimal control problem can therefore be stated as:

Problem 2.1 ($\mathcal{H}^\infty$ Optimal Control) *Find an internally stabilising controller* $\mathbf{K}$ *which ensures the* $\mathcal{H}^\infty$ *norm of the closed loop transfer function* $\mathbf{T}_{zw}$ *is bounded above by* γ*, where* γ *is in some prescribed tolerance of the minimal achievable* $\mathcal{H}^\infty$ *norm.*

The structure of $\mathbf{T}_{zw}$ has not yet been specified, but it turns out that a very general form can be used to describe the so-called generalised plant. Diagramatically this is shown in Figure 2.8, where $w(t)$ represents the exogenous inputs, $z(t)$ represents the controlled outputs, $y(t)$ the input to the controller, and $u(t)$ the control signal. $\mathbf{K}$ is to be generated from the given plant data, $\mathbf{P}$.

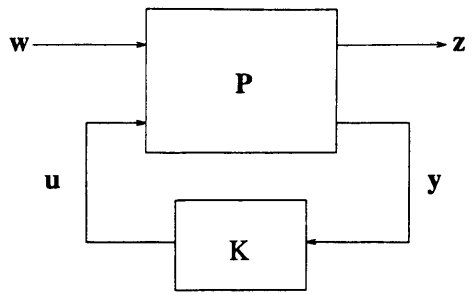

Figure 2.8: Generalised Plant in $\mathcal{H}^\infty$ Optimisation

In fact, if $\mathbf{P}$ is partitioned compatibly with its inputs and outputs as

$$\mathbf{P} = \left[\begin{array}{c|c} \mathbf{P}_{11} & \mathbf{P}_{12} \\ \hline \mathbf{P}_{21} & \mathbf{P}_{22} \end{array}\right] \tag{2.31}$$

we actually seek to minimise the $\mathcal{H}^\infty$ norm of the lower *linear fractional transformation* $\mathcal{F}_l(\mathbf{P},\mathbf{K}) = \mathbf{P}_{11} + \mathbf{P}_{12}\mathbf{K}(I - \mathbf{P}_{22}\mathbf{K})^{-1}\mathbf{P}_{21} =: \mathbf{T}_{zw}$.

This problem can be tackled using many different approaches, but is generally solved using two algebraic Riccati equations, whose solutions depend on plant data (see [13]). The derivation of the (sub-)optimal controller in all cases is non-trivial and the results will be not be stated here, due to the lengthy expressions for the controller in the general case. It suffices to say that commercially available software can be used to compute a controller meeting the prescribed bound, γ([4]). However 'standard assumptions' are needed for these optimisation processes to function (these are useful for the design techniques described later).

Given that the plant $\mathbf{P}$ has the following state space representation

$$\mathbf{P} \sim \left[\begin{array}{c|c|c} A & B_1 & B_2 \\ \hline\hline C_1 & D_{11} & D_{12} \\ \hline C_2 & D_{21} & D_{22} \end{array}\right] \tag{2.32}$$

the following assumptions are made

1. (A, B_2, C_2) is stabilisable and detectable
2. D_{12} has full column rank; D_{21} has full row rank
3. $$\left[\begin{array}{cc} A - j\omega I & B_2 \\ C_1 & D_{12} \end{array}\right]$$ has full column rank for all real ω;

$$\begin{bmatrix} A - j\omega I & B_1 \\ C_2 & D_{21} \end{bmatrix}$$

has full row rank for all real ω;

The first assumption is required for the existence of stabilising controllers; the second is sufficient to ensure that the synthesised controller is proper; the last assumption ensures the existence of stabilising solutions to the two Riccati equations associated with the $\mathcal{H}^\infty$ synthesis procedure.

These assumptions are made for the standard algorithms described in [13], and are the ones used in many commercial software packages ([4]). Some of these assumptions can be dropped in the formulations of [71] and [63], which consider the singular $\mathcal{H}^\infty$ problem, and the $\mathcal{H}^\infty$ problem without assumption on the plant zeros respectively. Furthermore, the paper by Gahinet ([18]), gives an LMI interpretation of relaxing some of the above assumptions. These methods are less well understood than the conventional $\mathcal{H}^\infty$ method ([13]) and, moreover, are not needed in the work here, so will not be discussed further.

The algorithm used in $\mathcal{H}^\infty$ controller synthesis is based on the bisection method and proceeds as follows. For a given value of gamma (usually specified by the designer) the following conditions are checked:

1. $D_{11}'D_{11} \leq \gamma$.
2. Positive semi-definite solutions to the two Riccati equations exist.
3. A spectral radius condition is satisfied.

If such conditions are satisfied, γ is reduced, if not γ is increased. The algorithm then repeats; it terminates when γ has been calculated to a prescribed tolerance. The outcome of the algorithm is a controller, which is usually sub-optimal, of the same order as the plant, $\mathbf{P}$, which enforces $\|\mathcal{F}_l(\mathbf{P},\mathbf{K})\|_\infty \leq \gamma$. As the Riccati equation associated with $\mathcal{H}^\infty$ control has an indefinite quadratic term, for arbitrary γ, a solution is not guaranteed. For more information about the algorithm, see, for example, [99].

$\mathcal{H}^\infty$ Mixed Sensitivity Design

The controller which is the result of the $\mathcal{H}^\infty$ optimisation process guarantees that the closed loop system is stable against certain types of uncertainty. It is often the case that the model of

the plant is known to a prescribed accuracy in a particular frequency range, but is uncertain in another. For this reason, the transfer functions whose $\mathcal{H}^\infty$ norms are to be minimised are often frequency weighted. To understand why this is the case, note that most uncertainty can be approximated as $\Delta = W_a(j\omega)\tilde{\Delta}W_b(j\omega)$, where W_a, W_b are used to reflect the frequency content of the uncertainty. Pairing these with the nominal transfer function, call it $M(s)$, and applying the Small Gain Theorem we see that robust stability is ensured for all $\|\tilde{\Delta}\|_{i/\Delta,2} < \frac{1}{\gamma}$, where

$$\gamma = \|W_b(j\omega)M(j\omega)W_a(j\omega)\|_\infty \tag{2.33}$$

Thus if some information about the frequency content of the uncertainty is known or can be estimated, this can help reduce conservatism in the results and also allow performance specifications to be included alongside the robustness considerations.

Here, the two common $\mathcal{H}^\infty$ design procedures which are used for controller design in this thesis are described. In particular, these descriptions serve as background for the helicopter control work discussed in later chapters.

S/KS *Design*

As the name suggests this procedure centres around the minimisation of a weighted combination of the sensitivity and **KS** functions. These are normally frequency weighted to accommodate the variation of $\bar{\sigma}(\Delta(j\omega))$ with ω, and 'stacked' to allow performance and robustness specifications to be considered simultaneously. We seek a controller which enforces

$$\left\| \begin{array}{c} \mathbf{W}_1\mathbf{S}_i \\ \mathbf{W}_2\mathbf{K}\mathbf{S}_o \end{array} \right\|_\infty \leq \gamma \tag{2.34}$$

which implies

$$\|\mathbf{W}_1\mathbf{S}_i\|_\infty \leq \gamma \tag{2.35}$$

$$\|\mathbf{W}_2\mathbf{K}\mathbf{S}_o\|_\infty \leq \gamma \tag{2.36}$$

where $\mathbf{W}_1$ and $\mathbf{W}_2$ are the weights representing the frequency shaping requirements. Normally $\mathbf{W}_1$ is chosen as a low-pass filter to enforce good set-point tracking and disturbance rejection, but often is chosen proper (rather than strictly proper) to limit the peak of the sensitivity function which impairs robustness. [5] $\mathbf{W}_2$ is normally chosen as a high-pass filter to capture

[5] It is sometimes not prudent to do this due to the *waterbed* effect

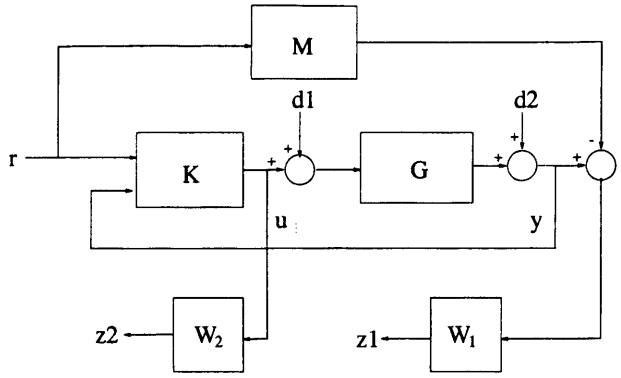

Figure 2.9: $\mathcal{H}^\infty$ 2 DOF Mixed Sensitivity Configuration

robustness requirements and also, since the expression for the control signal can be written as $u = \mathbf{KS}r$, it can be manipulated to influence the energy and frequency content of the control signal. Note that to satisfy the rank condition (point 2) in the above assumptions $\mathbf{W}_2$ must be chosen as proper rather than strictly proper.

In terms of the Small Gain Theorem inequalities (2.35) and (2.36) imply that the system is robust, at low frequencies, to output feedback multiplicative uncertainty, Δ_f, of induced $\mathcal{L}_2$ norm (or incremental gain) less than $\frac{1}{\gamma}$; and at high frequencies to additive uncertainty, Δ_a of induced $\mathcal{L}_2$ norm (or incremental gain) less than $\frac{1}{\gamma}$.

2 DOF Mixed Sensitivity

The configuration shown in Figure 2.9 provides a convenient way of enforcing performance requirements in addition to robustness requirements. The objective is to minimise.

$$\left\| \begin{bmatrix} \mathbf{W}_1(\mathbf{M} - \mathbf{S}_o\mathbf{G}\mathbf{K}_1) & \mathbf{W}_1\mathbf{S}_o\mathbf{G} & \mathbf{W}_1\mathbf{S}_o \\ \mathbf{W}_2\mathbf{S}_i\mathbf{K}_1 & \mathbf{W}_2\mathbf{T}_i & \mathbf{W}_2\mathbf{S}_i\mathbf{K}_2 \end{bmatrix} \right\|_\infty \tag{2.37}$$

Essentially the cost function associated with this transfer function ensure performance requirements through the $\mathbf{W}_1$ weight, which is again chosen as a low pass filter to ensure good agreement at low frequency between the closed loop system and the ideal model $\mathbf{M}$. $\mathbf{W}_2$ again is chosen as a high pass filter to ensure that the $\mathbf{KS}$ and $\mathbf{T}$ functions remain small at high frequencies to impart robustness against additive and multiplicative uncertainties to the closed-loop. Again, $\mathbf{W}_2$ must be proper but not strictly proper to satisfy the technical conditions.

The synthesis procedure for this plant, $\mathbf{G}$, could, for the most effective solution, take place in two stages: the first to enforce robustness criteria (i.e. the design of the feedback controller), the second to give good nominal performance (the design of the feed-forward controller). Unfortunately for a generalised plant of dimension n, this would yield a high order compensator

of the order $3n$, plus any the dimension of any weights used. Instead the synthesis is normally one-step and the transfer function above is normally minimised in one optimisation process.

2.2 Systems with Input Nonlinearities

2.2.1 Overview

Most practical systems are subjected to the presence of nonlinearities at their input, the most common probably being the saturation nonlinearity, but others such as control selectors, rate-limits and hysteresis are also common. These are often not included with the actual plant model, and instead are treated as separate entities. One common reason for this is that most of these nonlinearities have a piecewise linear nature, and can, by suitable design technique, sometimes be ignored, providing the plant input remains in this linear region for the majority of the time. Another reason for their neglect is that, while conceptually simple to understand, they often have a mathematical structure which is difficult to handle in a straightforward manner; many of these elements are non-smooth (for example the saturation and deadzone nonlinearities), or even discontinuous (for example switching functions, hysteresis).

The aim of this section is to introduce some of the preliminary ideas associated with linear systems subject to input nonlinearities and briefly review some of the more important results that have been established. Although not as vast as the robust control literature, a comprehensive exposition of the input-nonlinearity literature is possibly more difficult due to the diversity and complexity of the mathematical techniques used.

This thesis considers two types of input nonlinearity: the amplitude saturation nonlinearity and the controller substitution nonlinearity. The former has a great deal more literature devoted to it and will be studied from two angles: the first will consider how a controller can be designed to take into account saturation limits *a priori*; the second will examine how the control system can be modified if the controller was designed without due regard for actuator limits - this is often referred to as *anti-windup compensation* or *conditioning*. The controller substitution literature considers the problem of how transient effects due to a switch in controllers can be effectively handled, and is often associated with the anti-windup literature. The notion of reducing these transients is often referred to as 'bumpless transfer'. The formulation of anti-windup and bumpless transfer problems can be similar, but in this thesis a distinction is made. This is partly due to the fact that, although the problems seem similar and it is possible to solve each in a similar manner, there are some unique properties which the bumpless transfer problem has which need careful attention.

In fact, there are few results available for systems which experience switching in of different controllers. Some results have appeared for some cases of switched linear systems, particularly in the context of stochastic stability ([50]), but very few concerning the type of situation in a general bumpless transfer context. Some exceptions exist and [9] gives examples of certain types of control selectors which belong to Conic Sectors, and thus absolute stability results such as the Circle and Popov Criterion can then be used. Due to their sparsity and the fact that these results are not applicable to many parts of the thesis, a fuller discussion of bumpless transfer techniques is delayed until Chapter 3.

2.2.2 Constrained Input Systems

The discussion given here pertains to general properties of linear systems subject to input saturation; that is systems whose controls are component-wise bounded in magnitude. These systems are simply standard linear systems which are cascaded with a memoryless saturation nonlinearity, whose general form is given below.

Definition 2.5 (General Saturation Function) *A function $\sigma : \mathbb{R}^m \mapsto \mathbb{R}^m$ is called a saturation function if*

1. *$\sigma(u)$ is decentralised; that is $\sigma(u) = [\sigma_1(u_1) \quad \sigma_2(u_2) \quad \dots \quad \sigma_m(u_m)]'$*
2. *σ_i is globally Lipschitz.*
3. *$s\sigma_i(s) > 0$ whenever $s \neq 0$.*
4. *$\min\{\lim_{s\to 0+} \sigma_i(s)/s, \lim_{s\to 0-} \sigma_i(s)/s\} > 0$.*
5. *$\liminf_{|s|\to\infty} |\sigma_i(s)| > 0$.*

This definition follows Lin *et al.*, [47], and is a very general description of saturation-type nonlinearities. It basically allows the nonlinearity to be any 'first and third' quadrant sector bounded continuous function, such as tanh(.), arctan(.) etc, and to be mathematically well-posed. Some of the results in this thesis will hold for this general saturation nonlinearity, others will not and require the use of the standard saturation nonlinearity.

Definition 2.6 (Standard Saturation Nonlinearity) *The standard saturation function,* $sat(.) : \mathbb{R}^m \mapsto \mathbb{R}^m$ *is defined as*

$$sat(u) := \begin{bmatrix} sat_1(u_1) \\ sat_2(u_2) \\ \cdots \\ sat_m(u_m) \end{bmatrix} \tag{2.38}$$

where

$$sat_i(u_i) := sign(u_i)\min(|u_i|, \bar{u}_i) = \begin{cases} \bar{u}_i, & u_i > \bar{u}_i \\ u_i, & |u_i| \leq \bar{u}_i \\ -\bar{u}_i, & u_i < \bar{u}_i \end{cases} \tag{2.39}$$

and $\bar{u}_i > 0$ *is the componentwise saturation limit of the* u_i.

Note that this definition of the standard saturation nonlinearity requires the saturation to be symmetric and satisfies all the conditions of the more general definition.

2.2.3 Stability Properties of Input Saturated Linear Systems

The subject of stability is one of prime importance when dealing with feedback control systems. In this section some results which have appeared in the literature are introduced as background to some of the material in the remainder of the thesis. Many results in the literature pertain to specific control schemes or system structures, but here it is preferred to state only the most general.

Of prime importance, certainly for the regulator problem, is the region of the state space from which all states can be driven to zero. Formally, this is termed the *null controllable* region and is defined below

Definition 2.7 (Null Controllability) *A state-space system's* [6] null controllable *region is the region of the state-space where all states starting in that region can be driven to the origin using an appropriate control.*

Definition 2.8 (Global Null Controllability) *A state-space system with state vector* $x \in \mathbb{R}^n$ *system is termed* globally null controllable *if its region of null controllability is* $\mathbb{R}^n$ *i.e. every state can be driven to the origin.*

[6] A system is called a state-space system if it permits an internal state-space representation. Not all systems qualify for this representation

The following result is taken from [60], who in turn took it from [42] with the generalisations of [64]. It is a essentially a controllability result for input-saturated systems

Theorem 2.4 (Global Null Controllability) *The system*

$$\dot{x}(t) = Ax(t) + B\sigma(u(t)) \tag{2.40}$$

is globally null controllable if and only if (A, B) *is stabilisable, and* A *has all its eigenvalues lying in the closed left-half complex plane.*

Romanchuk ([60]) also states the result for discrete-time systems, which is equivalent except the eigenvalues of A must lie in the closed unit disk. Note that the type of control, $u(t)$ is not stated and it was proved in [17], that purely *linear* feedback could not stabilise an integrator chain of order greater than 3. In fact, for systems with eigenvalues on the imaginary axis, the best a linear feedback can do is to achieve *semi-global* stabilisation, which will be considered shortly. Nonlinear feedbacks which achieve global stabilisation are rare, but have been reported in [74], where an integrator chain of arbitrary order is stabilised by a nonlinear law of 'nested' saturations. The importance of Theorem 2.4 is that it prohibits global stability results for open-loop exponentially unstable linear systems with input saturation.

One of the more important results concerning linear feedbacks will now be stated. The results in Chapter 3 are based on work closely related to this concept. The following definition is adapted from [46]

Definition 2.9 (Semi Global Stabilisation) *A linear system subject to input saturation is said to be semi-globally stabilisable if there exists a control law* $u(.)$ *and an arbitrarily large bounded set,* $\mathcal{X} \subset \mathbb{R}^n$*, such that the equilibrium* $x = 0$ *is locally asymptotically stable with* $\mathcal{X}$ *contained within its basin of attraction.*

It can be seen that semi-global stabilisation is a powerful result and is arguably as practically significant as global stabilisation; realistically one can always bound the set of states a system will reach. The next result is taken from the papers of Lin and Saberi (see [45], [46] for example).

Theorem 2.5 (Null Controllable Semi-global Stabilisation) *The system (2.40) is semi-globally stabilisable by a linear control law if and only if* (A, B) *is stabilisable and the eigenvalues of* A *reside in the closed left-half complex plane.*

In [45] and [46] a family of linear control laws which achieve semi-global stabilisation of the asymptotically null controllable system, (2.40), is constructed. Moreover, the family suggested in [46] enable an arbitrarily large high gain parameter to be added to improve transient response and such like. Results related to this will be given in Chapter 4.

Many other results have appeared in this field, most of which have not been mentioned. A comprehensive survey of many of these papers appears in [5]. One notable group of papers which has not been mentioned is those concerned with optimal control of saturated systems. The problem with many of these results is that they either ignore stability completely (see the latter part of chapter 2 of [43], for example), or they give rise to extremely complicated solutions ([61]); due to the practical nature of this thesis they therefore fall outside its scope.

2.2.4 Anti-Windup Schemes

The main difference between this set of schemes from those arising in the constrained input literature just surveyed is that account of input saturation is taken after a nominal linear controller has been designed. [7] In other words, an extra block of compensation is added to the system and most often this only affects the system's behaviour during, or immediately after, saturation has occurred. This is sometimes referred to as 'conditioning'.

Anti-windup compensation is attractive because it allows arbitrary linear methods to be used for the controller design, and thus circumvents much of the mathematical intractability associated with many of the constrained input *a priori* synthesis techniques. Furthermore, the system functions as the linear design for the majority of its operation, and the anti-windup compensator is only excited during saturation, which one hopes is occasional [8]. It is perhaps for these two reasons why anti-windup compensators are virtually the only type of input-saturation handling apparatus used in practice.

Figure 2.10 shows probably the most general form of anti-windup compensator; $u \in \mathbb{R}^m$ is the nominal linear control signal, and $u_m \in \mathbb{R}^m$ is the actual input to the plant. Most often it is the case that the difference between u and u_m is used to drive the AWC (anti-windup compensator), although some particularly novel schemes, such as that of [75], allow for other functions to be used and also need part of the state vector to be available. In actual fact it has been suggested by Sternby *et al.*([86]) that the majority of AWC's could be interpreted as state feedback terms in the original linear controller. This is not however true of all schemes.

[7] This is not absolutely correct as some anti-windup schemes such as [83] and [40], suggest controllers that are specifically designed to be 'anti-windup compensated'

[8] If saturation is frequent, it is debatable whether anti-windup compensators are most suitable, and the previous input constraint techniques may yield better results.

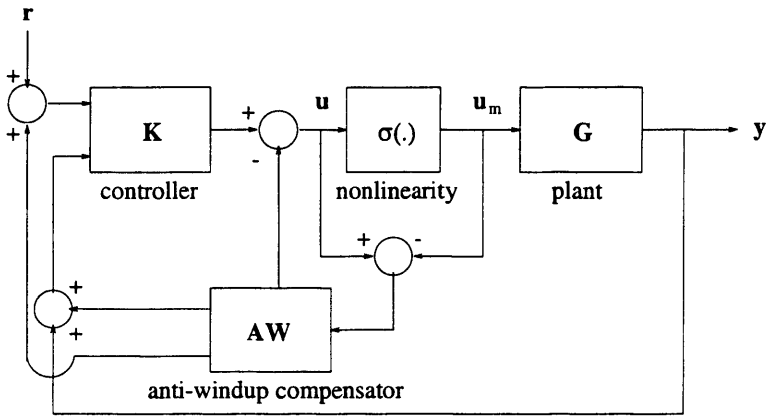

Figure 2.10: General Anti-windup Scheme

The existing work on anti-windup compensators will now briefly be reviewed. Unlike the remainder of the constrained input literature, this has several convenient evolutionary stages and two unifying interpretations. Note that two more comprehensive discussions of AWC's can be found in [10] and [15].

Classical AW Compensation and the Hanus Conditioning Technique

These two approaches to anti-windup are probably the most widely used conditioning schemes for both anti-windup and bumpless transfer. Classically, anti-windup was associated with integrator 'windup' and is how the term originated. It was tackled by placing a high gain in a loop around the integrator which came into effect when saturation occurred. Of course, whenever the controller contains zeros in the right-half complex plane, there is a definite limit on the amount of gain which can be applied; this may not be enough to prevent windup, and this method can only be considered ad hoc.

One of the most significant occurances in AWC design was the development of the Hanus Conditioning technique ([31]), which has remained popular since its introduction. Essentially the idea behind the Hanus scheme is to interpret the mismatch between nominal and saturated control signal as an inconsistency in the controller states to what was actually injected into the plant. To overcome this inconsistency, a 'realisable reference' is created by partially inverting the controller and driving it with the difference $u - u_m$. If the original (2DOF) controller has the state space realisation

$$K(s) \sim \left[\begin{array}{c|cc} A & B_1 & B_2 \\ \hline C & D_1 & D_2 \end{array}\right] \tag{2.41}$$

then the state-space realisation of the Hanus self-conditioned controller is given as

$$\left[\begin{array}{c}\dot{x}\\ \hline u\end{array}\right] = \left[\begin{array}{c|ccc} A & B_1 & B_2 & -B_1 D_1^{-1} \\ \hline C & D_1 & D_2 & 0 \end{array}\right] \left[\begin{array}{c} x \\ \hline r \\ y \\ u - u_m \end{array}\right] \tag{2.42}$$

where u_m is the actual plant input. In fact, substitution of u in $u - u_m$ gives the equivalent representation as

$$\left[\begin{array}{c}\dot{x}\\ \hline u\end{array}\right] = \left[\begin{array}{c|ccc} A - B_1 D_1^{-1} C & 0 & B_2 - B_1 D_1^{-1} D_2 & B_1 D_1^{-1} \\ \hline C & D_1 & D_2 & 0 \end{array}\right] \left[\begin{array}{c} x \\ \hline r \\ y \\ u_m \end{array}\right] \tag{2.43}$$

The main advantages of the Hanus Scheme are

- Conceptually simple.
- Simple to implement - no need to add extra controller dynamics.
- Does not alter the nominal behaviour when the control is un-saturated.

Its main disadvantage is that it, in its original form, can only be applied to certain controllers.

- The controllers must be bi-proper; that is, they must be invertible at $s = \infty$. This requires D_1 to be nonsingular
- The controllers must be minimum phase to ensure the conditioned configuration is stable (the conditioned controller is partially inverted, so non-minimum phase transmission zeros manifest themselves as right-half plane poles in the conditioned scheme).

Some of these points will be alluded to in the bumpless transfer work of the next chapter. It is also worth noting that some attempts have been made to remove these restrictions, notably the generalised conditioning scheme ([30]), but this requires the solution of a quadratic programming problem, and the attractive simplicity of the original scheme is lost. Walagama [87] also proposed a modification based on coprime factors, although no insight to choosing a particular factorisation was given.

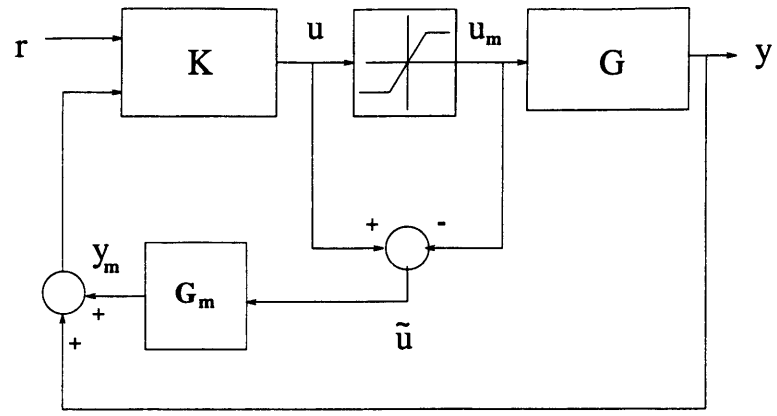

Figure 2.11: Model Based Anti-windup Compensation

Model Based Techniques

These are another important sub-class of anti-windup compensators; they are of particular interest in this thesis as some of the work in later chapters takes these as a basis. The basic diagram of model based compensators is shown in Figure 2.11. From the diagram it can be seen that the anti-windup compensator takes the form of the so-called *direct model*, $G_m(s)$ which operates on the difference $u - u_m$. Unlike the Hanus scheme which uses the concept of a 'realisable reference', to modify the controller, the objective of the model based schemes is to modify the plant output, before it is added to the controller, by using a signal y_m generated by the direct model. Note that in order for internal stability to be preserved, $G_m(s)$ must be stable [9]itself and also stabilise $\mathbf{K}$ (and of course be mathematically well-posed).

One of the advantages of the model based scheme is that one has more degrees of freedom available than in static schemes (the Hanus scheme gives no degrees of freedom; the high gain gives only one), and in principle allows greater control over the transient response; albeit at the expense of adding extra dynamics.

There are also disadvantages: firstly there are no concrete guidelines for choosing $G_m(s)$ [10]; secondly, as pointed out by Walagama *et al.*([87]), if the direct model contains lightly damped modes, the scheme often behaves unsatisfactorily (y_m can be oscillatory).

An important subclass of the model based schemes actually turns out to be internal model control (IMC - [53]): this is the case whereby the direct model $G_m(s)$ is simply chosen as the (stable) linear plant. The anti-windup properties of this scheme have been established by Campo and Morari ([8]) and other modifications to improve the scheme have been made by various authors.

[9]In fact, if G_m shares the same state-space as K, some unstable poles can occur in $\mathbf{G}_m$ providing they are cancelled by some transmission zeros in $\mathbf{K}$

[10]This is elaborated on later in the thesis - see Chapter 6.

The Unifying Theories

Several unifying theories connecting various anti-windup schemes are in existence. Two are considered here, before going on to discuss more contemporary work.

One of the first unifying theories to emerge in the control literature was given in the text [1], where the *observer based* realisation of anti-windup schemes was suggested, which takes the following form in the 2DOF case

$$K_{AW}(s) \sim \left[\begin{array}{c|ccc} A & B_1 & B_2 & -L \\ \hline C & D_1 & D_2 & 0 \end{array}\right] \tag{2.44}$$

Essentially this is the nominal linear controller with the inclusion of the term $-L(u - u_m)$ in the state equation, where necessarily L is chosen to ensure $\mathbf{spec}(A - LC) \in \mathcal{C}^-$. The object of L is to modify the behaviour of the system when saturation occurs.

The observer based modification of the controller is a technique in its own right, but it can easily be seen that the classical *high gain* approach as well as the Hanus technique are both particular flavours of this general form of anti-windup compensator. Obviously one of the attractive features of such a technique is the fact that it does not increase the dimension of the compensator, as no extra dynamics are needed. As well as the two cases mentioned already, Walagama *et al.*([87]) have claimed that more general types of anti-windup compensators can be interpreted as being of the observer type - see also the paper [40].

Probably one of the most important developments in the anti-windup field after the conditioning technique of Hanus, was the *general theory* of [10]. Although the observer based parametrisation captured several common anti-windup schemes, it could not capture all due to the fact that it excluded the possibility of adding extra dynamics. It has been shown, for example in [14], that there are some cases where extra dynamics must be included to obtain acceptable transient responses.

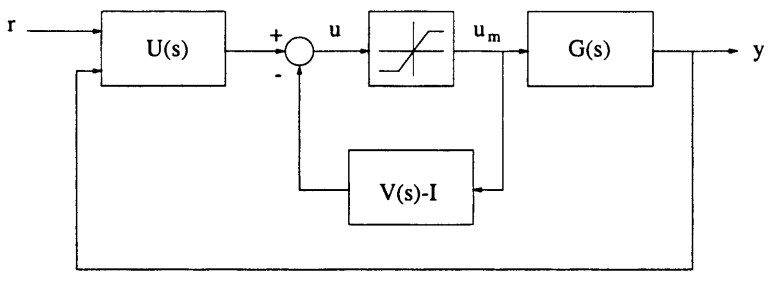

Figure 2.12: Unified Anti-windup

The scheme of Campo *et al.*captures virtually all linear conditioning schemes[11], which constitutes most of the anti-windup literature. A diagram of their scheme is shown in Figure 2.12, where the controller is split into a pair of left coprime factors

$$K(s) = V(s)^{-1}U(s), \quad U(s), V(s) \in \mathcal{RH}^{\infty} \tag{2.45}$$

For some of the schemes in the literature, the use of a non-minimal coprime factorisation is needed; that is the coprime factors have higher order than the controller to capture the extra dynamics introduced by some schemes. However, all coprime factors of identical order to that of the controller can be described as

$$[U(s) \quad V(s)] \sim \left[\begin{array}{c|cc} A - H_1C & -H_1 & B - H_1C \\ \hline H_2C & H_2 & H_2D \end{array}\right] \tag{2.46}$$

where $\mathbf{spec}(A - H_1C) \in \mathcal{C}^-$ and

$$H_1 = \Lambda_1(I + \Lambda_2)^{-1} \tag{2.47}$$

$$H_2 = (I + \Lambda_2)^{-1} \tag{2.48}$$

In certain cases, namely when $H_2 = I$, this scheme reduces to the observer based scheme previously mentioned. This scheme is attractive due to its ability to unify most schemes and provide new interpretations of choosing parameters in terms of the gains H_1 and H_2; unfortunately it does not always give a great deal of insight into the selection of these gains.

Contemporary Schemes

Some of the more important and well developed contemporary schemes will now be discussed: recent nonlinear schemes and a new interpretation of linear conditioning schemes for stable systems. The latter will be introduced first as it follows on conveniently from the Campo *et al.* unifying theory, and in actual fact has a precise relationship to that scheme. The scheme is diagramatically shown in Figure 2.13, where anti-windup compensation is considered in terms of choosing $M(s)$.

It has been shown that this can be re-drawn as Figure 2.14, where all signals are labelled identically and $\mathbf{G} \in \mathcal{RH}^{\infty}$. Note that in this equivalent configuration, the system has three distinct parts.

[11] An anti-windup scheme is said to employ linear conditioning if all of its elements are linear

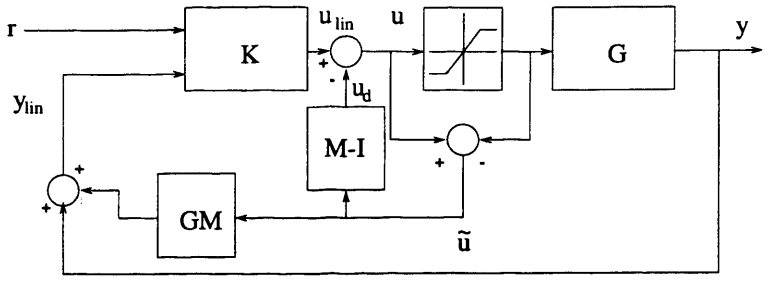

Figure 2.13: Conditioning with $M(s)$

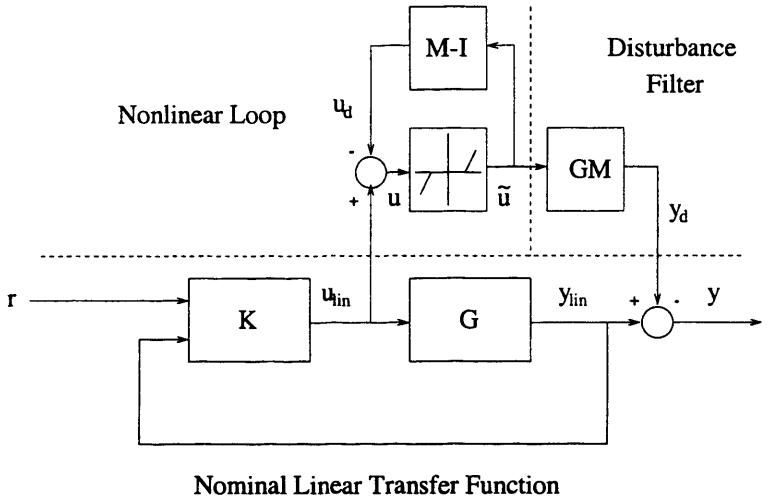

Figure 2.14: Equivalent Representation of Conditioning with $M(s)$

1. Nominal Linear System - this operates purely linearly
2. Nonlinear Loop - whenever saturation occurs, this part of the system becomes active
3. Disturbance filter - During and after saturation this linear system creates a 'disturbance' which is added to the output of the original linear system.

There are three modes of operation associated with these distinct parts of the system: when no saturation occurs and the system operates linearly; when saturation occurs and the nonlinear loop is driven; and after saturation when the nonlinear loop is no longer active, but the disturbance filter dissipates energy. This scheme was introduced in [92] and a detailed discussion can be found in [93].

This has an important relationship to the Campo *et al.* scheme because the scheme can be interpreted as a coprime factorisation of the plant. That is, $\mathbf{M}$ can be viewed as one half of the right coprime factorisation of the plant $\mathbf{G} = \mathbf{N}\mathbf{M}^{-1}$. In fact it has been shown in [93] that this scheme is the dual of the Campo scheme: this being represented as a right coprime factorisation of the plant, whereas the Campo scheme was interpreted as a left coprime factorisation of the controller.

The advantages of such an interpretation is that it gives the engineer a certain amount of intuition in devising the transfer function **M**. Another of its major strengths is that the stability of the scheme can be determined from the nonlinear loop, from which the nominal linear loop is decoupled. Currently, however, it is only applicable to stable plants (as **G** appears open-loop in the disturbance filter), and, as this thesis is concerned mainly with open-loop unstable plants, will not be considered further.

Another class of contemporary schemes which is worth mentioning is that of *nonlinear* conditioning schemes; as their name suggests the anti-windup compensator is not necessarily linear. In fact, it might be argued that as the presence of saturation causes the scheme to behave in a nonlinear way, there is no reason to believe why purely linear compensation should be used [12].

One of the first nonlinear schemes was given in [39] and even today is regarded as having provided excellent results. However this was only applied to a simple system and is considered slightly academic ([93]). Apart from this, few nonlinear results have appeared, probably due to their complexity and lack of intuition, except a series of papers by Teel and co-authors ([76], [40], [75]). One of the objectives of these papers is to give a strategy whereby the behaviour of the saturated loop recovers to that of the linear loop in some sense, which is often taken as the $\mathcal{L}_2$ sense. This does not necessarily mean that linear anti-windup compensation is required and in [75] a quite general anti-windup compensator is given which is applicable to most types of problem and consists of both linear and nonlinear functions.

No further mention of nonlinear conditioning schemes will be made in the remainder of the dissertation. Little is known about the choice of nonlinear parameters in the context of engineering design and the subject is left open for research.

2.2.5 Stability Results for Constrained Input System

This section will contain a brief summary of some of the stability results commonly in use in the analysis of constrained input systems - both conditioned and *a priori* synthesised systems. One of the key results, The Small Gain Theorem, has already been reviewed and the reader is referred to the previous section. The techniques discussed here are mainly Lyapunov based or those from the absolute stability literature.

[12] Some results in the constrained input literature - for example [48] - have proved that in some cases nonlinear compensation can do no better than linear compensation

Lyapunov Stability

The history of Lyapunov stability is long and rich. Many would argue that the Lyapunov stability theorems have the most diverse applications in systems and control theory. What has come to be called *Lyapunov's Second Method* will be discussed here, and from now on when Lyapunov stability is mentioned it will mean stability in this sense.

The following definition of a Lyapunov function is taken from Stalford [69] and is mathematically quite precise, although more general than we shall typically need.

Definition 2.10 *Consider the system*

$$\dot{x} = f(x, u) \tag{2.49}$$

where $x \in \mathcal{X} \subset \mathbb{R}^n$ and the terminal set Θ is contained in $\mathcal{X}$. Then a scalar function, $V : \mathcal{X} \mapsto \mathbb{R}$ is called a Lyapunov function for the above system if it satisfies the following conditions

1. $V(x) = 0, \quad x \in \Theta,$
2. $V(x) > 0, \quad x \in \mathcal{X}/\Theta,$
3. $lim_{\|x\| \to \infty} V(x) = \infty,$
4. $\frac{\partial V(x)}{\partial x} f(x, u) < 0, \quad x \in \mathcal{X}/\Theta.$

It has been proven that if there exists a Lyapunov function, as defined above, for a system then the system is stable over the domain $\mathcal{X}$, provided that $f(.)$ and $V(.)$ are both continuously differentiable. Certain relaxations in the definition of the Lyapunov function have also been given which allows its application to wider classes of system - see for example [69].

The essence of the above is that a function $V(x)$ is called a Lyapunov function for a given system if it is positive definite and its time derivative, $\dot{V}(x) = \frac{\partial V(x)}{\partial x} f(x, u)$ is negative definite.

In the special case of linear systems, we have the following theorem, constructed from [41]

Theorem 2.6 *The system*

$$\dot{x} = Ax + Bu \tag{2.50}$$

is stable or Hurwitz, that is $\mathbf{spec}(A) \in \mathcal{C}^-$*, if and only if for any given positive definite matrix Q, $\exists P > 0$ which satisfies*

$$A'P + PA = -Q \tag{2.51}$$

Moreover if A is Hurwitz, then P is the unique solution to (2.51).

This is a well known theorem and it will be extensively used in later parts of this thesis. Equation (2.51) is known as a *Lyapunov Equation*, and is actually a symmetric form of a more general class of linear matrix equations, the *Sylvester Equations.*

Closely associated with Lyapunov theory is the concept of *positively invariant sets*, which are often simply termed *invariant sets.*

Definition 2.11 (Positive Invariance) *A connected set $\mathcal{X}$ is said to be* positively invariant *or* forward invariant, *for the system*

$$\dot{x} = f(x,t) \tag{2.52}$$

if $x(0) \in \mathcal{X} \Rightarrow x(t) \in \mathcal{X} \forall t \in \mathbb{R}_+$.

It actually transpires that Lyapunov level sets have the property of positive invariance (see [41] for example). More formally,

Lemma 2.1 *Consider the system $\dot{x} = f(x)$ and the Lyapunov function $V(x) > 0$, such that for some connected set $\mathcal{X} \subset \mathbb{R}^n$ contained within the system's domain of attraction, it is true that $\dot{V}(x) < 0$. Then if there exists a positive real number c and a set*

$$\{x : V(x) \leq c\} \subset \mathcal{X} \tag{2.53}$$

then this set has the property of positive invariance.

A fuller description of Lyapunov theory can be found in the book by Khalil ([41]) and, with reference to *Lyapunov Equations*, in ([99]).

Dissipation Theory

Dissipation theory can be roughly summarised as a generalisation of Lyapunov theory to an input-output context. Whereas Lyapunov type ideas tend to be used in more of a regulation context, dissipation ideas tend to be used in a more input-output context. The origins of dissipation theory can be found in many physical studies, but the abstract generalisation which

today is termed dissipation theory by control engineers was first developed by Willems - see for example [94].

In essence a system is said to be dissipative if the stored energy in a system at a given time does not exceed the stored energy at an earlier time, plus the energy injected externally. In fact the notion of a *supply rate* is used; this is the net amount of abstract energy being injected into the system. The notion of a storage function, which is rather like a Lyapunov function, is used to represent energy stored in the system. A more complete discussion of these ideas are contained within, for example, [60] and [84], but we will review some of the basic ideas.

If we consider the system, $S : U \mapsto Y$, with input u and output y, then its associated supply rate is a function of the form $r(u, y) : U \times Y \to \mathbb{R}_+$. A candidate storage function has similar properties to a Lyapunov function candidate and often is also denoted $V(x) \geq 0$.

Theorem 2.7 *A system $S : U \to Y$, with input u and output y is said to be dissipative with respect to the supply rate, $r(u, y)$ if there exists a candidate storage function, $V(x)$ with the following properties:-*

1. *$V : \mathbb{R}^n \to \mathbb{R}$ is uniformly Lipschitz over any compact set and $V(0) = 0$.*
2. *$V(x) \geq 0$*
3. *$\dot{V}(x) - r(u, y) \leq 0$*

Note that dissipation theory is not quite as 'strict' as Lyapunov theory, in the sense that many of the inequalities in the above theorem are not strict. However, the ideas are similar and many functions which act as Lyapunov functions also double as storage functions (the converse is also true - see [84], chapter 3). This approach is often used in $\mathcal{L}_2$ gain analysis of nonlinear systems, and in [60] extensive use of these ideas were made in computing $\mathcal{L}_2$ induced norms and incremental gains of input-saturated linear systems. In this thesis, however, dissipation theory does not play a large part, although its usefulness is recognised.

The Circle and Popov Criteria

The Circle and Popov Criteria have been used for the analysis of linear systems with memoryless nonlinearities for years in the control field. In the case of SISO systems they both have a graphical interpretation, but now their popularity for MIMO analysis and synthesis is growing due to the advent of LMIs - see [7].

The idea behind both of these criteria is similar to that of the Small Gain Theorem, except with the inclusion of more information about the structure of the nonlinearities, namely that

they belong to a certain *conic sector.* In fact due to this similarity both Zames ([98]) and Romanchuk ([60]), view them as corollaries to the Small Gain Theorem. The crucial difference in both criteria is the sector condition imposed. The following definition is taken from [41]

Definition 2.12 *The function* $\phi : [0,\infty) \times \mathbb{R}^p \mapsto \mathbb{R}^p$ *is a memoryless, possibly time-varying nonlinearity which is piecewise continuous in* t *and locally Lipschitz in* y*. Moreover,* $\phi(.,.)$ *is said to lie in* Sector$[\bar{V}, \underline{V}]$ *if*

$$[\phi(t,y) - \bar{V}y]'[\phi(t,y) - \underline{V}y] \leq 0, \forall t, \quad \forall y \in \Gamma \subset \mathbb{R}^p \tag{2.54}$$

where $\bar{V}, \underline{V}$ *are real matrices such that* $\bar{V} - \underline{V} > 0$ *and the interior of* Γ *is connected and contains the origin. If this inequality holds for all* $y_i \in (-\infty, \infty), \quad i = 1, 2, \ldots, p$*, then the sector condition is said to hold globally.*

Central to the classical proofs and definitions of the Circle and Popov criteria is the notion of strict positive realness, which is given below ([41]).

Definition 2.13 *Let* $Z(s) \in \mathbb{R}^{p \times p}$ *be a proper, rational transfer function matrix and suppose* $\det[Z(s) + Z'(-s)]$ *is not identically zero. Then* $Z(s)$ *is strictly positive real if and only if*

- $\det(Z(s))$ *is a Hurwitz polynomial,*
- $Z(j\omega) + Z'(-j\omega) > 0, \quad \forall \omega \in \mathbb{R},$
- *One of the following conditions is satisfied:*
  1. $Z(\infty) + Z'(\infty) > 0,$
  2. $Z(\infty) + Z'(\infty) = 0$ *and* $\lim_{\omega \to \infty} \omega^2 [Z(j\omega) + Z'(-j\omega)] > 0,$
  3. $Z(\infty) + Z'(\infty) \geq 0$ *(but not zero nor nonsingular) and there exist positive constants* σ_0 *and* ω_0 *such that*

$$\omega^2 \sigma_{min}[Z(j\omega) + Z'(-j\omega)] \geq \sigma_0, \forall |\omega| \geq |\omega_0| \tag{2.55}$$

The Circle and Popov Criteria will now be stated ([41])

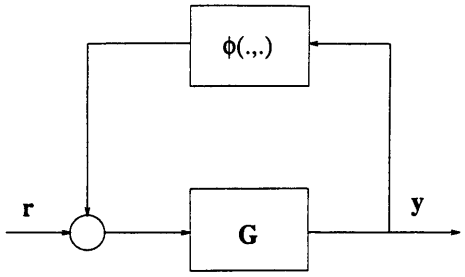

Figure 2.15: Linear System with Sector Bounded Nonlinearity if Feedback path

Theorem 2.8 (Circle Criterion) *Consider the feedback system in Figure 2.15, where* $G(s) \in \mathcal{RH}^\infty$ *has the minimal state-space realisation*

$$\left[\begin{array}{c|c} A & B \\ \hline C & D \end{array}\right] \tag{2.56}$$

and the nonlinear function $\phi(.,.)$ *satisfies, globally the sector condition, (2.54). Then the system is absolutely stable if*

$$G_T(s) := G(s)[I + YG(s)]^{-1} \tag{2.57}$$

is Hurwitz and

$$Z_T(s) := [I + \bar{V}G(s)][I + YG(s)]^{-1} \tag{2.58}$$

is strictly positive real. If the sector condition is only satisfied within a certain domain, $\Gamma \subset \mathbb{R}^p$, *then the conditions on* $G_T(s)$ *and* $Z_T(s)$ *ensure the system is stable with a finite domain.*

The circle criterion is quite cumbersome to handle in this form, but can be conveniently represented by an equivalent set of LMI's which are given in [93].

The Popov criterion is similar to the Circle Criterion, except that it is slightly less general, but also slightly less conservative. In fact in [41], its proof is identical, except that a different Lyapunov function (of the *L'ure* type) is used to prove stability.

Theorem 2.9 (Popov Criterion) *Consider the feedback system in Figure 2.15, where the minimal realisation of* $G(s) \in \mathcal{RH}^\infty$ *is given by*

$$\left[\begin{array}{c|c} A & B \\ \hline C & D \end{array}\right] \tag{2.59}$$

and the time invariant *nonlinearity $\phi(.,.)$ satisfies the sector condition with $\underline{V} = 0$ globally. Also suppose that $\bar{V}\phi(y)$ is the gradient of a scalar function* [13]. *Then the system is absolutely stable if there is an $\eta \geq 0$, with $-\frac{1}{\eta}$ not an eigenvalue of A such that*

$$Z(s) := I + (1 + \eta s)\bar{V}G(s) \tag{2.60}$$

is strictly positive real. If the sector condition (2.54) is satisfied and $\bar{V}\phi(y)$ is the gradient of a scalar function in a domain $\Gamma \subset \mathbb{R}^p$, then the same condition on $Z(s)$ ensures the system is absolutely stable in a finite domain.

Again, for multivariable systems, the result in this form is quite cumbersome, but it can be equivalently represented by a set of LMI's as described, for example, by [7]. In fact the LMI description is slightly more general as it instead uses a diagonal positive definite matrix instead of the scalar $\eta \geq 0$.

Note that both the Circle and Popov criteria require the linear transfer function, $G(s)$ to be stable. In some cases this difficulty can be surmounted by making loop transformations, such that $\tilde{G}(s) := G(s)[G(s) + V]^{-1} \in \mathcal{RH}^\infty$, and $\tilde{\phi}(.,.) := \phi(.,.) + V$; then the circle or Popov criteria can be applied to the loop-shifted system.

It is important to emphasise that, in the case of unstable plants with $\phi(.,.)$ being a saturation nonlinearity, that this type of result cannot be applied, because the validity of this transformation holds only when the state of the linear system is within its domain of attraction. This has been alluded to before in the literature in the case of the Small Gain Theorem (see [40]), but an example is given in the appendix to demonstrate that the same type of problem can occur in the case of absolute stability results.

In Chapter 6, this fact explains why no rigorous stability analysis was attempted with the anti-windup scheme: the helicopter is open-loop unstable, so no global stability guarantees can be given.

[13] This is true for a vector $g(y)$ if and only if $\frac{\partial g}{\partial y}$ is symmetric.

Chapter 3

Linear Quadratic Bumpless Transfer

3.1 Overview

This chapter considers the problem of dynamic transfer among two or more controllers. The tendency in such a situation is for a degradation in performance to occur when controllers are switched; often an undesirable transient or 'bump' occurs at or shortly after the switching instant. The so-called *bumpless transfer* problem is that of designing a mechanism which enables transfer between different controllers to take place as smoothly as possible.

Introduced in this chapter is a new mechanism which can help to facilitate bumpless transfer. This mechanism borrows the basic mathematical machinery from linear quadratic (LQ) optimal control and enables a feedback matrix to be derived, which attempts to force the output of the off-line controller to match the output of the current on-line controller. The idea is that when switching does occur, as the control signals generated by the controllers about to be transferred are the same (or close), the 'bump' which results is very small.

Formulae are derived for linear continuous time and linear discrete time controllers in both one-degree-of-freedom (1DOF) and two-degrees-of-freedom (2DOF) configurations. Results are first given for the finite-horizon case but then, under certain assumptions, these formulae are extended to the infinite-horizon case. When certain additional assumptions are made it is shown that the formulae actually reduce to those given by Hanus in [31]. This chapter is based on [81] and the modification given in [80].

3.2 Introduction

The problem of bumpless transfer is one of the oldest input-nonlinearity stumbling blocks in the control community and its study is both theoretically interesting and practically important. It arises most often in two instances. The first is when a system has several types of controllers which are selected for different circumstances, each controller being more appropriate for one

task than any other. The second set of circumstances can be found when controlling a highly nonlinear system, which prevents linear controllers (for example) from providing satisfactory performance over the whole operating regime; instead several controllers are designed for use at different operating points.

The second instance is of more concern to the helicopter work of this thesis, and is probably the more practically prevalent of the two. Of course, a related branch of study is that of *gain-scheduled* controllers; that is controllers which are able to give satisfactory performance throughout the whole operating envelope of a nonlinear system by having certain parameters scheduled as a function of the system's position in that envelope. We will not be concerned with this, and good references for this type of control theory can found in [55]. Note that switched controllers may be preferable to scheduled controllers for reason of their ease of implementation and, often, less complex computational issues [1].

Traditionally the study of bumpless transfer has been linked to that of anti-windup, and indeed the problems are similar by virtue of the fact that they are both input nonlinearity problems. Furthermore, several techniques have been found to be applicable to both problems, although recently it has been suggested ([24]) that even though the two problems often share the same basic framework, the objectives of the compensator designed to avoid them can be markedly different.

The history of bumpless transfer compensators is long and the reader is referred to Chapter 2 and the references cited there for more detail. However we shall consider some of the more important techniques, specifically devoted to bumpless transfer rather than anti-windup generally, which have arisen.

Classically, for SISO systems, the problem of bumpless transfer was tackled by placing a large gain in a feedback loop around the off-line controller (the 'High Gain' technique described in Chapter 2). This is then driven by the error or reference in addition to the on-line control signal. Effectively this forces the off-line controller to track the on-line control signal. Of course problems with this approach are the fact that for good tracking high gains are needed and this is not always possible; simple root-locus ideas show that, if the controller has any RHP zeros - including those at infinity - the gain cannot be raised beyond a limit, or instability will occur.

One of the most celebrated and widely used transfer schemes to date was proposed by Hanus ([31]) and has been successfully applied to many real-life projects, for example a VSTOL aircraft ([37]) and ([56]). A discussion of this technique is given in Chapter 2. In the bumpless transfer context, the Hanus Conditioning Scheme attempts to initialise the states of the off-line

[1] LPV-based scheduled controllers involve a significant modelling task and a large computational effort is required to solve the resulting LMI's

controller to those of the on-line controller by creating a feedback loop around the off-line controller that partially inverts it. This feedback loop is only active if the on-line and off-line control signals are different, and takes as its input the difference between these two. This results in the synthesis of the *realisable reference* signal which is fed to the off-line controller to initialise its states. Due to the partial controller inversion however, the Hanus Scheme requires the off-line controller to be bi-proper [2] and minimum phase, when used in the linear setting. The latter condition imposes few problems for most controllers, but the former can be restrictive. Various suggestions have been made as to how to choose a direct feed-through term (see for example [37] for a promising proposal), but none has been universally accepted. Furthermore, if the controller is non-square, the inverse of the direct-feedthrough term does not exist and this renders the Hanus method redundant.

The work described here aims to develop a technique for bumpless transfer for fairly general linear time invariant controllers, but one which uses little computational power, therefore making it easy to implement in practice. As already stated, the mathematical machinery has been borrowed from established LQ theory and the cost function minimised is deemed appropriate for the bumpless transfer scenario.

The structure of this chapter is as follows. First the additional notation needed, together with the assumptions under which the work is conducted, are introduced. Next a brief review of some optimal control basics is given. Following this, results are derived in detail for the 1DOF continuous time case which will prepare the reader for the later briefer treatment of the 2DOF continuous time case and the discrete time cases. A link to the Hanus conditioning Scheme is then given and a comment on the stability of the proposed scheme will be made. The scheme's potential is illustrated with some examples. Next some of the possible pitfalls with the basic scheme are pointed out, and an enhanced configuration suggested. This enhanced scheme is then demonstrated through an example. Finally some concluding remarks are made.

3.3 Assumptions and Additional Notation

For the most part the notation used is that introduced at the beginning of the thesis, but with several additional definitions. Where possible, the notation will be as discreet as possible so not to detract from the main ideas.

The controllers considered are all finite dimensional linear time invariant (FDLTI) in nature and the modest assumption that all their states are available for feedback, along with any other signals fed into or produced by the controllers, is made. This is not an unreasonable assumption

[2] That is, it must be invertible at infinity

as most modern controllers will be implemented in computer or micro-controller form, so their states will just be computer variables. Importantly it is assumed that all controllers' realisations are completely controllable, observable and locally stabilise the plant in question.

Both 1DOF and 2DOF controllers are considered, which are respectively assigned the following state-space realisations

$$\left[\begin{array}{c|c} A & B \\ \hline C & D \end{array}\right] \tag{3.1}$$

$$\left[\begin{array}{c|cc} A & B_1 & B_2 \\ \hline C & D_1 & D_2 \end{array}\right] \tag{3.2}$$

In the continuous time case it shall be assumed that the controller state equation is of the form

$$\dot{x} = f(x, w, \alpha, t) \tag{3.3}$$

and in the discrete time case it be shall assumed that the next state is determined from

$$x_{k+1} = f(x_k, w_k, \alpha_k, k) \tag{3.4}$$

The dimensions of the problem are summarised as follows: the state is $x \in \mathbb{R}^n$, the control is $u \in \mathbb{R}^m$. In the 1DOF case, the error (between reference and output) is denoted $e \in \mathbb{R}^p$ and the vector generated by the bumpless transfer block is $\alpha \in \mathbb{R}^p$; in the 2DOF case the plant output is denoted by $y \in \mathbb{R}^{p_1}$, the reference signal, $r \in \mathbb{R}^{p_2}$ and the signal generated by the bumpless transfer mechanism is $\alpha \in \mathbb{R}^{p_2}$. An arbitrary exogenous vector is sometimes used and is labelled $w \in \mathbb{R}^q$. All other vectors and matrices are assumed of compatible dimensions.

Following the ideas introduced in Chapter 2, the Lebesgue space of all square integrable functions is given by

$$\mathcal{L}_2 := \{x : \|x\|_2 < \infty\} \tag{3.5}$$

where $x = x(t)$ and the the $\mathcal{L}_2$ norm, $\|x\|_2$, is defined as

$$\|x\|_2 := \sqrt{\int_0^\infty x'x dt} \tag{3.6}$$

Similarly, the Lebesgue space of all absolutely square summable sequences is given by

$$l_2 := \{x : \|x\|_2 < \infty\} \tag{3.7}$$

where $x = x_k, \quad k =\in \{1, 2, ...\}$ and the the l_2 norm, $\|x\|_2$, is defined as

$$\|x\|_2 := \sqrt{\sum_0^\infty x'x} \tag{3.8}$$

Although the notation for both the $\mathcal{L}_2$ and l_2 norms is the same, it should be clear from the context which one is meant.

The Extended Lebesgue space of continuous square integrable functions, $\mathcal{L}_{2e}$, is identical to the the Lebesgue space, $\mathcal{L}_2$, except that the upper limit of the norm's integral is taken as some finite time, so that functions with an infinite $\mathcal{L}_2$ norm may still belong to $\mathcal{L}_{2e}$. The Extended Lebesgue space of discrete square summable sequences, l_{2e}, is defined similarly. It is assumed that all continuous signals belong to $\mathcal{L}_{2e}$ and that all discrete signals belong to l_{2e} here, as we are concerned with what amounts to weighted combinations of these norms. Recall that the majority of signals encountered have finite $\mathcal{L}_\infty$ (resp. l_∞) norms if they have finite $\mathcal{L}_{2e}$ (resp. l_{2e}) norms.

3.4 Concepts from Optimal Control

3.4.1 Continuous Time

The aim of this section is to introduce some concepts associated with continuous time LQ theory. A comprehensive and highly readable discussion of much of the material here can be found in, for example, [43] or [2]. These ideas will be drawn heavily on in subsequent sections.

The performance index considered is of the form

$$J(x, w, T) = \int_0^T L(x, w, t)dt + \phi(x(T), T) \tag{3.9}$$

which is to be minimised under the constraint of the state equation (3.3). This constraint can be adjoined to the performance index by using a dynamic Lagrange multiplier, $\lambda(t) \in \mathbb{R}^n$. The modified performance index is thus

$$\tilde{J}(x, w, T) = \int_0^T [L(x, w, t) + \lambda'(t)(f(x, w, t) - \dot{x})]dt + \phi(x(T), T) \tag{3.10}$$

Defining the *Hamiltonian* function as

$$H(x,w,\lambda,t) := L(x,w,t) + \lambda'(t)f(x,w,t) \tag{3.11}$$

(3.10) can be re-written as

$$\tilde{J}(x,w,T) = \int_0^T [H(x,w,\lambda,t) - \lambda'(t)\dot{x})]dt + \phi(x(T),T) \tag{3.12}$$

It is assumed that the functions $f(x,w,t)$, $L(w,x,t)$ and $\phi(x(T),T)$ belong to a sufficiently smooth class, to enable the gradients defined later to be taken.

Given a performance index of this type, it is well known that first order necessary conditions are given by ([43])

$$\frac{\partial H}{\partial \lambda} = \dot{x} = f(x,w,t) \tag{3.13}$$

$$\frac{\partial H}{\partial x} = -\dot{\lambda} \tag{3.14}$$

$$\frac{\partial H}{\partial w} = 0 \tag{3.15}$$

with the terminal condition

$$\frac{\partial \phi}{\partial x(T)} = \lambda(T) \tag{3.16}$$

Note that equations (3.13) and (3.14) constitute the *state* and *co-state* equations, respectively, where the co-state equation is a differential equation which is solved from the terminal condition, and describes the system's adjoint. Equation (3.15) is often referred to as the *stationarity* condition.

Note that thus far only necessary conditions for an extremum have been given; sufficient conditions have not been discussed. For general nonlinear systems and costs it is difficult to enforce sufficient conditions. However due to the linearity of the systems considered in this chapter and as the function $L(x,w,t)$ has a specific form, namely

$$L(x,w,t) = \begin{bmatrix} x \\ w \end{bmatrix}' \begin{bmatrix} Q & S \\ S' & R \end{bmatrix} \begin{bmatrix} x \\ w \end{bmatrix}, \quad Q,R > 0 \tag{3.17}$$

As $R > 0$ the function is convex in w, the *Legendre-Clebsch* condition is satisfied, which is a sufficient condition for a local minimum to exist [3]. Moreover, as the systems we are concerned

[3] Other, possibly more general, sufficient conditions are available

with are both linear and stabilisable, this local result can be strengthened to global - see [70].

More thorough investigation of these concepts can be found in ([43]), ([27]) and ([2]) for example, and related theory concerning the *calculus of variations* on which this is based can be found, for example in ([20]).

3.4.2 Discrete Time

The discrete time versions of the LQ theory we will use subsequently is very similar to that of the continuous time case. There are certain subtleties in the derivation of some of the necessary conditions (see [43] for example), but there will be no need to explore such intricacies here.

The performance index considered is

$$J = \sum_{0}^{T-1} L(x_k, w_k, k) + \phi(x_T, T) \tag{3.18}$$

which is to be minimised subject to the state equation, (3.4), and T is the terminal time.

The constraining state equation can be combined with the cost, (3.18) using a dynamic Lagrange multiplier, $\lambda_{k+1} \in \mathbb{R}^n$, yielding

$$\tilde{J} = \sum_{0}^{T-1} L(x_k, w_k, k) + \lambda'_{k+1}(f(x_k, w_k, k) - x_{k+1}) + \phi(x_T, T) \tag{3.19}$$

The Hamiltonian function in discrete time is defined as

$$H(x_k, \lambda_k, w_k, k) := L(x_k, w_k, k) + \lambda'_{k+1} f(x_k, w_k, k) \tag{3.20}$$

The modified performance index can now be written as

$$\tilde{J} = \sum_{0}^{T-1} H(x_k, \lambda_k, w_k, k) - \lambda'_{k+1} x_{k+1} + \phi(x_T, T) \tag{3.21}$$

First order necessary conditions for an extremum are given by

$$\frac{\partial H}{\partial \lambda_{k+1}} = x_{k+1} \tag{3.22}$$

$$\frac{\partial H}{\partial x_k} = \lambda_k \tag{3.23}$$

$$\frac{\partial H}{\partial w_k} = 0 \tag{3.24}$$

$$\frac{\partial \phi}{\partial x_T} = \lambda_T \tag{3.25}$$

These are similar conditions to the continuous time case and are the *state equation*, *co-state equation*, *stationarity condition* and *boundary condition* respectively. Again observe that the co-state equation evolves backwards in discrete-time from a terminal point.

The fact that a minimum actually exists is not yet demonstrated, but as the items of concern are actually quadratic forms of $L(x_k, w_k, k)$, defined as

$$L(x_k, w_k, k) = \begin{bmatrix} x_k \\ w_k \end{bmatrix}' \begin{bmatrix} Q & S \\ S' & R \end{bmatrix} \begin{bmatrix} x_k \\ w_k \end{bmatrix}, \quad Q, R > 0 \tag{3.26}$$

the convexity of this function ensures that a minimum of the cost function will actually exist.

3.5 The Continuous Time Case

3.5.1 Derivation of Continuous Time 1 D.O.F. Bumpless Transfer Matrix

This section will explain in detail the idea behind the proposed method of bumpless transfer and how it can be solved using LQ theory. 1DOF controllers are initially considered due to their slightly simpler structure and also because the accompanying algebra is easier to follow.

The basic idea of the proposal will now be described. As previously stated, it is assumed that there is access to the on-line controller's states, together with all signals fed into, and produced by, the on-line controller: i.e. the full-information scenario. With reference to Fig. 3.1, the proposal is to synthesise a static feedback gain, F, which can be used to drive the off-line controller in such a way that, at the time of transfer between on and off-line controllers, the transients produced by this switching are minimal.

To achieve a 'minimal' amount of transient behaviour during switching a quadratic cost function is minimised. The minimisation of a weighted combination of two signals is proposed. Firstly, at the time of switching, it is desirable for the on and off-line controllers to be producing control signals which are as close to each other as possible: this would reduce the magnitude of the discontinuity which occurs during transfer. Secondly, account must also be taken of the signals driving the controllers. Note that the off line control signal is being driven by the signal produced by the feedback gain and that, in the 1 D.O.F. case, the on-line controller is being driven by the error signal. It is desirable to avoid a large difference in these signals because, in order to maintain good tracking, the signal driving the off-line controller will be switched to the error signal. That is, after switching the off-line controller becomes the current on-line controller. This situation is described diagramatically in Figure 3.1.

To recapitulate, the objective is to minimise the difference between two sets of signals: the difference between the two control signals, and the difference between the signals driving the two controllers. To pose this problem in the LQ context, the following functional is to be minimised

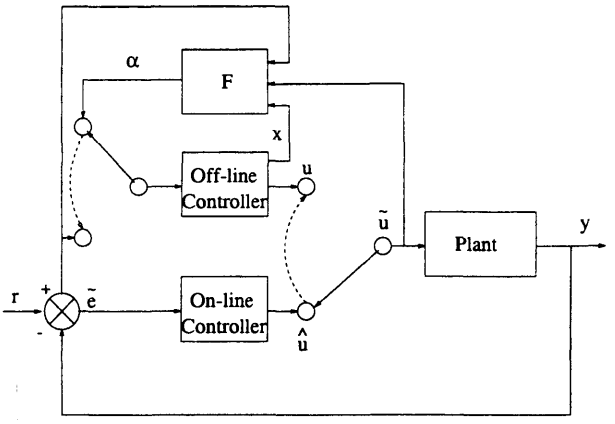

Figure 3.1: Bumpless Transfer Scheme

$$J(u,\alpha,T) = \frac{1}{2}\int_0^T z_u(t)'W_u z_u(t) + z_e(t)'W_e z_e(t)dt + \frac{1}{2}z_u(T)'Pz_u(T) \tag{3.27}$$

where

$$z_u(t) = u(t) - \tilde{u}(t) \tag{3.28}$$

$$z_e(t) = \alpha(t) - \tilde{e}(t) \tag{3.29}$$

and where $\tilde{u}(t)$ and $\tilde{e}(t)$ are the on-line control signal and error signal respectively; $u(t)$ is the off-line control signal; $\alpha(t)$ is the signal produced by the feedback gain which drives the off-line controller. W_u and W_e are constant positive definite weighting matrices of appropriate dimensions which are used to tailor the design as required. Finally, $z_u(T) = u(T) - \tilde{u}(T)$ is the difference between the two control signals at the switching (terminal) time T (which may be taken as infinity), and P is the positive semi-definite terminal weighting matrix; although this may well be set to zero and is introduced only for the benefit of derivation, and, indeed, generality.

To synthesise a feedback matrix, F, the problem of minimising this quadratic performance index is therefore solved. The signal $\alpha(t)$ produced by F, is a function of the off-line controller states, the error signal, and the on-line control signal. The gain F can be regarded as a full-information 'sub-controller', which temporarily controls the off-line controller.

Formally, the problem addressed in the remainder of this chapter is the following:-

Problem 3.1 *Consider the configuration in Figure 3.1 (1 D.O.F.) or Figure 3.2 (2 D.O.F.), where the on-line control signal, $\tilde{u}$, is given by*

$$\tilde{u} = \begin{cases} \hat{u} & \forall t \leq T \\ u & \forall t > T \end{cases} \tag{3.30}$$

Find the signal, $\alpha(t)$, $\forall t \leq T$ which ensures optimal transfer in the sense of minimising a prescribed performance index.

The following is the main result of the section.

Theorem 3.1 *Consider the system in Figure 3.1 where the continuous time off-line controller has the minimal state-space realisation given in (3.1). Given that the switch takes place at time T, then the signal, $\alpha(t)$, $\forall t \leq T$ which ensures optimal transfer between the two controllers, in the sense of the performance index (3.27), is given by*

$$\alpha = \Delta \begin{bmatrix} (D'W_uC)' \\ B \\ -(D'W_u)' \\ -W_e \end{bmatrix}' \begin{bmatrix} x \\ \lambda \\ \tilde{u} \\ \tilde{e} \end{bmatrix} \tag{3.31}$$

where the co-state, $\lambda(t)$, is obtained from

$$\lambda(t) = \Pi(t)x(t) - g(t) \tag{3.32}$$

and $\Pi(t)$ solves the differential Riccati equation

$$-\dot{\Pi} = \Pi\tilde{A} + \tilde{A}'\Pi + \Pi\tilde{B}\Pi + \tilde{C} \tag{3.33}$$

subject to the terminal condition

$$\Pi(T) = (I - C'PD\Delta B)^{-1}(C'PC + C'PD\Delta D'W_uC) \tag{3.34}$$

and $g(t)$ is found from the differential equation

$$-\dot{g} = (\tilde{A}' + \Pi\tilde{B})g + B_g\tilde{w} \tag{3.35}$$

which is solved subject to the terminal condition

$$g(T) = -(I - C'PD\Delta B)^{-1} D_g \tilde{w}(T) \tag{3.36}$$

where

$$\Delta = -(D'W_uD + W_e)^{-1} \tag{3.37}$$

$$\tilde{A} = A + B\Delta D'W_uC \tag{3.38}$$

$$\tilde{B} = B\Delta B' \tag{3.39}$$

$$\tilde{C} = C'W_u(I + D\Delta D'W_u)C \tag{3.40}$$

and

$$B_g := \begin{bmatrix} (C'W_u + C'W_uD\Delta D'W_u + \Pi B\Delta D'W_u)' \\ (C'W_uD\Delta W_e + \Pi B\Delta W_e)' \end{bmatrix}' \tag{3.41}$$

$$D_g := \begin{bmatrix} -(C'PD\Delta D'W_u + C'P)' \\ -(C'PD\Delta W_e)' \end{bmatrix}' \tag{3.42}$$

$$\tilde{w} := \begin{bmatrix} \tilde{u} \\ \tilde{e} \end{bmatrix} \tag{3.43}$$

Proof: To derive $\alpha(t)$ the LQ procedures which were briefly reviewed in the previous section are invoked. If the off-line controller is being driven by the signal $\alpha(t)$, then its state-space equations are,

$$\dot{x} = Ax + B\alpha \tag{3.44}$$

$$u = Cx + D\alpha \tag{3.45}$$

Substituting for u, in the performance index (3.27), one obtains:

$$J = \frac{1}{2}\int_0^T (Cx + D\alpha - \tilde{u})'W_u(Cx + D\alpha - \tilde{u}) + (\alpha - \tilde{e})'W_e(\alpha - \tilde{e})dt + \frac{1}{2}z_u(T)'Pz_u(T) \tag{3.46}$$

Forming the Hamiltonian,

$$H = \frac{1}{2}[(Cx + D\alpha - \tilde{u})'W_u(Cx + D\alpha - \tilde{u}) + (\alpha - \tilde{e})'W_e(\alpha - \tilde{e})] + \lambda'(Ax + B\alpha) \quad (3.47)$$

Equations (3.13) - (3.15) provide the first-order necessary conditions for a minimum in the index (3.46) subject to the controller's state equation, and are equivalent to,

$$\begin{aligned}
\frac{\partial H}{\partial \lambda} &= Ax + B\alpha && (3.48)\\
\Rightarrow \dot{x} &= Ax + B\alpha && (3.49)\\
\frac{\partial H}{\partial x} &= A'\lambda + C'W_uCx - C'W_u\tilde{u} + C'W_uD\alpha && (3.50)\\
\Rightarrow \dot{\lambda} &= -A'\lambda - C'W_uCx + C'W_u\tilde{u} - C'W_uD\alpha && (3.51)\\
\frac{\partial H}{\partial \alpha} &= (D'W_uD + W_e)\alpha + D'W_uCx + B'\lambda - D'W_u\tilde{u} - W_e\tilde{e} && (3.52)\\
\Rightarrow \alpha &= \Delta(D'W_uCx + B'\lambda - D'W_u\tilde{u} - W_e\tilde{e}) && (3.53)
\end{aligned}$$

If this expression for α is used in the state and co-state equations, (3.50) and (3.52) respectively, one obtains:

$$\begin{bmatrix} \dot{x} \\ \dot{\lambda} \end{bmatrix} = \begin{bmatrix} \tilde{A} & \tilde{B} \\ -\tilde{C} & -\tilde{A}' \end{bmatrix} \begin{bmatrix} x \\ \lambda \end{bmatrix} + \begin{bmatrix} -B\Delta W_e \\ C'W_uD\Delta W_e \end{bmatrix} \tilde{e} + \begin{bmatrix} -B\Delta D'W_u \\ C'W_u(I + D\Delta D'W_u) \end{bmatrix} \tilde{u} \quad (3.54)$$

The above non-homogenous differential equation is of the form which often arises in LQ minimisation and can be solved by the Method of Sweep (see [43]), which stipulates the affine relationship

$$\lambda(t) = \Pi(t)x(t) - g(t) \quad (3.55)$$

Differentiating,

$$\dot{\lambda}(t) = \dot{\Pi}(t)x(t) + \Pi(t)\dot{x}(t) - \dot{g}(t) \quad (3.56)$$

If (3.55), (3.56) and (3.54) are combined the following two expressions for $\dot{\lambda}$ result:

$$\dot{\lambda} = (\dot{\Pi} + \Pi\tilde{A} + \Pi\tilde{B}\Pi)x - \Pi\tilde{B}g - \Pi B\Delta D'W_u\tilde{u} - \Pi B\Delta W_e\tilde{e} - \dot{g} \quad (3.57)$$

and

$$\dot{\lambda} = -(\tilde{C} + \tilde{A}'\Pi)x + C'(W_u + W_u D\Delta D' W_u)\tilde{u} + C' W_u D\Delta W_e \tilde{e} + \tilde{A}' g \tag{3.58}$$

Equating coefficients of x the differential Riccati Equation (3.33) is obtained. Equating the remaining coefficients yields (3.59)

$$\begin{aligned} -\dot{g} = &(C'W_u + C'W_u D\Delta D'W_u + \Pi B\Delta D'W_u)\tilde{u} \\ &+(C'W_u D\Delta W_e + \Pi B\Delta W_e)\tilde{e} + (\tilde{A}' + \Pi\tilde{B})g \end{aligned} \tag{3.59}$$

which can be simplified to yield (3.35). Evaluating the boundary conditions from (3.16) gives the terminal conditions (3.36) and (3.34) stated in the theorem. These terminal conditions are used in (3.35) and (3.33) to determine the time varying matrix Π and vector g. In turn this can be used in the adjoint equation (3.32) to determine the co-state vector, λ. Recalling the definition of α (equation (3.53)), the following expression for the minimising feedback is obtained

$$\alpha = \Delta \begin{bmatrix} (D'W_u C)' \\ B \\ -(D'W_u)' \\ -W_e \end{bmatrix}' \begin{bmatrix} x \\ \lambda \\ \tilde{u} \\ \tilde{e} \end{bmatrix} \tag{3.60}$$

which is that given in the theorem.

◇◇

A problem now exists; for implementation, the co-state vector λ, which is obtained from a differential equation which develops backward in time from the terminal values of $\tilde{u}$ and $\tilde{e}$, is needed: future knowledge is required in order to arrive at a solution. For certain systems, which have a pre-planned trajectory, for example, this information can be determined and the co-state calculated. However, for most systems, it is difficult to calculate the co-state directly, which motivates the next section.

Extension to Infinite Horizon

Although conditions for a finite horizon bumpless transfer have been derived, there are two important points to note about this general case: the output of the closed-loop system adjoint,

λ, can only be computed on a finite horizon if the reference signals ($\tilde{e}$ and $\tilde{u}$) are known *a priori*; moreover, it is normally the case that these signals are *not* known *a priori*. In the case that these signals *are* known beforehand, either the values of $\lambda(t)$ would have to be determined off-line before implementation; or (3.32) solved for the initial condition $\lambda(0)$ off-line, using (3.36) and (3.34), and then the adjoint equation (3.32) would be solved on-line to obtain the values of $\lambda(t)$ needed by F. These two points limit the usefulness of the finite horizon results for many real-life applications.

However, if the results are extended to an infinite time support, these problems are not applicable; practical implementation then becomes possible. Here arguments to extend the finite horizon results are developed, and conditions which must apply for this to be achieved are stated. To aid us a theorem is presented, which gives conditions for the Riccati Equation (3.33) to have a steady-state, constant solution, $\Pi(\infty)$, which is the same as the corresponding algebraic Riccati equation (ARE):

$$\Pi\tilde{A} + \tilde{A}'\Pi + \Pi\tilde{B}\Pi + \tilde{C} = 0 \tag{3.61}$$

The theorem is essentially from [43].

Theorem 3.2 *Assume $(\tilde{A}, \tilde{B})$ is stabilisable, $(\tilde{A}, \sqrt{\tilde{C}})$ is detectable and the terminal solution to the Riccati differential equation (3.33) is positive semi-definite, then:*

- *The Riccati equation (3.33) has a steady state solution, independent of the terminal value, such that $\Pi = \Pi(\infty) = \lim_{T\to\infty} \Pi(t) \geq 0$*
- *The solution $\Pi(\infty) = \Pi$ is positive semi-definite and stabilising*

Remark

Our assumption on the controllability of (A, B) implies that the pair $(\tilde{A}, \tilde{B})$ are controllable. To see this note that due to the full rank assumption on Δ, controllability of $(\tilde{A}, \tilde{B})$ is equivalent to controllability of $(\tilde{A}, B)$. Also as $\Delta D'W_uC$ is equivalent to a state feedback term in $\tilde{A}$, and state feedback does not alter controllability, then controllability of $(\tilde{A}, \tilde{B})$ is ensured. By a similar argument, observability of (A, C) can be seen to imply observability of $(\tilde{A}, \sqrt{\tilde{C}})$ if the term $W_uD\Delta D'W_u$ is positive definite. This is not ensured as $\Delta < 0$, but can be made so by appropriate choice of weighting matrices.

Furthermore, if $D = 0$, controllability and observability of $(\tilde{A}, \tilde{B}, \sqrt{\tilde{C}})$ is ensured. This can be seen by noting that, when $D = 0$, the following expressions hold:

$$\tilde{A} = A \tag{3.62}$$

$$\tilde{B} = -BW_e^{-1}B' \tag{3.63}$$

$$\tilde{C} = C'W_uC \tag{3.64}$$

As W_u and W_e have both been chosen positive definite, their ranks are full and therefore neither $\tilde{B}$, nor $\tilde{C}$ lose rank. This implies the controllabilty and observability statement made above. Hence from Theorem 3.2, it can be concluded that the steady state solution of equation (3.33) converges to that of the ARE (3.61); thus in the infinite horizon it is sufficient to solve an algebraic equation and, moreover, this solution is stabilising.

◇◇

The following theorem formally states the results for a form infinite horizon bumpless transfer.

Theorem 3.3 *Consider Theorem 3.1, let $T \to \infty$ and assume that $\tilde{e}$ and $\tilde{u}$ are unknown but constant for all time. Then providing $(\tilde{A}, \tilde{B}, \sqrt{\tilde{C}})$ is stabilisable and detectable and $\Pi(T) \geq 0$, the signal $\alpha(t)$ ensuring optimal bumpless transfer in the sense of the performance index (3.27), is given by*

$$\alpha = F \begin{bmatrix} x \\ \tilde{u} \\ \tilde{e} \end{bmatrix} \tag{3.65}$$

where F is obtained as

$$F = \Delta \begin{bmatrix} (B'\Pi + D'W_uC)' \\ (-D'W_u + B'M(C'W_u + C'W_uD\Delta D' + \Pi B\Delta D'W_u))' \\ (-W_e + B'M(C'W_uD\Delta W_e + \Pi B\Delta W_e))' \end{bmatrix}' \tag{3.66}$$

and $\Pi \geq 0$ solves the ARE (3.61) and $M = (\tilde{A}' + \Pi\tilde{B})^{-1}$. Furthermore, the off-line control loop is stable.

Proof: First, following Theorem 3.2, it is evident that, under the stabilisability and detectability assumptions made in the theorem, as $T \to \infty$, then the solution of the differential Riccati equation will converge to that of (3.61) provided that $\Pi(T) \geq 0$.

Now consider the differential equation (3.35). It is well known from optimal control that such a differential equation does not converge to a constant solution for an arbitrary exogenous vector

$\tilde{w}$. Thus, even in the infinite horizon a differential equation, using future information, must be solved to obtain an exact solution.

We suggest using an approximation for g, as used in LQ tracking and described in [2]. To this end, we make the additional assumption that the exogenous signals $\tilde{u}$ and $\tilde{e}$ are constant. Then, noting that $\mathbf{spec}(A_g) := \mathbf{spec}((\tilde{A}+\tilde{B}\Pi)') \in \mathcal{C}^-$ (by the stabilising property of the ARE solution), it can be shown that,

$$\lim_{T\to\infty} g(t) = g = -A_g^{-1}B_g\tilde{w} \tag{3.67}$$

where $A_g := (\tilde{A}+\tilde{B}\Pi)'$ and g is a constant as a consequence of $\tilde{w}$ being a constant. Using the expressions for A_g and B_g this can be written as a linear equation:

$$\begin{aligned} g = -(\tilde{A}'+\Pi\tilde{B})^{-1}[&(C'W_u + C'W_uD\Delta D'W_u + \Pi B\Delta D'W_u)\tilde{u} + \\ &(C'W_uD\Delta W_e + \Pi B\Delta W_e)\tilde{e}] \end{aligned} \tag{3.68}$$

Equation (3.68) no longer needs the exogenous signals to be known *a priori* (as long as they are constant) as it too is purely algebraic. Hence both Π and g can be computed for substitution into (3.32) (in turn this can be inserted into (3.53)). Thus in the infinite horizon α can be computed as given in (3.65). Furthermore note that the ARE, (3.61), has a positive definite stabilising solution, which always exists providing the stabilisability and detectability conditions are satisfied, and hence ensures the stability of the off-line control loop.

◇◇

Note that if $D = 0$, then the formula for F simplifies considerably.

Remark

The infinite horizon solution relies heavily upon the approximation for g, which assumes the exogenous signals are unknown but constant. However, many signals in real systems, such as steps, can be considered constant over a certain period of time. For these signals, the signal α is optimal, but for others it is suboptimal. Thus if the system responds quickly enough (large poles), the approximation may serve as quite satisfactory and these infinite horizon results may be applied.

The justification of allowing $T \to \infty$ is more difficult, in the context of controller switching, as T will always be finite in reality. One argument for allowing $T \to \infty$ is practical: along with assumption that the exogenous signals are constant, it allows for a simple construction of the bumpless transfer element, F. Another justification of the infinite horizon length is that, as

optimality of $\alpha(t)$ is dependant on horizon length, which only has meaning, generally, when the precise moment of switching is known *a priori*. With the infinite horizon formulae applied to real systems, where switching takes place in some finite time, $\alpha(t)$ will never be 'optimal' but it will get close to optimal the larger t is. Furthermore, simulation has indicated that in many cases the infinite horizon solution is quite adequate.

◇◇

To summarise, Problem 3.1 has been solved in the finite horizon case and in the constant-input infinite horizon case, for 1DOF continuous time controllers and the performance index (3.27).

3.5.2 2 Degrees of Freedom Design

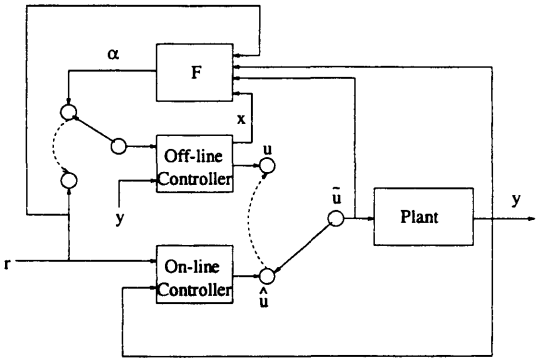

Figure 3.2: 2 D.O.F Configuration

The ideas developed can also be applied to the 2 D.O.F. configuration[4] where the on-line controller is driven by the reference signal, r, and the plant output, y; and the off-line controller is driven by the plant output and the output from the feedback matrix, α. The main objective will remain the same in the 2 D.O.F configuration: to minimise the difference between the off-line and on-line control signals in the sense of a quadratic cost. However, as neither controller is driven by the error signal, and both controllers are partly driven by the plant output signal, for the subsidiary minimisation one must minimise the difference between the other signals that are driving the two controllers: the reference, and the feedback matrix output. Hence the performance index becomes,

$$J(u,\alpha,T) = \frac{1}{2}\int_0^T z_u'(t)W_u z_u(t) + z_e'(t)W_e z_e(t)dt + \frac{1}{2}z_u(T)'Pz_u(T) \qquad (3.69)$$

where

[4]Note that 1 D.O.F. controllers may be considered a special case of the 2 D.O.F. configuration. Hence, this bumpless transfer scheme may easily be adapted to switch between 1 D.O.F. and 2 D.O.F. controllers.

$$z_u(t) = u(t) - \tilde{u}(t) \tag{3.70}$$

$$z_e(t) = \alpha(t) - r(t) \tag{3.71}$$

Formally, the following theorem is the main result of the section:-

Theorem 3.4 *Consider the system in Figure 3.2, where the continuous time controller has minimal state-space realisation given in (3.2). Given that the switch takes place at time T, then the signal $\alpha(t), \forall t \leq T$, which ensures optimal transfer between the two controllers, in the sense of the performance index (3.69), is given by*

$$\alpha = \Delta \begin{bmatrix} (D_1' W_u C)' \\ B_1 \\ (D_1' W_u D_2)' \\ -(D_1' W_u)' \\ -W_e \end{bmatrix}' \begin{bmatrix} x \\ \lambda \\ y \\ \tilde{u} \\ r \end{bmatrix} \tag{3.72}$$

where the co-state, $\lambda(t)$, is obtained from

$$\lambda(t) = \Pi(t)x(t) - g(t) \tag{3.73}$$

where $\Pi(t)$ solves the differential Riccati equation

$$-\dot{\Pi} = \Pi\tilde{A} + \tilde{A}'\Pi + \Pi\tilde{B}\Pi + \tilde{C} \tag{3.74}$$

subject to the terminal condition

$$\Pi(T) = (I - C'PD_1\Delta B_1')^{-1}(C'PC + C'PD_1\Delta D_1' W_u C) \tag{3.75}$$

and $g(t)$ is determined from

$$-\dot{g} = (\tilde{A}' + \Pi\tilde{B})g + \begin{bmatrix} -(C'W_uD_1\Delta D_1'W_uD_2 + C'W_uD_2 + \Pi(B_2 + B_1\Delta D_1'W_uD_2))' \\ (C'W_uD_1\Delta D_1'W_u + C'W_u + \Pi B_1\Delta D_1'W_u)' \\ (C'W_uD_1\Delta W_e + \Pi B_1\Delta W_e)' \end{bmatrix}' \begin{bmatrix} y \\ \tilde{u} \\ r \end{bmatrix} \tag{3.76}$$

which is solved subject to the terminal conditions:

$$g(T) = -(I - C'PD_1\Delta B_1')^{-1} \begin{bmatrix} (C'PD_2 + C'PD_1\Delta D_1 W_u C)' \\ -(C'P + C'PD_1\Delta D_1 W_u)' \\ -(C'PD_1\Delta W_e)' \end{bmatrix}' \begin{bmatrix} y(T) \\ \tilde{u}(T) \\ r(T) \end{bmatrix} \quad (3.77)$$

where

$$\Delta := -(D_1' W_u D_1 + W_e)^{-1} \quad (3.78)$$

$$\tilde{A} = A + B_1\Delta D_1' W_u C \quad (3.79)$$

$$\tilde{B} = B_1\Delta B_1' \quad (3.80)$$

$$\tilde{C} = C'(W_u + W_u D_1\Delta D_1' W_u)C \quad (3.81)$$

Proof: The proof follows along similar lines as before. The state space description of the off-line controller is now,

$$\dot{x} = Ax + B_1\alpha + B_2 y \quad (3.82)$$

$$u = Cx + D_1\alpha + D_2 y \quad (3.83)$$

Appending this to the cost (3.69), and solving the first order necessary conditions yields the expressions given in the theorem.

◇◇

If the same assumptions as in the 1 D.O.F. case are made, the results can be extended to an infinite time support. Specifically:-

Theorem 3.5 *Consider Theorem 3.4, let $T \to \infty$ and assume y, r and $\tilde{u}$ are unknown but constant for all time. Then providing $(\tilde{A}, \tilde{B}, \sqrt{\tilde{C}})$ is stabilisable and detectable and $\Pi(T) \geq 0$, the signal $\alpha(t)$ ensuring optimal transfer between the two controllers, in the sense of the performance index (3.69) is given by*

$$\alpha = \Delta \begin{bmatrix} (D_1' W_u C + B_1'\Pi)' \\ (D_1' W_u D_2 - B_1' M\hat{Y})' \\ (-D_1' W_u + B_1' M\hat{U})' \\ (-W_e + B_1' M\hat{R})' \end{bmatrix}' \begin{bmatrix} x \\ y \\ \tilde{u} \\ r \end{bmatrix} \quad (3.84)$$

where

$$M := (\tilde{A}' + \Pi\tilde{B})^{-1} \tag{3.85}$$

$$\hat{Y} := (C'W_uD_1 + \Pi B_1)\Delta D_1'W_uD_2 + \Pi B_2 + C'W_uD_2 \tag{3.86}$$

$$\hat{U} := C'W_u + (C'W_uD_1 + \Pi B_1)\Delta D_1'W_u \tag{3.87}$$

$$\hat{R} := (C'W_uD_1 + \Pi B_1)\Delta W_e \tag{3.88}$$

and Π *is the positive semi-definite stabilising solution to the ARE (3.61). Furthermore, the off-line control loop is stable.*

Proof: The proof follows in the same manner as with the 1 D.O.F. case. In the infinite horizon, stability of the off-line loop is ensured as the solution to the Riccati equation converges to a constant, positive definite solution, provided that $(\tilde{A}, \tilde{B})$ and $(\tilde{A}, \sqrt{\tilde{C}})$ stabilisable and detectable repsectively, and that $\Pi(T) \geq 0$. This in turn ensures that M exists as $\mathbf{spec}(\tilde{A} + \tilde{B}\Pi) \in \mathcal{C}^-$.

$\Diamond\Diamond$

Note that the infinite horizon formula requires no prior knowledge of the external inputs to determine F, providing they are constant. As with the 1 D.O.F. case the formula simplifies significantly in the case that $D = 0$.

3.6 The Discrete Time Case

The discrete time versions of the formulae for bumpless transfer are similar to their continuous time counterparts, and are derived here for completeness.

3.6.1 Derivation for 1 D.O.F. Discrete-Time Case

The aim, as before, is to minimise the difference between the on and off-line control signals and also the difference between the signals driving the controllers: α, the signal produced by the 'subcontroller', and the control error. Hence, the corresponding discrete quadratic performance index to be minimised is:

$$J = \frac{1}{2}\sum_{0}^{T-1}[z_u(k)'W_uz_u(k) + z_e(k)'W_ez_e(k)] + \frac{1}{2}z_u(T)'Pz_u(T) \tag{3.89}$$

in which

$$z_u(k) = u_k - \tilde{u}_k \tag{3.90}$$

$$z_e(k) = \alpha_k - \tilde{e}_k \tag{3.91}$$

$$z_u(T) = u_T - \tilde{u}_T \tag{3.92}$$

Theorem 3.6 *Consider the configuration in Figure 3.1, where the discrete time off-line controller has minimal state-space realisation given in (3.1). Given that the switch takes place at time T, then the signal α_k, $\forall k \leq T$, which ensures optimal transfer between the two controllers, in the sense of performance index (3.89), is given by*

$$\alpha_k = \Delta \begin{bmatrix} (D'W_uC)' \\ B \\ -(D'W_u)' \\ -W_e \end{bmatrix}' \begin{bmatrix} x_k \\ \lambda_{k+1} \\ \tilde{u_k} \\ \tilde{e_k} \end{bmatrix} \tag{3.93}$$

where λ_{k+1} is obtained from

$$\lambda_{k+1} = \Pi_{k+1}x_{k+1} - g_{k+1} \tag{3.94}$$

Π_{k+1} is the solution to the discrete-time Riccati equation

$$\tilde{A}'(I - \Pi_{k+1}\tilde{B})^{-1}\Pi_{k+1}\tilde{A} - \Pi_k + \tilde{C} = 0 \tag{3.95}$$

and g_{k+1} is the solution to the difference equation

$$\begin{aligned} -g_k = & -\tilde{A}'(I - \Pi_{k+1}\tilde{B})^{-1}g_{k+1} - \\ & \begin{bmatrix} (C'W_u(I + D\Delta D'W_u) + \tilde{A}'(I - \Pi_{k+1}\tilde{B})^{-1}B\Delta D'W_u)' \\ (C'W_uD\Delta W_e + \tilde{A}'(I - \Pi_{k+1}\tilde{B})^{-1}B\Delta W_e)' \end{bmatrix}' \begin{bmatrix} \tilde{u}_k \\ \tilde{e}_k \end{bmatrix} \end{aligned} \tag{3.96}$$

which are solved subject to the boundary conditions

$$\Pi_T = (I - C'PD\Delta B')^{-1}(C'PC + C'PD\Delta D'W_uC) \tag{3.97}$$

$$g_T = (I - C'PD\Delta B')^{-1} \begin{bmatrix} -(C'PD\Delta D'W_u + C'P)' \\ -(C'PD\Delta W_e)' \end{bmatrix} \begin{bmatrix} \tilde{u}_T \\ \tilde{e}_T \end{bmatrix} \tag{3.98}$$

where

$$\Delta := -(D'W_uD + W_e)^{-1} \tag{3.99}$$

$$\tilde{A} := A + B\Delta D'W_uC \tag{3.100}$$

$$\tilde{B} := B\Delta B' \tag{3.101}$$

$$\tilde{C} := C'W_uC + C'W_uD\Delta D'W_uC \tag{3.102}$$

Proof: The off-line controller is described by the difference equations:

$$x_{k+1} = Ax_k + B\alpha_k \tag{3.103}$$

$$u_k = Cx_k + D\alpha_k \tag{3.104}$$

Substituting the control signal into (3.89), one can write

$$\begin{aligned} J = & \frac{1}{2}\sum_{0}^{T-1}[(Cx_k + D\alpha_k - \tilde{u}_k)'W_u(Cx_k + D\alpha_k - \tilde{u}_k) + (\alpha_k - \tilde{e}_k)W_e(\alpha_k - \tilde{e}_k)] \\ & + \frac{1}{2}z_u(T)'P(T)z_u(T) \end{aligned} \tag{3.105}$$

Applying a Lagrange multiplier, $\lambda_k \in \mathbb{R}^n$, to equation (3.105) and the discrete state equation gives the Hamiltonian as

$$\begin{aligned} H = \frac{1}{2}\{(Cx_k + D\alpha_k - \tilde{u}_k)'W_u(Cx_k + D\alpha_k - \tilde{u}_k) + (\alpha_k - \tilde{e}_k)'W_e(\alpha_k - \tilde{e}_k)\} \\ + \lambda'_{k+1}(Ax_k + B\alpha_k) \end{aligned} \tag{3.106}$$

Solving the (discrete) first order necessary conditions, and using the Method of Sweep (i.e. $\lambda_k = \Pi_k x_k - g_k$) the expression for α_k can be derived in a similar manner to the continuous time case.

$\Diamond\Diamond$

As with the continuous time case, note that the determination of F relies on the *a priori* knowledge of the on-line error and control sequences as the equations for g_k and Π_k develop backwards in time. In most situations this information is unavailable so the results have to be extended to the infinite horizon, providing the assumption of the external inputs being constant is made. Thus we have the discrete-time counterpart of the continuous time infinite horizon results.

Theorem 3.7 *Consider Theorem 3.6, let $T \to \infty$ and assume that $\tilde{e}$ and $\tilde{u}$ are unknown but constant. Then providing $(\tilde{A}, \tilde{B}, \sqrt{\tilde{C}})$ are stabilisable and detectable and $\Pi(T) \geq 0$, the signal α_k which ensures optimal transfer between the two controllers, in the sense of the performance index (3.89), is given by*

$$\alpha_k = F \begin{bmatrix} x_k \\ \tilde{u}_k \\ \tilde{e}_k \end{bmatrix} \tag{3.107}$$

$$F = (I - \Delta B'\Pi B)^{-1}\Delta \begin{bmatrix} (D'W_uC + B'\Pi A)' \\ -(D'W_u + B'(I-M)^{-1}\hat{U})' \\ -(W_e + B'(I-M)^{-1}\hat{E})' \end{bmatrix}' \tag{3.108}$$

where,

$$M := \tilde{A}'(I - \Pi\tilde{B})^{-1} \tag{3.109}$$

$$\hat{U} := M\Pi B\Delta D'W_u + C'W_u + C'W_uD\Delta D'W_u \tag{3.110}$$

$$\hat{E} := M\Pi B\Delta W_e + C'W_uD\Delta W_e \tag{3.111}$$

and Π is the stabilising solution to the Discrete-time algebraic Riccati Equation:

$$-\Pi + \tilde{A}'\Pi\tilde{A} - \tilde{A}'\Pi B(B'\Pi B + \Delta^{-1})^{-1}B'\Pi\tilde{A} + \tilde{C} \tag{3.112}$$

Furthermore, the off-line control loop is stable.

Proof: It is well known that, following Theorem 3.2, providing that $\tilde{A}$, $\tilde{B}$, and $\sqrt{\tilde{C}}$ are stabilisable and detectable, and that $\Pi(T) \geq 0$, then the solution of the Riccati equation converges to a constant value in the infinte horizon: a value identical to the solution of the discrete algebraic Riccati equation. Importantly, this solution is stabilising for the off-line control loop. Thus in the infinite horizon Π is the stabilising solution to the Discrete-time algebraic Riccati Equation:

$$\tilde{A}'(I - \Pi\tilde{B})^{-1}\Pi\tilde{A} - \Pi + \tilde{C} = 0 \tag{3.113}$$

which, using the Matrix Inversion Lemma, can be written as (3.112).

◇◇

It is important to realise that, as with the continuous time case, as the extension to the infinite horizon has been made, F is written in purely algebraic terms . Otherwise, F would be written in terms of difference equations and would require *a priori* knowledge of the reference signal to be able to be computed off-line. Once again, note that if $D = 0$, the expression for F reduces somewhat.

This section has given conditions under which Problem 3.1 is solved for the finite horizon case, and also for the infinite horizon case with constant exogenous signals.

3.6.2 Discrete-Time 2 D.O.F Bumpless Transfer

The discrete-time first-order necessary conditions are now applied to the discrete time 2 D.O.F. case. As in the continuous time case, the feedback matrix, F, has access to the off-line controller states, the on-line control signal, the reference input, and the plant output. Proceeding in exactly the same manner as before, the static feedback gain which will enable bumpless transfer is derived.

$$J = \frac{1}{2}\sum_{0}^{T-1}[(u_k - \tilde{u}_k)'W_u(u_k - \tilde{u}_k) + (\alpha_k - r_k)W_e(\alpha_k - r_k)] + \frac{1}{2}z_u(T)'Pz_u(T) \tag{3.114}$$

Theorem 3.8 *Consider the system in Figure 3.2, where the discrete-time off-line controller has minimal state-space realisation as given in (3.2). Given that the switch takes place at time T, the signal α_k, $\forall k \leq T$ which ensures optimal transfer between the two controllers in the sense of performance index (3.114), is given by*

$$\alpha_k = \Delta \begin{bmatrix} (D_2'W_uC)' \\ B_1 \\ (D_1'W_uD_2)' \\ -(D_1'W_u)' \\ -W_e \end{bmatrix}' \begin{bmatrix} x_k \\ \lambda_{k+1} \\ y_k \\ u_k \\ r_k \end{bmatrix} \tag{3.115}$$

The co-state, λ is obtained from:

$$\lambda_{k+1} = \Pi_{k+1}x_{k+1} - g_{k+1} \tag{3.116}$$

where Π_k and g_k are the solutions to:

$$\tilde{A}'(I - \Pi_{k+1}\tilde{B})^{-1}\Pi_{k+1}\tilde{A} - \Pi_k + \tilde{C} = 0 \tag{3.117}$$

$$-\tilde{A}'(I - \Pi_{k+1}\tilde{B})^{-1}g_{k+1} = -g_k + \begin{bmatrix} [C'W_uD_2 + C'W_uD_1\Delta D_1'W_uD_2 + \tilde{A}'(I - \Pi_{k+1}\tilde{B})^{-1}\Pi_{k+1}(B_2 + B_1\Delta D_1'W_uD_2)]' \\ -(C'W_u + C'W_uD_1\Delta D_1'W_u + \tilde{A}'(I - \Pi_{k+1}\tilde{B})^{-1}\Pi_{k+1}B_1\Delta D_1'W_u)' \\ -(C'W_uD_1\Delta W_e + \tilde{A}'(I - \Pi_{k+1}\tilde{B})^{-1}\Pi_{k+1}B_1\Delta W_e)' \end{bmatrix}' \begin{bmatrix} y_k \\ \tilde{u_k} \\ r_k \end{bmatrix} \tag{3.118}$$

The terminal conditions are:

$$\Pi_T = (I - C'PD_1\Delta B_1')^{-1}(C'PC + C'PD_1\Delta D_1W_uC) \tag{3.119}$$

$$g_T = (I - C'PD_1\Delta B_1')^{-1} \begin{bmatrix} (C'PD_2 + C'PD_1\Delta D_1'W_uD_2)' \\ -(C'P + C'PD_1\Delta D_1'W_u)' \\ -(C'PD_1\Delta W_e)' \end{bmatrix} \begin{bmatrix} y_T \\ \tilde{u}_T \\ r_T \end{bmatrix} \tag{3.120}$$

where

$$\Delta := -(D_1'W_uD_1 + W_e)^{-1} \tag{3.121}$$

$$\tilde{A} := A + B_1\Delta D_1'W_uC \tag{3.122}$$

$$\tilde{B} := B_1\Delta B_1' \tag{3.123}$$

$$\tilde{C} := C'W_uC + C'W_uD_1\Delta D_1'W_uC \tag{3.124}$$

Proof: The discrete 2 D.O.F. off-line controller has the following state-space representation:

$$x_{k+1} = Ax_k + B_1\alpha_k + B_2y_k \tag{3.125}$$

$$u_k = Cx_k + D_1\alpha_k + D_2y_k \tag{3.126}$$

Appending this to the cost function (3.114), solving the first order necessary conditions and using the Method of Sweep gives, similarly to the 1 D.O.F. case, the formulae in the theorem.

◇◇

Extension of this result to the infinite horizon gives the following theorem.

Theorem 3.9 *Consider Theorem 3.8 and let $T \to$ and assume that r, y and $\tilde{u}$ are unknown but constant. Then, providing $(\tilde{A}, \tilde{B}, \sqrt{\tilde{C}})$ is stabilisable and detectable and $\Pi(T) \geq 0$, the signal ensuring optimal transfer between the two controllers in the sense of performance index (3.114), is given by*

$$\alpha_k = F \begin{bmatrix} x_k \\ y_k \\ \tilde{u}_k \\ r_k \end{bmatrix} \tag{3.127}$$

where the constant matrix F is given by,

$$F = (I - \Delta B_1' \Pi B_1)^{-1} \Delta \begin{bmatrix} (D_1' W_u C + B_1' \Pi A)' \\ (D_1' W_u D_2 + B_1' \Pi B_2 + B_1'(I - M)^{-1} \hat{Y})' \\ -(D_1' W_u + B_1'(I - M)^{-1} \hat{U})' \\ -(W_e + B_1'(I - M)^{-1} \hat{R})' \end{bmatrix}' \tag{3.128}$$

where $\Pi \geq 0$ is the stabilising solution to the discrete time ARE:

$$\tilde{A}(I - \Pi \tilde{B})^{-1} \Pi \tilde{A} - \Pi + \tilde{C} = 0 \tag{3.129}$$

where

$$M := \tilde{A}'(I - \Pi \tilde{B})^{-1} \tag{3.130}$$

$$\hat{Y} := C' W_u D_2 + C' W_u D_1 \Delta D_1' W_u D_2 + M \Pi (B_2 + B_1 \Delta D_1' W_u D_2) \tag{3.131}$$

$$\hat{U} := C' W_u + C' W_u D_1 \Delta D_1' W_u + M \Pi B_1 \Delta D_1' W_u \tag{3.132}$$

$$\hat{R} := C' W_u D_1 \Delta W_e + M \Pi B \Delta D_1' W_u \tag{3.133}$$

Proof: The proof is similar to the proof of Theorem 3.7.

◇◇

As before, the expression for the subcontroller, F, simplifies somewhat if the direct feedthrough term is zero.

This section has provided a solution to Problem 3.1 in the finite horizon cases and also in the infinite horizon case, given constant exogenous signals, for the performance index (3.114)

3.7 An Extension to the Hanus Conditioning Scheme

Thus far formulae have been derived for a full-information static gain (in the infinite horizon case) which can be used to drive the off-line controller in such a way that when this controller is switched on-line, the transient effects are small. It is emphasized that no assumptions have been made concerning the properness of the conditioned controllers. Nor have any minimum-phase conditions been imposed, as the stability of the off-line control loop is guaranteed by the stabilising property of the solution to the algebraic Riccati equation.

It is interesting to note however, that if the following assumptions are made:

- The controllers are bi-proper i.e. a D-matrix exists and is square
- The controller is minimum phase
- W_e is zero

then the formulae derived here reduce to the Hanus Scheme. This follows from some basic matrix algebra, and the fact that the solutions to the respective Riccati equations are singular when these conditions are enforced.

For both continuous and discrete 1 D.O.F. configurations, the expression for F becomes:

$$F = [-D^{-1}C \;\; D^{-1} \;\; 0] \tag{3.134}$$

while in the 2 D.O.F. cases:

$$F = [-D_1^{-1}C \;\; -D_1^{-1}D_2 \;\; -D_1^{-1} \;\; 0] \tag{3.135}$$

These expressions are exactly the Hanus Conditioning Scheme for the respective cases. Note that Hanus requires the controllers to be minimum phase to ensure stability of the off-line control loop.

However, although the feedback portion of the schemes are identical, the implementation is different: the Hanus still maintains an advantage in this respect, as the controller is constantly driven by the error or reference signal, and thus no switching is required (see [31] and [10] for details).

3.8 Stability

In the infinite horizon all the various formulae for F ensure the stability of the off-line control loop (i.e. the loop consisting of the off-line controller and the 'subcontroller', F) by virtue

of the fact that the solution of the corresponding ARE is stabilising. In the finite horizon, stability is not an issue, and the solutions to the Riccati equations depend upon the terminal weights and boundary conditions.

The assumption that both on and off-line controllers are stabilising for the plant in question, around a certain operating point, guarantees stability of the closed loop system around this operating point, without switching occurring. However nothing can be concluded in general about the stability of the overall system when arbitrary switching occurs. Recent results based on passivity theory have appeared in [9], which guarantee stability for both anti-windup and bumpless transfer. That analysis stems from an earlier paper [10], where a unification of many existing schemes is developed. The results arguably lend themselves more conveniently to anti-windup schemes, than to bumpless transfer, however, and require assumptions to be made which are not satisfied by the LQ scheme proposed here.

If the number of switches which takes place is finite, then it can be concluded that after the final switch takes place, the state will remain bounded and hence stability will hold. More general switching is not as easy to handle, but some recent results of Hespanha and Morse [34] have claimed that, for given controller realisations, stability will result for arbitrary switching strategies, provided the controllers themeselves are stabilising.

It is also worth noting that most results concerning stability of anti-windup and bumpless transfer schemes pertain to the stability of linear systems with a single nonlinearity between the controller and plant. This is a realistic representation for anti-windup configurations, but in the case of bumpless transfer, the reason for switching between two controllers is usually due to the actual nonlinearity of the plant. Hence, it would be more desirable to prove stability of bumpless transfer schemes taking into account the nonlinear nature of the plant.

From a practical point of view, however, experience based on nonlinear simulations is that stability, as defined by any practical measure, is maintained providing both controllers are stabilising, and the off-line control loop is also stable. This is the case with the LQ scheme, and thus it is opined that a stable closed loop will result. Notwithstanding, no concrete conclusions may be drawn about stability, although the LQ method seems as likely to result in a stable system as most other methods.

3.9 Simulation Results

Simulation results which illustrate how the methods derived in this chapter fare in practice are now presented. The plant to be controlled is a helicopter model: the Westland Lynx, a nonlinear model of which was provided by GKN Westland. This models the nonlinear variations

that occur in the dynamics over the flight envelope. A high degree of inter-axis coupling and open loop instability make this a challenging control problem. A more complete description of this problem can be found in Chapter 5.

The controllers were designed using $\mathcal{H}^\infty$ 2 D.O.F. mixed sensitivity techniques (the high and low speed controllers were designed using 15-state linearisations taken at 70 and 30 m/s respectively), which are described in Chapter 2 in some detail.

The following outputs were chosen for control:

- Roll Attitude
- Pitch Attitude
- Yaw Rate
- Vertical Velocity

and, additionally the two rate outputs, were chosen to enhance the design:

- Roll Rate
- Pitch Rate

The control inputs to the helicopter were:

- Lateral Cyclic
- Longitudinal Cyclic
- Tail Rotor Collective
- Main Rotor Collective

The outputs were scaled by $3.3m/s$ (vertical velocity), 0.2 radians (pitch attitude), 0.2 radians (roll attitude), and 0.2 radians/second (yaw rate).

The situation where the helicopter is making the transition from low speed to high speed in forward flight is considered. First observe the effects of not switching between controllers, as shown in Figs 3.3 and 3.4. Both plots show a step demand in pitch attitude: the first using a low-speed controller and the second using a high speed controller. A step in pitch attitude will cause the helicopter's velocity to increase and hence it can be seen that the low speed controller's performance degrades considerably in the roll channel (Fig 3.3) as the helicopter attains high

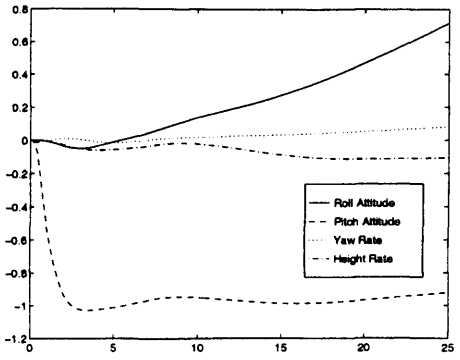

Figure 3.3: Helicopter Response to Step in Pitch Attitude using Low Speed Controller

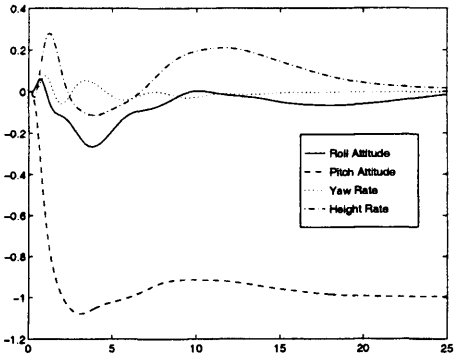

Figure 3.4: Helicopter Response due to Step in Pitch Attitude using High Speed Controller

velocities. Similarly, from Fig 3.4, it can be seen that using the high-speed controller at low air speeds causes significant coupling between channels and consequently a loss of performance.

To overcome the degradation of performance which occurs as the helicopter increases speed, a controller switching strategy is introduced. The inclusion of rate feedback to enhance performance and stability, led to a non-square controller, which, combined with the strict properness of the resulting $\mathcal{H}^\infty$ controllers, renders the Hanus technique inapplicable in this instance. However, the LQ scheme can cope with both strictly proper and non-square controllers.

The infinite horizon formulae are implemented as they require no prior knowledge of the external signals. There is some practical justification for this as the inputs to controllers of this type will often be steps and pulses, which can be appproximated as constant inputs over short periods. Hence the formulae of Theorem 3.4 were used, as the controllers were 2 D.O.F.

Initial tests have indicated that the scheme works well when it 'tends to' the Hanus Scheme. This implies that the control signals should be weighted heavily in comparison to the other signals. Therefore the weights were chosen as:

- $W_u = diag(10^3, 10^3, 10^3, 10^3)$
- $W_e = diag(0.1, 0.1, 0.1, 0.1, 0.1, 0.1)$

This reflects the diagonal nature of the plant which we attempted to preserve, as well as the relative importance of each channel during transfer. It is also possible to use non-diagonal, positive definite weighting matrices. This flexibility in the scheme could prove useful in practice, although more research is required on the selection of these matrices. These matrices were used in the continuous time 2 D.O.F. formulae derived earlier, and a static feedback gain, F was determined.

It was decided to switch from the high speed to the low speed controller at $40m/s$. For purposes of illustration, only the high speed controller was 'conditioned' off-line before it was switched in. When the low speed controller was switched off-line, it was left open-loop so the difference between the control signals could be clearly seen. It is noted that in practice, as soon as a controller is switched off-line it would be conditioned immediately, so that it could be switched on-line again rapidly.

Fig. 3.5 shows the responses of the helicopter using the LQ bumpless transfer scheme. First a step in pitch attitude is applied to increase the helicopter's speed; then a step in roll is instigated to change the vehicle's direction. A very smooth transition in the pitch and yaw channels results. In the height channel, a small 'bump' occurs at the time of switching which gradually decays; similarly in the roll channel there is a slight transient degradation. Neither of these effects were considered excessive.

From inspecting the actuator signals in Figure 3.5, it can be seen that the control signals produced by the two controllers are virtually identical until switching occurs. This is very close to what might be expected in the Hanus Scheme, and reinforces the idea that it is a special case of the LQ scheme presented here.

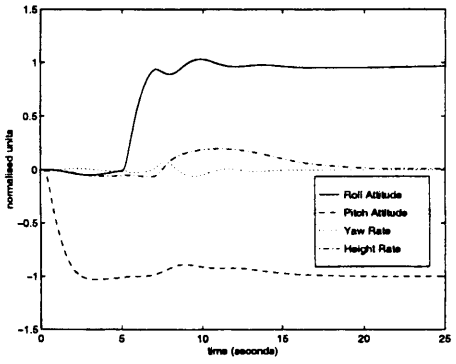

Response to Steps in Pitch and Roll

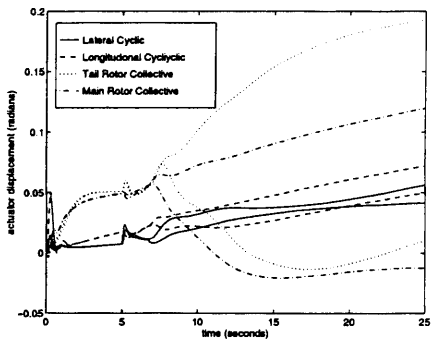

Actuator Reponses to Steps in Pitch and Roll

Figure 3.5: Helicopter Responses due to Steps in Pitch and Roll Attitude using LQ Bumpless Transfer Scheme

3.10 Merits and Deficiencies

It is now appropriate to point out the merits of the proposed design method, before going on to add some cautionary notes on its use. The comments here apply equally to continuous and discrete time cases in both 1DOF and 2DOF configurations.

This method is attractive from several points of view, particularly when compared to the popular Hanus Conditioning technique. Firstly it is able to be applied to *general* linear controller types, whereas the Hanus technique is not able to be directly applied [5] if the controller is not bi-proper and minimum-phase.

The LQ method does give the engineer scope to tailor the design accordingly, through use of two positive definite weighting matrices, which can shape the type of F matrix obtained. This could be useful in a practical situation. Furthermore, as F is simply a static gain it requires little extra on-line computation, as it does not increase the order of the overall control system.

It has also been shown that the formulae derived here can, under certain assumptions, simplify to those given by Hanus. This is both theoretically interesting, and practically encouraging, considering the success of the Hanus Scheme in industrial applications. In a certain sense this relationship makes the new results a generalisation of Hanus' technique; it also shows that, in a linear quadratic context, Hanus' results can constitute an optimal bumpless transfer strategy.

However, the method as it stands does have a possible deficiency which will now be discussed. Recall that the object of the minimisation is to ensure that the on and off line control signals are close to each other at the time of switching, in an attempt to minimise any detrimental transient behaviour. This is done under the secondary constraint that the signals driving the controllers must also be close to each other at the time of switching, although this constraint is often weighted lightly in the minimisation process.

In other words it is possible that even though F has been designed such that u and $\tilde{u}$ are similar at the time of transfer, α and either e or r will still be significantly different. This may not matter as generally both plant and controller will have some high frequency attenuation property meaning that the discontinuity at the controller input may not manifest itself malevolently at the plant output. However, if the controller has fast poles and direct feedthrough terms (a PI controller for example), this discrepancy between α and e or y could still result in unsatisfactory behaviour.

[5] Walagama *et al.*have proposed a coprime factorisation approach to circumvent some of these difficulties, but it depends heavily upon the choice of coprime factors, which is not unique; it is not clear how to choose a particular coprime factorisation.

3.11 Modified LQ Bumpless Transfer

This section introduces a slight modification of the scheme whose objective is to remedy the problem identified in the last section; namely that of a possibly large discontinuity at the controller input during switching. For this reason the configuration in Figure 3.6 is proposed. Note that this is for a 2DOF scheme, but by setting $B_1 = B, \quad B_2 = -B$ and $D_1 = D, \quad D_2 = -D$, the equivalent 1DOF scheme can be obtained.

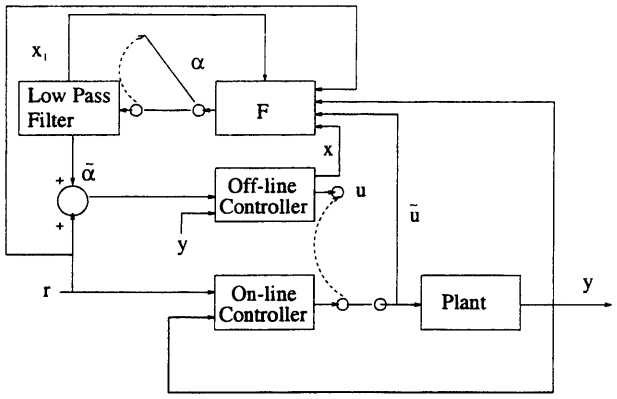

Figure 3.6: Modified Bumpless Transfer Scheme

The scheme is a slight modification of the previous one, except the off-line controller is driven by $\tilde{\alpha}$ and r simultaneously. Note that $\tilde{\alpha}$ is α, which is derived differently here, fed through a filter, $L(s)$. When the controller is switched on-line, the switch between F and $L(s)$ is opened, thus disconnecting $L(s)$ from α. However, as the controller is driven by $\tilde{\alpha}$, and as $L(s)$ is a continuous linear system, $\tilde{\alpha}$ will die away gradually, and thus the controller input will not be subject to a discontinuity.

Generally, $L(s)$ will be chosen as a unity gain low pass filter so that $\tilde{\alpha}$ is identical to α in every respect, except that its high frequency components will be removed. This will mean the same cost function can be used, and also no discontinuity will be present at the controller input.

We consider the modified problem for the continuous time (2DOF) case; analagous results for the discrete time case are deferred to the appendix due to their similarity.

The following minimal state-space realisation is assigned to the low-pass filter, $L(s)$

$$\dot{x}_l = A_l x_l + B_l \alpha \tag{3.136}$$

$$\tilde{\alpha} = C_l x_l \tag{3.137}$$

where $x_l \in \mathbb{R}^{n_l}$, $\tilde{\alpha} \in \mathbb{R}^{p_1}$ and the matrices' dimensions are implicitly given by those of the vectors.

Referring to Figure 3.6, when the controller is off-line its state-space equations are given by [6]

$$\dot{x} = Ax + B_1(r + \tilde{\alpha}) + B_2 y \tag{3.138}$$

$$u = Cx + D_1(r + \tilde{\alpha}) + D_2 y \tag{3.139}$$

These dynamics can then be combined with those of the low-pass filter to obtain

$$\dot{\tilde{x}} = \tilde{A}\tilde{x} + \tilde{B}_1 w + \tilde{B}_2 \alpha \tag{3.140}$$

$$u = \tilde{C}\tilde{x} + \tilde{D}_1 w \tag{3.141}$$

where

$$\tilde{A} = \begin{bmatrix} A & B_1 C_l \\ 0 & A_l \end{bmatrix} \quad \tilde{B}_1 = \begin{bmatrix} B_1 & B_2 \\ 0 & 0 \end{bmatrix} \quad \tilde{B}_2 = \begin{bmatrix} 0 \\ B_l \end{bmatrix}$$

$$\tilde{C} = [C \quad 0] \quad \tilde{x} = \begin{bmatrix} x \\ x_l \end{bmatrix} \quad w = \begin{bmatrix} r \\ y \end{bmatrix}$$

Observe that with the current configuration, the performance index must be chosen slightly differently: it is still desirable to minimise the difference, $u - \tilde{u}$, but as $\tilde{\alpha}$ now enters additively to r, we now simply want to minimise α (as $\tilde{\alpha}$ is just a low-pass filtered version of α, minimising α will make $\tilde{\alpha}$ small in some sense). Thus the modified performance index is

$$\frac{1}{2}\int_0^T z_u' W_u z_u + \alpha' W_e \alpha dt + \frac{1}{2} z_u(T)' P z_u(T) \tag{3.142}$$

where z_u, W_u and W_e are as previously defined. Making the appropriate substitutions this can be written as

$$\frac{1}{2}\int_0^T (\tilde{C}\tilde{x} + \tilde{D}_1 w - \tilde{u})' W_u (\tilde{C}\tilde{x} + \tilde{D}_1 w - \tilde{u}) + \alpha' W_e \alpha dt + \frac{1}{2} z_u(T)' P z_u(T) \tag{3.143}$$

Thus the *Hamiltonian* becomes

$$H = \frac{1}{2}\left\{(\tilde{C}\tilde{x} + \tilde{D}_1 w - \tilde{u})' W_u (\tilde{C}\tilde{x} + \tilde{D}_1 w - \tilde{u}) + \alpha' W_e\right\} + \lambda'(\tilde{A}\tilde{x} + \tilde{B}_1 w + \tilde{B}_2 \alpha) \tag{3.144}$$

[6] These equations are slightly more general than those considered in [80] where only a stricly proper controller is studied

Evaluating the first order necessary conditions for a minimum yields

$$\frac{\partial H}{\partial \lambda} = \tilde{A}\tilde{x} + \tilde{B}_1 w + \tilde{B}_2 \alpha \tag{3.145}$$

$$\frac{\partial H}{\partial \tilde{x}} = \tilde{C}' W_u \tilde{C}\tilde{x} + \tilde{A}' + \tilde{C}' W_u \tilde{D}_1 w - \tilde{C}' W_u \tilde{u} \tag{3.146}$$

$$\frac{\partial H}{\partial \alpha} = W_e \alpha + \tilde{B}_2' \lambda \tag{3.147}$$

These can be combined to obtain

$$\begin{bmatrix} \dot{\tilde{x}} \\ \dot{\lambda} \end{bmatrix} = \begin{bmatrix} \tilde{A} & -\tilde{R} \\ -\tilde{Q} & -\tilde{A}' \end{bmatrix} \begin{bmatrix} \tilde{x} \\ \lambda \end{bmatrix} + \begin{bmatrix} \tilde{B}_1 & 0 \\ -\tilde{C}' W_u \tilde{D}_1 & \tilde{C}' W_u \end{bmatrix} \begin{bmatrix} w \\ \tilde{u} \end{bmatrix} \tag{3.148}$$

where the following definitions have been made

$$\tilde{R} := \tilde{B}_2 W_e \tilde{B}_2' \tag{3.149}$$

$$\tilde{Q} := \tilde{C}' W_u \tilde{C} \tag{3.150}$$

Using the Method of Sweep (i.e. assume the linear relationship $\lambda = \Pi\tilde{x} - g$) as before and combining this with Equation (3.148) the formulae for α is obtained as

$$\alpha = -W_e^{-1} \tilde{B}_1 \lambda \tag{3.151}$$

where $\lambda := \Pi\tilde{x} - g$ is found from the differential equations

$$\dot{\Pi} + \Pi\tilde{A} + \tilde{A}'\Pi - \Pi\tilde{R}\Pi + \tilde{Q} = 0 \tag{3.152}$$

$$(\tilde{A} - \tilde{R}\Pi)' - (\tilde{C}' W_u \tilde{D} + \Pi\tilde{B}_1) w + \tilde{C}' W_u \tilde{u} = -\dot{g} \tag{3.153}$$

which are respectively solved from the terminal points

$$\Pi(T) = \tilde{C}' P \tilde{C} \tag{3.154}$$

$$-g(T) = \tilde{C}' P \tilde{D}_1 w(T) - \tilde{C}' P \tilde{u}(T) \tag{3.155}$$

3.11.1 Extension to the Infinite Horizon

As with the un-modified formulue, the finite horizon results require the signals $w(t)$ and $\tilde{u}(t)$ to be known beforehand to allow results to be computed. They also suffer from the same problems such as having a time-varying state-feedback and having optimality very much associated with horizon length. Therefore these finite horizon results are complemented by deriving infinite horizon results which are more useful from a practical point of view.

Note that (refer to Theorem 3.2) in order for the solution of the differential Riccati equation, (3.152), to converge to the positive semi-definite stablising solution of

$$\tilde{A}'\Pi + \Pi\tilde{A} - \Pi\tilde{R}\Pi + \tilde{Q} \tag{3.156}$$

we require $(\tilde{A}, \tilde{R}, \sqrt{\tilde{Q}})$ to be stabilisable and detectable. Note from the definitions of $\tilde{R}$ and $\tilde{Q}$ and strict positive definteness of W_u and W_e that, as it was assumed that our controller controllable and observable, then it follows that $(\tilde{A}, \tilde{R}, \sqrt{\tilde{Q}})$ is indeed stabilisable and detectable (in fact it is controllable and observable). Hence a positive semi-definite stablising solution to (3.156) always exists and furthermore it satifies

$$\lim_{T\to\infty} \Pi(t) = \Pi(\infty) = \Pi \geq 0 \tag{3.157}$$

Now consider the equation (3.153) and note that as this develops backwards in time and as $\tilde{A} - \tilde{R}\Pi$ is Hurwitz implies $-(\tilde{A} - \tilde{R}\Pi)$ is anti-Hurwitz, the LQ tracking technique of the previous section (see [2]) can again be applied. With the assumption that w and $\tilde{u}$ are constant then it follows that

$$\lim_{T\to\infty} g(t) = g = -(\tilde{A} - \tilde{R}\Pi)^{-T}\left[-(\Pi\tilde{B}_1 + \tilde{C}'W_u\tilde{B}_1)w + \tilde{C}'W_u\tilde{u}\right] \tag{3.158}$$

Inserting this into the expression for α gives

$$\alpha = F\begin{bmatrix} \tilde{x} \\ w \\ \tilde{u} \end{bmatrix} \tag{3.159}$$

where F is given by

$$F = \begin{bmatrix} \Pi \\ -(\tilde{A} - \tilde{R}\Pi)^{-T}(\Pi\tilde{B}_1 + \tilde{C}'W_u\tilde{D}_1) \\ (\tilde{A} - \tilde{R}\Pi)^{-T}\tilde{C}'W_u \end{bmatrix} \tag{3.160}$$

Note that the off-line control loop will be stable as $\Pi \geq 0$ is the stabilising solution to the ARE, (3.156); therefore it follows that the off-line 'A' matrix, $(\tilde{A} - \tilde{R}\Pi)$, is Hurwitz (which also ensures the existence of $(\tilde{A} - \tilde{R}\Pi)^{-1}$).

Other than stability of the two separate linear systems (the on and off-line closed loops) no guarantees about stability during switching are given. This is the same as was described in the previous section and the difficulties mentioned there apply here also. Like before, it is conjectured that stability will prevail providing the switching speed is of sufficiently low frequency; in a practical situation a hysteresis loop could be inserted to ensure that transfer from one controller to another does not occur often.

3.11.2 Examples

The example we consider here is much the same as in Section 3.9: the controllers are mulivariable $\mathcal{H}^\infty$ 2DOF controller designed for the Westland Mk7 Lynx helicopter. This time however we consider controllers which have been designed to deliver good performance around their operating point, but are not as robust to changes in flight condition. Their fast poles make the original method unsuitable, but is amenable to the second method.

Again the transition from low speed (5m/s) and high speed (70m/s) is considered. Figure 3.7 shows the aircraft's response to a pulse in pitch using just the 5m/s controller and just the 70m/s controller. In both cases it can be seen that unacceptable transient behaviour occurs.

Figure 3.8 shows the response to an identical pitch pulse using the modified LQ bumpless transfer scheme. The weighting matrices were chosen as $W_u = I_4 \times 1000$ and $W_e = I_6 \times 0.1$. The low pass filter was chosen as

$$L(s) = I_6 \times \frac{10}{s + 10} \tag{3.161}$$

Note how an almost undetectable transition between the controllers occur. From the actuator responses it can be observed that the off-line control signal gracefully, continuously deforms into the on-line one. It is interesting to note that, when simulated on the nonlinear model, if no bumpless transfer scheme were to be used, the extent of the transient occuring when the controllers are switched is enough to cause instability. This is evidently not the case when the modified LQ method is used.

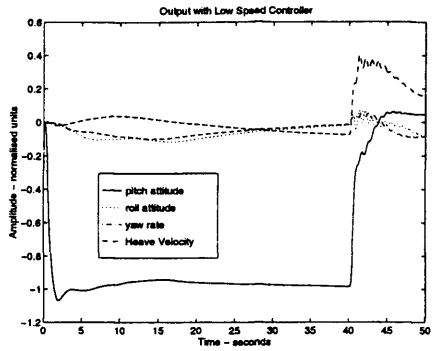

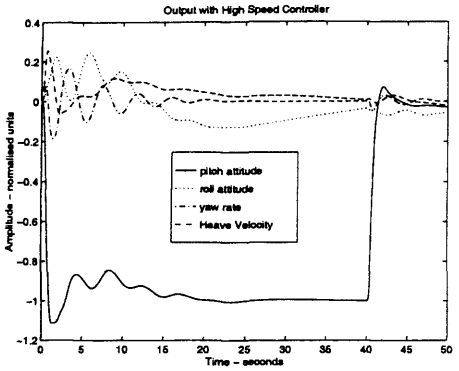

Response to Pulse in Pitch using 5m/s Controller Response to Pulse in Pitch using 70m/s Controller

Figure 3.7: Helicopter Responses due to Pulse in Pitch Attitude

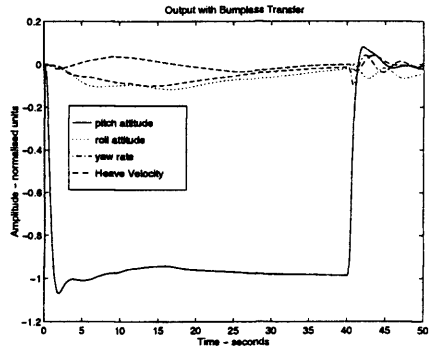

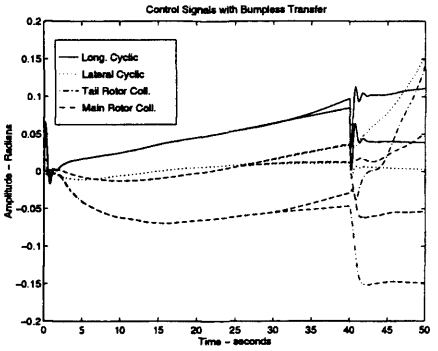

Response to Pulse in Pitch using modified LQ scheme Actuator Responses using modified LQ scheme

Figure 3.8: Helicopter Responses due to Pulse in Pitch Attitude

3.12 Conclusion

This chapter has discussed the use of LQ techniques in the bumpless transfer problem. Initially formulae were derived for a feedback element which attempts to force the off-line controller output to that of the on-line controller in the $\mathcal{L}_2$ sense. Acknowledging that these formulae are generally difficult to implement, infinite horizon versions were then derived. In this case the feedback element is simply a static, full-information feedback gain. These formulae are purely algebraic and computationally un-demanding as they only require the solution to a single Riccati equation. The formulae were demonstrated successfully on the Lynx helicopter example.

The modified version of the formulae retains most of the advantages of the un-modified version, except is slightly more expensive in terms of on-line computation, due to the low-pass filter inserted in each control output. Thus the number of extra states to be integrated increases, albeit only slightly providing low order filters are used and the system has few control inputs. However, this version also has the advantage that it seems to enable a slightly smoother transfer to occur, and may also be applied to problems where the first version would give poor results.

Both formulae are widely applicable due to the few assumptions they make on the controllers, and even those which are made are, in most practical cases, not unreasonable. This gives them an advantage over some of the bumpless transfer schemes in the literature (the famous example is the Hanus scheme, [31]).

Future work may concentrate on how the choice of weighting matrices influences the design, and if there are any guidelines for choosing them in an optimal fashion. The stipulation of controllability and observability may also be investigated. Due to the link often made between anti-windup and bumpless transfer, the possibility of using a similar technique to this for anti-windup compensation could be considered.

Chapter 4

Nonlinear Tracking for Constrained Input Linear Systems

4.1 Overview

As mentioned in chapter 1, the control of linear systems subject to input constraints is an important and frequently occuring control problem, although a simple, effective and general algorithm for its solution has, so far, been elusive. The anti-windup approach to tackling such problems is examined later in the thesis; this chapter discusses the alternative approach whereby account of the control limits is taken explicitly in the controller design.

This chapter makes a contribution to the expanding body of knowledge on this subject, and in particular substantially expands an existing methodology already available in the literature. Specifically, a certain type of low-and-high gain methodology (see later and Chapter 2 for a related discussion) is embellished to enable high order and multivariable systems to be considered.

Preliminary results given towards the end of the chapter seem to indicate that this is a promising approach towards control system design for constrained input linear systems.

This chapter is based on [78], which considers the general case. Also a shortened version which only considers the strictly proper case can be found in [79]. Briefly detailed in Appendix C, are some alternative formulae suggested by [28], which can be used in place of the matrices $H = [H_1' \; H_2']'$ and G, which are defined later.

4.2 Introduction

The *a priori* control of linear systems subject to input constraints has been fraught with many theoretical problems due to the mathematical difficulty in handling the saturation function. This has, by and large, manifested itself in two ways: resulting design methods are either too conservative, or too complicated. Hence the application of such methods to practical problems is very rare.

However in the last decade the low-and-high gain technique, which was discussed in Chapter 2, emerged as an effective tool for handling linear, constrained-input systems. As already discussed in Chapter 2, for the class of globally null-controllable systems, it allowed a saturated linear control law to be used which semi-globally stabilised the system under consideration. This was first discussed in [46], but later extended in [62] to include some robustness and performance criteria.

The basic idea behind the scheme was simple (although the proofs were generally non-trivial): first a linear low gain was designed which ensured that for a certain, *arbitrarily large*, set in the state-space, the control law did not saturate; then a high gain control law was added to achieve better performance, disturbance rejection and such like. These two control laws were then both saturated and semi-global stability was ensured. This was similar to an earlier scheme proposed by [29], which had the same idea but the stability guaranteed was only local.

In [44] a modification to the low-and-high gain methodology was proposed. Essentially this was to use a *nonlinear* high gain instead of a linear one with the aim of increasing performance. Furthermore, while only local stability was ensured, this relaxation also allowed open-loop unstable systems to be considered (open-loop unstable systems are not globally null controllable). Computer simulations demonstrated on an F-16 aircraft example indicated excellent results.

In fact the power of [44] results was only limited by their scope: only second order SISO systems were considered. The aim of this chapter will therefore be to extend these results to higher-order and multivariable systems. In other words a nonlinear composite control law which locally stabilises a, possibly MIMO, constrained input linear system of arbitrary order is sought. Guidelines will also be given for choosing this nonlinear parameter so that the transient response is improved.

4.3 Preliminaries

The notation and defintions are as given at the beginning of the thesis, although a few more are required specifically for this chapter. In particular, we take the *component-wise* magnitude of a vector x, to be denoted as $|x|$. Although not consistent with the remainder of the thesis, this reduces notational encumbrance somewhat.

Under consideration is the class of finite-dimensional linear time invariant systems subject to standard symmetric saturation constraints on the control:

$$\dot{x} = Ax + Bsat(u) \tag{4.1}$$

$$y = Cx + Dsat(u) \tag{4.2}$$

where $x \in \mathbb{R}^n$, $u \in \mathbb{R}^m$, $y \in \mathbb{R}^p$ and the pair (A, B), with B full column rank, is assumed to be fully controllable. The saturation function is the standard saturation function defined in Chapter 2. [1]

The control signal, u, is restricted to be a function of the state and the reference signal, $r \in \mathbb{R}^p$; that is

$$u = g(x, r, t) \tag{4.3}$$

Before proceeding further, it is assumed that the system has the following state-space realisation

$$\begin{bmatrix} \dot{x}_1 \\ \dot{x}_2 \end{bmatrix} = \begin{bmatrix} A_{11} & A_{12} \\ A_{21} & A_{22} \end{bmatrix} \begin{bmatrix} x_1 \\ x_2 \end{bmatrix} + \begin{bmatrix} 0 \\ \bar{B} \end{bmatrix} sat(u) \tag{4.4}$$

where $\bar{B} \in \mathbb{R}^{m \times m}$ is nonsingular and the other vectors and matrices are partitioned compatibly. For systems not already in this form, there exists an orthogonal transformation matrix $\bar{T}$, which can be computed [2] in commercially available software packages, and applied to yield the above form. Note also that, as (A, B) is controllable, (A_{11}, A_{12}) is also controllable, which implies A_{11} can be chosen nonsingular through a further state similarity transformation (if necessary).

4.4 Main Results

The main results are obtained in the following manner. First a linear state feedback is derived in some conventional manner, which respects the control limits. Then a constant feedforward gain is added to achieve asymptotic tracking of a constant (step) input. Following this, it is shown how a control law of the form

$$u = u_L + u_N \tag{4.5}$$

can be constructed so that the nonlinear part of the control law not only ensures stability of the system, but enhances the linear design. Section 4.5 discusses the selection of this nonlinear parameter. Note that the majority of this section consists of a multivariable generalisation of the results in [44].

[1] In the low-and-high gain control law design advocated in [62], the general saturation nonlinearity, $\sigma(.)$ - as defined in Chapter 2 - was used. These results do not hold for this general nonlinearity, although extensions in this direction are anticipated in the future

[2] A convenient routine for this is the one given in [16], for example, which takes advantage of the stable QR decomposition, which is discussed in [23]

4.4.1 Nominal Linear Design

This section introduces the method by which we transform the tracking problem posed into a regulator; a process which is intimately related to the state-space realisation imposed. It is shown how asymptotic tracking is achieved through the choice of a linear state feedback and input feed-forward defined by

$$u_L = Fx + Gr \tag{4.6}$$

First it is assumed that the state feedback gain, F, has been designed by some means so that the control constraints are not violated, and that the nominal closed-loop $A + BF$ is Hurwitz. In other words, it is assumed that F has been designed such that, for some x and r (to be quantified later), and some specific G (also to be defined later),

$$|u_L| = |Fx + Gr| \preceq \bar{u} \tag{4.7}$$

where $\preceq$ (.) denotes componentwise inequality and $\bar{u} = [\bar{u}_1 \quad \bar{u}_2 \quad \dots \quad \bar{u}_m]$ is the maximum magnitude, component-wise, of the control signal vector. The first result is now introduced.

Lemma 4.1 *Given the non-autonomous linear system*

$$\dot{x} = Ax + Bu_L \tag{4.8}$$

and the matrix $F \in \mathbb{R}^{m\times n}$ such that $A_c := A + BF$ is Hurwitz. Then for arbitrary $H_2 \in \mathbb{R}^{m\times p}$ selecting

$$H_1 := -A_{11}^{-1}A_{12}H_2 \tag{4.9}$$

$$G: = -\bar{B}^{-1}[(A_{21} + \bar{B}F_1)H_1 + (A_{22} + \bar{B}F_2)H_2] \tag{4.10}$$

and applying the control $u_L = Fx + Gr$ with r a constant, yields the autonomous system

$$\dot{\tilde{x}} = A_c\tilde{x} \tag{4.11}$$

under the state co-ordinate transformation

$$\tilde{x} = \begin{bmatrix} \tilde{x}_1 \\ \tilde{x}_2 \end{bmatrix} = \begin{bmatrix} x_1 \\ x_2 \end{bmatrix} - \begin{bmatrix} H_1 \\ H_2 \end{bmatrix} r \tag{4.12}$$

where $F := [F_1 \quad F_2]$ *and* $\tilde{H} := \begin{bmatrix} H_1 \\ H_2 \end{bmatrix}$ *are conformably partitioned with* x.

Proof: Using the standard form derived earlier, the closed loop system can be written as

$$\begin{bmatrix} \dot{x}_1 \\ \dot{x}_2 \end{bmatrix} = \begin{bmatrix} A_{11} & A_{12} \\ A_{21} + \bar{B}F_1 & A_{22} + \bar{B}F_2 \end{bmatrix} \begin{bmatrix} x_1 \\ x_2 \end{bmatrix} + \begin{bmatrix} 0 \\ \bar{B}G \end{bmatrix} r \tag{4.13}$$

Using the definition of $\tilde{x}$, and noting that, as r is constant, $\dot{\tilde{x}} = \dot{x}$, it follows that

$$\begin{bmatrix} \dot{\tilde{x}}_1 \\ \dot{\tilde{x}}_2 \end{bmatrix} = \begin{bmatrix} A_{11} & A_{12} \\ A_{21} + \bar{B}F_1 & A_{22} + \bar{B}F_2 \end{bmatrix} \left(\begin{bmatrix} \tilde{x}_1 \\ \tilde{x}_2 \end{bmatrix} + \begin{bmatrix} H_1 \\ H_2 \end{bmatrix} r \right) + \begin{bmatrix} 0 \\ \bar{B}G \end{bmatrix} r \tag{4.14}$$

Collecting the terms in r yields

$$\begin{bmatrix} \dot{\tilde{x}}_1 \\ \dot{\tilde{x}}_2 \end{bmatrix} = \begin{bmatrix} A_{11} & A_{12} \\ A_{21} + \bar{B}F_1 & A_{22} + \bar{B}F_2 \end{bmatrix} \begin{bmatrix} \tilde{x}_1 \\ \tilde{x}_2 \end{bmatrix} + \begin{bmatrix} A_{11}H_1 + A_{12}H_2 \\ \bar{B}G + (A_{21} + \bar{B}F_1)H_1 + (A_{22} + \bar{B}F_2)H_2 \end{bmatrix} r \tag{4.15}$$

In order for the system to be autonomous, the last term on the right hand side must be zero. Choosing H_1 and G as stipulated yields

$$A_{11}H_1 + A_{12}H_2 = -A_{11}A_{11}^{-1}A_{12}H_2 + A_{12}H_2 = 0 \tag{4.16}$$

$$\begin{aligned} \bar{B}G + (A_{21} + \bar{B}F_1)H_1 + (A_{22} + \bar{B}F_2)H_2 &= -\bar{B}\bar{B}^{-1}[(A_{21} + \bar{B}F_1)H_1 + (A_{22} + \bar{B}F)_2)H_2] + \\ &\quad (A_{21} + \bar{B}F_1)H_1 + (A_{22} + \bar{B}F_2)H_2 = 0 \end{aligned} \tag{4.17}$$

Inserting these into equation (4.15) gives

$$\begin{bmatrix} \dot{\tilde{x}}_1 \\ \dot{\tilde{x}}_2 \end{bmatrix} = \begin{bmatrix} A_{11} & A_{12} \\ A_{21} + \bar{B}F_1 & A_{22} + \bar{B}F_2 \end{bmatrix} \begin{bmatrix} \tilde{x}_1 \\ \tilde{x}_2 \end{bmatrix} \tag{4.18}$$

This proves the lemma.

◇◇

Another result is now introduced. This states the conditions under which asymptotic tracking may be achieved for the saturated system using the linear feedback, u_L (providing that r is a constant (step) input).

Lemma 4.2 *Consider the system (4.1)-(4.2) with the linear control, $u = u_L = Fx + Gr$ applied, where r is a constant, F has been designed such that $A_c = A + BF$ is Hurwitz, G is as given in (4.10) and H_1 is as defined in (4.9). Furthermore assume the matrix*

$$\tilde{C} := \{C_2 - C_1 A_{11}^{-1} A_{12} + D\bar{B}^{-1}(-A_{22} + A_{21}A_{11}^{-1}A_{12})\} \tag{4.19}$$

has full row rank and let $H_2 = \tilde{C}^R$, where $(.)^R$ denotes right inverse.

Given that $P > 0$ solves the Lyapunov equation

$$A_c'P + PA_c = -Q \tag{4.20}$$

for some $Q > 0$, and c is the largest positive real number such that

$$\tilde{x} \in \mathcal{E} \Longrightarrow |F\tilde{x}| \preceq (1 - \Delta)\bar{u} \tag{4.21}$$

where $\mathcal{E} = \{\tilde{x} : \tilde{x}'P\tilde{x} \leq c\}$ and $\tilde{x}$ is defined in (4.12). Then, $\forall \Delta \in [0, 1]$, the output $y(t)$ asymptotically tracks the input r if the following conditions are satisfied:

1. *The initial state satisfies*

$$(x_1(0) - H_1 r, x_2(0) - H_2 r) \in \mathcal{E} \tag{4.22}$$

2. *The reference, r, satisfies*

$$|\bar{B}^{-1}(A_{21}H_1 + A_{22}H_2)r| \preceq \Delta\bar{u} \tag{4.23}$$

Proof: First recall that as long as the control limits are not violated, the system remains linear and may be written in its autonomous form. To see that the above conditions guarantee that this is indeed the case, note that

$$\begin{aligned} u_L &= Fx + Gr && (4.24)\\ &= F\tilde{x} - \bar{B}^{-1}(A_{21}H_1 + A_{22}H_2)r && (4.25) \end{aligned}$$

So if, as stipulated by the lemma, $\tilde{x}(0) \in \mathcal{E}$, then $|F\tilde{x}| \preceq (1 - \Delta)\bar{u}$. As it is also required that $|\bar{B}^{-1}(A_{21}H_1 + A_{22}H_2)r| \preceq \Delta\bar{u}$, it is easy to see that $|u_L| \preceq \bar{u}$. Hence the system remains linear and can be written as

$$\dot{\tilde{x}} = A_c\tilde{x} \tag{4.26}$$

As $\mathcal{E}$ is positively invariant for the system (4.26), it is evident that $\forall\tilde{x}(0) \in \mathcal{E},\ \tilde{x}(t) \in \mathcal{E}\ \forall t \in \mathbb{R}_+$. Thus the system remains linear for all time.

Furthermore, as F was designed so that A_c is Hurwitz this implies that, $\lim_{t\to\infty}\tilde{x}(t) = 0$; which in turn implies that $\lim_{t\to\infty} x(t) = \begin{bmatrix} H_1 \\ H_2 \end{bmatrix} r$, and

$$\begin{aligned} \lim_{t\to\infty} y(t) &= \lim_{t\to\infty}\{C_1x_1(t) + C_2x_2(t) + Dsat(u(t))\} && (4.27)\\ &= [(C_1 + DF_1)H_1 + (C_2 + DF_2)H_2 + DG]r && (4.28)\\ &= \tilde{C}H_2r = r && (4.29) \end{aligned}$$

where the last equality follows from the assumption that H_2 is chosen as defined by as $\tilde{C}^R$ (and it exists). Thus the output vector asymptotically tracks the input vector, and the lemma is proven.

$\Diamond\Diamond$

For all of the outputs to track all of the inputs the right inverse is necessary in this formulation, but may be restrictive for some systems. This condition requires $\tilde{C}$ to have full row rank, which implies that the matrix must be square or flat. This means that the number of controls must satisfy $p \leq m$, which is in keeping with the fact that a system cannot be expected to track a greater number of demands than there are inputs.

Note in the above lemma that the maximum c such that $\tilde{x} \in \mathcal{E} \Longrightarrow |F\tilde{x}| \preceq (1-\Delta)\bar{u}$ can be treated as a quadratic programming problem, which can be solved by packages such as the MATLAB Optimisation ToolBox. In fact, this can be calculated explicitly, as proved for example in [33], where the maximum c is given as

$$c = \min_i \frac{\bar{u}_i^2}{F_iP^{-1}F_i'} \tag{4.30}$$

where F_i is the i'th row of the matrix F.

Note that the domain of guaranteed stability, $\mathcal{E}$, may be a poor approximation of the system's actual domain of attraction. Less conservative estimates of the maximum invariant set exist and take the form of polyhedral sets - see [6] for a detailed survey of set invariance.

4.4.2 Nonlinear Augmentation

The next part of the strategy is as in [44] whereby the linear feedback is augmented with a nonlinear term

$$u = u_L + u_N \tag{4.31}$$

The nonlinear term is given by

$$u_N = -R(x,r)B'P(x - \tilde{H}r) \tag{4.32}$$

where $\tilde{H} := \begin{bmatrix} H_1 \\ H_2 \end{bmatrix}$. The main result of the section is now stated, which gives conditions under which the output can asymptotically track the input vector. This amounts to a multivariable generalisation of Theorem 2.1 in [44].

Theorem 4.1 *Consider the saturated linear system (4.1) - (4.2), with the control law (4.31) applied, where F is such that $A + BF$ is Hurwitz and $P > 0$ solves the Lyapunov equation (4.20). Define $R(x,r) \in \mathbb{R}^{m\times m}$ as*

$$R(x,r) = diag(\rho_1(x,r), \rho_2(x,r), \ldots, \rho_m(x,r)) \tag{4.33}$$

and let H_1, G be defined by equations (4.10) and (4.9). Also let $H_2 = \tilde{C}^R$.

Then for any non-negative functions $\rho_i(x,r)$ which are locally Lipschitz in x and such that $R(x,r)$ is uniformly bounded, the output vector $y(t)$ will asymptotically track a step in the input vector r for any initial state and input vector satisfying conditions 1 and 2 of lemma 4.2.

Proof: The proof of the theorem is quite long; the reason being, for the most part, fairly tedious algebra. To start the now-familiar state transformation is made

$$\tilde{x} = x - \tilde{H}r \Leftrightarrow x = \tilde{x} + \tilde{H}r \tag{4.34}$$

where $\tilde{H}$ is as defined above. Thus in the $\tilde{x}$ co-ordinates, the closed loop system may be written as

$$\dot{\tilde{x}} = A_c\tilde{x} + A\tilde{H}r - BF\tilde{x} + Bsat(u) \tag{4.35}$$

and, after simplification, u is given by

$$\begin{aligned} u &= -R(x,r)B'P\tilde{x} + F\tilde{x} + (G + F\tilde{H})r && (4.36)\\ &= -R(x,r)B'P\tilde{x} + F\tilde{x} - \bar{B}^{-1}(A_{21}H_1 + A_{22}H_2)r && (4.37)\\ &= -R(x,r)B'P\tilde{x} + F\tilde{x} - Jr && (4.38) \end{aligned}$$

where the aforementioned definition of G has been used to simplify the expression and J has been defined as $J := \bar{B}^{-1}(A_{21}H_1 + A_{22}H_2)$. Thus in closed-loop

$$\dot{\tilde{x}} = A_c\tilde{x} + A\tilde{H}r - BF\tilde{x} + Bsat\left(-R(x,r)B'P\tilde{x} + F\tilde{x} - Jr\right) \quad (4.39)$$

Re-arranging and simplifying $A\tilde{H}$, this becomes

$$\dot{\tilde{x}} = A_c\tilde{x} + B\left(sat(-R(x,r)B'P\tilde{x} + F\tilde{x} - Jr) - F\tilde{x} + Jr\right) \quad (4.40)$$

Now, the theorem requires that conditions 1 and 2 of Lemma 4.2 be satisfied. These conditions ensure that $u_L \preceq \bar{u}\ \forall(\tilde{x}(0), r) \in \mathcal{E} \times \mathcal{V}_r$, where

$$\mathcal{V}_r := \left\{r : |\bar{B}^{-1}(A_{21}H_1 + A_{22}H_2)r| \preceq \Delta\bar{u}\right\} \quad (4.41)$$

It must now be proven that $\mathcal{E}$ remains positively invariant when the composite control is applied. Choosing $v(\tilde{x}) = \tilde{x}'P\tilde{x} > 0$ as a Lyapunov function, and differentiating this along the trajectories of the closed-loop system yields

$$\dot{v}(\tilde{x}) = \tilde{x}'(A_c'P + PA_c)\tilde{x} + 2\tilde{x}'PB\left(sat(-R(x,r)B'P\tilde{x} + F\tilde{x} - Jr) - F\tilde{x} + Jr\right) \quad (4.42)$$

For stability it is desirable that $\dot{v}(\tilde{x}) < 0$ and as A_c is Hurwitz, this is guaranteed if the second term on the right-hand side is negative semi-definite. First consider the case where

$$|-R(x,r)B'P\tilde{x} + F\tilde{x} - Jr| \preceq \bar{u} \quad (4.43)$$

i.e. the system is unsaturated and remains linear. Then the following is obtained

$$\dot{v}(\tilde{x}) = \tilde{x}(A_c'P + PA_c)\tilde{x} - 2\tilde{x}'PBR(x,r)B'P\tilde{x} < 0 \quad (4.44)$$

Thus stability is ensured, as one would expect. Next consider the case where all of the controls are saturated; hence

$$|-R(x,r)B'P\tilde{x}+F\tilde{x}-Jr| \succeq \bar{u} \tag{4.45}$$

Since, $\forall(\tilde{x},r) \in \mathcal{E} \times \mathcal{V}_r, \quad Fx+Gr = F\tilde{x}-Jr \preceq \bar{u}$ by construction, then

$$sat(-R(x,r)B'P\tilde{x}+F\tilde{x}-Jr)-F\tilde{x}+Jr \succeq 0 \tag{4.46}$$

Also, as $Fx+Gr = F\tilde{x}-Jr \preceq \bar{u}, \quad \forall(\tilde{x},r) \in \mathcal{E} \times \mathcal{V}_r$, then for (4.45) to hold

$$-R(x,r)B'P\tilde{x} \succeq 0 \tag{4.47}$$

As $R(x,r) = diag\{\rho_1(x,r),\rho_2(x,r),\ldots\} \geq 0$, then this implies that $B'P\tilde{x} \preceq 0$, which in turn implies that $\tilde{x}'BP(\bar{u}-F\tilde{x}+Jr) \leq 0$; thus $\dot{v}(\tilde{x}) < 0$, and stablity is ensured and, moreover $\mathcal{E}$ is positively invariant (i.e. for any $\tilde{x}(0) \in \mathcal{E}$, $\tilde{x}(t)$ will remain in that set for all time thereafter). In a similar manner, it can be shown that stability and positive invariance is ensured when:

$$|-R(x,r)B'P\tilde{x}+F\tilde{x}-Jr| \preceq -\bar{u} \tag{4.48}$$

Thus far the proof has followed Lin's proof ([44]). Due to the multivariable nature of the problem however, cases which do not arise in SISO systems must now be considered. In the most general case it is possible that some controls do not saturate, others saturate at their upper limits, and others at their lower limits. In this case, it is convenient to define the sets

$$\mathcal{M} = \{i : |u_i| \leq \bar{u}_i\} \tag{4.49}$$

$$\mathcal{N} = \{i : u_i > \bar{u}_i\} \tag{4.50}$$

$$\mathcal{P} = \{i : u_i < -\bar{u}_i\} \tag{4.51}$$

where $i \in \{1,2,\ldots,m\}$. Note that one can write

$$\tilde{x}'BP(sat(u)-F\tilde{x}+Jr) = \sum_{i=1}^{m}(\tilde{x}'BP)_i(sat(u)-F\tilde{x}+Jr)_i \tag{4.52}$$

$$= \sum_{i\in\mathcal{M}}(\tilde{x}'BP)_i(sat(u)-F\tilde{x}+Jr)_i + \sum_{i\in\mathcal{N}}(\tilde{x}'BP)_i(sat(u)-F\tilde{x}+Jr)_i + \sum_{i\in\mathcal{P}}(\tilde{x}'BP)_i(sat(u)-F\tilde{x}+Jr)_i \tag{4.53}$$

Now from the previous part of the proof it is known that for $i \in \mathcal{N}$

$$sat(-R(x,r)B'P\tilde{x} + F\tilde{x} - Jr)_i - (F\tilde{x} - Jr)_i \geq 0 \tag{4.54}$$

or equivalently

$$sat(-R(x,r)B'P\tilde{x} + F\tilde{x} - Jr)_i - (F\tilde{x} - Jr)_i = \alpha_i \tag{4.55}$$

Similarly, for $i \in \mathcal{P}$, one has

$$sat(-R(x,r)B'P\tilde{x} + F\tilde{x} - Jr)_i - (F\tilde{x} - Jr)_i \leq 0 \tag{4.56}$$

or equivalently

$$sat(-R(x,r)B'P\tilde{x} + F\tilde{x} - Jr)_i - (F\tilde{x} - Jr)_i = -\alpha_i \tag{4.57}$$

where the α_i's are some positive constants. Borrowing more results from the previous part of the proof it is also known that, for some positive real numbers, β_i

$$(B'P\tilde{x})_i = -\beta_i \qquad \forall i \in \mathcal{N} \tag{4.58}$$

$$(B'P\tilde{x})_i = \beta_i \qquad \forall i \in \mathcal{P} \tag{4.59}$$

Hence, for $i \in \mathcal{N}$ it follows that

$$(\tilde{x}'PB)_i \left(sat(u) - F\tilde{x} + Jr\right)_i = -\sum_{i \in \mathcal{N}} \alpha_i \beta_i \leq 0 \tag{4.60}$$

and similarly for all $i \in \mathcal{P}$ it follows that

$$(\tilde{x}'PB)_i \left(sat(u) - F\tilde{x} + Jr\right)_i = -\sum_{i \in \mathcal{P}} \alpha_i \beta_i \leq 0 \tag{4.61}$$

Furthermore, for all $i \in \mathcal{M}$ we have

$$sat(u_i) - (F\tilde{x} - Jr)_i = (-R(x,r)B'P\tilde{x})_i \tag{4.62}$$

$$= -\rho_i(x,r)(B'P\tilde{x})_i \tag{4.63}$$

Thus in this case ($i \in \mathcal{M}$) it follows that ($\forall(\tilde{x}, r) \in \mathcal{E} \times \mathcal{V}_r$)

$$(\tilde{x}'PB)_i \left(sat(u) - F\tilde{x} + Jr\right)_i = -(\tilde{x}'PB)_i \rho_i(x,r)(\tilde{x}'PB)_i' \leq 0 \tag{4.64}$$

Then for every control signal, or $\forall i \in \{1, 2, \ldots, m\} = \mathcal{M} \cup \mathcal{N} \cup \mathcal{P}$ the following holds

$$\begin{aligned}
\tilde{x}'PB\left(sat(u) - F\tilde{x} + Jr\right) &= \sum_{i=1}^{m} (\tilde{x}'PB)_i \left(sat(u) - F\tilde{x} + Jr\right)_i && (4.65)\\
&= \sum_{i \in \mathcal{M}} (\tilde{x}'PB)_i \left(sat(u) - F\tilde{x} + Jr\right)_i \\
&\quad + \sum_{i \in \mathcal{N}} (\tilde{x}'PB)_i \left(sat(u) - F\tilde{x} + Jr\right)_i \\
&\quad + \sum_{i \in \mathcal{P}} (\tilde{x}'PB)_i \left(sat(u) - F\tilde{x} + Jr\right)_i && (4.66)\\
&= -\sum_{i \in \mathcal{M}} (\tilde{x}'PB)_i \rho_i(x,r)(\tilde{x}'PB)_i' - \sum_{i \in \mathcal{N} \cup \mathcal{P}} \alpha_i \beta_i && (4.67)\\
&\leq 0 && (4.68)
\end{aligned}$$

Thus $\dot{v}(\tilde{x}) < 0, \quad \forall(\tilde{x}, r) \in \mathcal{E} \times \mathcal{V}_r$ and stability and positive invariance are again ensured provided the conditions of the theorem are satisfied. It has been shown that as long as the conditions of the theorem are satisfied the regulator is stable for any non-negative $R(x,r)$ of the form stated in the theorem. To see that the output vector will asymptotically track the input observe that stability implies that $\lim_{t\to\infty} \tilde{x}(t) = 0$; it then follows that $\lim_{t\to\infty} u_N = 0$, noting that $R(x,r)$ is uniformly bounded. Asymptotically the output then becomes

$$\begin{aligned}
\lim_{t\to\infty} y(t) &= \lim_{t\to\infty} (Cx(t) + Dsat(u(t))) && (4.69)\\
&= C\tilde{H}r + D \lim_{t\to\infty} sat(u(t)) && (4.70)\\
&= C\tilde{H}r + D \lim_{t\to\infty} sat(u_L + u_N) && (4.71)\\
&= C\tilde{H}r + D \lim_{t\to\infty} u_L(t) && (4.72)
\end{aligned}$$

Thus asymptotic tracking follows as in the purely linear case.

$\Diamond\Diamond$

Note that the uniform boundedness assumption, is not required if either $D = 0$ or if only stability and not asymptotic tracking is required. In fact, for the local case, it is not required at all as it has been assumed that $R(x,r)$ is locally Lipschitz over the compact set $\mathcal{E}$; hence $R(x,r)$ is certainly bounded over that set.

In fact, it is the global case which motivated the uniform boundedness assumption. In this case we have the following result.

Theorem 4.2 *Consider the system (4.1)-(4.2) and assume A is Hurwtiz. Then*

1. *There does not exist a control such that $\lim_{t\to\infty} y(t) = r$ for all non-zero r.*
2. *When $r = 0$ (i.e. the regulator case)*
   (a) *The only linear control ensuring no saturation globally is $u_L = 0$.*
   (b) *A control law achieving global asymptotic regulation is given by*

$$u = u_N = -R(x)B'P(x - Hr) \tag{4.73}$$

where $R(x) := diag\{\rho_1(x), \ldots, \rho_m(x)\}$ is non-negative definite and globally Lipschitz in x, and $P > 0$ satisfies the Lyapunov equation

$$A'P + PA = -Q, \quad Q > 0 \tag{4.74}$$

Proof:

1. It is well known that, for a bounded input linear system, for tracking to be achieved for all $x(0) \in \mathbb{R}^n$ and any reference, the system must be globally reachable (see, for example, chapter 3 of [60] and references therein). Such a system is only globally reachable if its time-reversed counterpart is globally controllable, which requires A to be anti-Hurwitz. Thus, as it is stipulated that A is Hurwtiz, it is obvious that global asymptotic tracking can not be achieved for any reference, r.

2. To prove the first part, note that by linearity of $u = Fx$, it is evident that a set of the form

$$\Omega = \{x : |Fx| \preceq \bar{u}\} \tag{4.75}$$

is bounded in some directions, for all non-zero F. However when $F = 0$ it is obvious that $\Omega = \mathbb{R}^n$.

To prove the second part, note that our system under the given control is

$$\dot{x} = Ax + Bsat(u_N) \tag{4.76}$$

Choosing $v(x) = x'Px$ as a Lyapunov function and differentiating it along the trajectories of the above system yields

$$\dot{v}(x) = -x'Qx + 2x'PBsat(-R(x)B'Px) \tag{4.77}$$

$$= -x'Qx + 2\sum_{i=1}^{m}(x'PB)_i sat_i(-R(x)B'Px) \tag{4.78}$$

In a similar way to the proof of Theorem 4.1 it can be shown that $\dot{v}(x) < 0, \quad \forall x \in \mathbb{R}^n$. Thus global stability of the origin is ensured.

$\Diamond\Diamond$

This theorem is similar to the result of [46], except this reference considers the semi-global case and here there is extra freedom in choosing u_N nonlinear instead of a "high" linear gain.

4.5 Selection of the Nonlinear Parameter

The last section showed that for any nonnegative function $R(x, r)$ defined previously, the system with the control $u = u_L + u_N$ would cause the output vector to asymptotically track the step input demand r. It is, of course, desirable to choose $R(x, r)$ in such a way that transient performance is improved by the choice of this parameter.

In [44], it was shown how to choose $R(x, r)$ for a second order SISO system, such that the damping ratio tended, asymptotically, to infinity. This allowed, by choice of $R(x, r) = e^{-k|y-r|}$, the transient performance to be improved dramatically: a faster rise time, with less overshoot than the purely linear feedback was obtained in the flight control example given in the paper. For high order and multivariable systems, it is difficult to obtain such a fundamental relationship between $R(x, r)$ and the closed-loop behaviour of the resultant system. However, possible choices of $R(x, r)$ and the motivation behind them are discussed.

4.5.1 High Order SISO Systems

Here, although it is difficult to choose $R(x, r)$ such that it has an analytical relationship to basic properties of the closed-loop system's behaviour, it is believed there are guidelines and rules of thumb which allow an appropriate nonlinear parameter to be chosen; it is recognised that iterative simulation is likely nevertheless.

In fact it is thought that functions similar to the one originally proposed by [44] should, by appropriate tuning, be able to work for higher order systems. Specifically,

$$R(x,r) = c_1 e^{-k_1|y_1 - r_1|} \tag{4.79}$$

is anticipated to give similar results to Lin *et al's*, as the large initial 'burst' of control activity, will, as time passes, decay; resulting in a fast initial response which rapidly settles down as the error is decreased, meaning little overshoot. This guideline has been adequate for the examples tested (see later in this paper), but it is emphasised that it is not guaranteed to work for every system.

4.5.2 Multivariable (MIMO) systems

The difficulty in choosing $R(x,r)$ in MIMO systems is increased by the fact that the direction of the control input to a system is of paramount importance. Disregard for this fact can lead to choices of $R(x,r)$ which completely destroy the decoupling and performance of the linear system; that is $R(x,r)$ can degrade rather than improve the transient behaviour. In actual fact, as u_N enters directly into the system, it is generally difficult to choose $R(x,r)$ such that performance does not deteriorate - even without saturation present - as u_L and u_N are not guaranteed to have similar directions in the control space, $\mathbb{R}^m$.

However if the original state-feedback is synthesised by specific means which can be related conveniently to the direction of u_N, it may be possible to choose $R(x,r)$ such that the decoupling of the multivariable system is preserved or improved [3]. A proposal along these lines is given below. Note that even if u_L and u_N have similar directions, when saturation occurs the actual input directionality may change, and coupling may degrade. It is hoped that the effect of this will not be observed so readily if $R(x,r)$ is chosen correctly.

In the case that the c_i's are chosen correctly (i.e. such that the linear and nonlinear control have similar directions) it is then anticipated that an $R(x,r)$ of the form given below will give similar performance, channel-by-channel, to that advocated in [44].

$$R(x,r) = diag(c_1 e^{-k_1|y_1 - r_1|}, c_2 e^{-k_2|y_2 - r_2|}, \ldots, c_m e^{-k_m|y_m - r_m|}) \tag{4.80}$$

This choice of $R(x,r)$ can be thought of as a 'multivariable' version of the Lin's choice of the nonlinear parameter.

[3] As decoupling of a MIMO system is closely associated with the control gain, the system with only u_L may exhibit poor decoupling due to the requirement that $|u_L| \preceq \bar{u}$

4.5.3 Riccati based synthesis

A Riccati Based Synthesis of the Linear Feedback when $D = 0$

Here it is shown how the feedback matrix F can be synthesised such that $u_{fb} = Fx$ and u_N have similar directions. We assume here that $D = 0$, but the following section discusses an approach when $D \neq 0$. Note that other similar techniques could be used instead of this specific version.

First assume that the reference, r, is zero and the functional to be minimised is

$$\frac{1}{2}\int_0^\infty x'C'QCx + u'Eu \quad dt \tag{4.81}$$

where $Q > 0$ and $E := diag(\epsilon_1, \epsilon_2, \ldots, \epsilon_m)$ is positive definite with ϵ_i positive real constants, and C is assumed full rank [4] with (C, A) observable. It is well known that the control which minimises this functional and provides internal stability is given by $u = -E^{-1}B'\Pi x$, where $\Pi > 0$ solves the algebraic Riccati equation (ARE)

$$A'\Pi + \Pi A - \Pi BEB'\Pi + C'QC = 0 \tag{4.82}$$

Choose $u_{fb} = Fx = -E^{-1}B'\Pi x$ (which implies that $u_{fb} = F\tilde{x} = -E^{-1}B'\Pi\tilde{x}$, as $r = 0$ for the time being) and note that each component of the control is given by

$$u_{fb,i} = -\epsilon_i^{-1}(B'\Pi x)_i \tag{4.83}$$

In this case, it is easy to establish that with the nonlinear control u_N added to the feedback, the total control $u = u_L + u_N$ given, in the $\tilde{x}$ co-ordinates, by

$$u = -(R(x,r) + E^{-1})B'\Pi\tilde{x} + (-E^{-1}B'\Pi\tilde{H} + G)r \tag{4.84}$$

Now, if $R(x,r)$ is chosen such that it can be expressed, for each fixed x and r $R(x,r) = \alpha E$ (this requires, in other words the same weighting used on the individual ϵ_i's to be given to the ρ_i's). Thus it is obvious that the state feedback term, including the nonlinear parameter, will have the same direction as the linear state feedback, although with a different (greater) magnitude.

Of course this does not guarantee that the control law u will have the same direction as u_L, as there is also a feed-forward part to consider. Recall, however, that $R(x,r)$ is only present

[4] This will enable positive definite solutions to be obtained rather than positive semi-definite ones

to improve transient performance and will be small in the steady state. Providing it decays fast it is hoped that transient directionality changes caused by the nonlinear parameter will not be too great. Also, recall that the term $(-E^{-1}B'\Pi\tilde{H} + G)$ is chosen to ensure asymptotic tracking; the choice of nonlinear feedback does not affect the role of this if its direction in the steady state is the same as the linear feedback.

It now has to be shown that the choice $v(\tilde{x}) := \tilde{x}'P\tilde{x} = \tilde{x}'\Pi\tilde{x}$ is a legitimate choice for a Lyapunov function for the system: from the ARE (4.82) it follows that the expression

$$A_c'\Pi + \Pi A_c = -\Pi BEB'\Pi - C'QC \tag{4.85}$$

is only negative semi-definite, and thus using the procedures of Section 4 (which assume the term on the right hand side is definite) does not guarantee asymptotic stability of the origin $\tilde{x} = 0$. Setting $\Pi = P$, from Section 4, equation (4.42) it follows that

$$\begin{aligned}
\dot{v}(\tilde{x}) &= \tilde{x}'(A_c'P + PA_c)\tilde{x} + 2\tilde{x}'PB\left(sat(-R(x,r)B'P\tilde{x} + F\tilde{x} - Jr) - F\tilde{x} + Jr\right) && (4.86)\\
&= -\tilde{x}'[PBEB'P + C'QC]\tilde{x} + 2\tilde{x}'PB\left(sat(-R(x,r)B'P\tilde{x} + F\tilde{x} - Jr) - F\tilde{x} + Jr\right) && (4.87)\\
&\leq -\tilde{x}'C'QC\tilde{x} + 2\tilde{x}'PB\left(sat(-R(x,r)B'P\tilde{x} + F\tilde{x} - Jr) - F\tilde{x} + Jr\right) && (4.88)
\end{aligned}$$

Obviously at the origin $\tilde{x} = 0$, $\dot{v}(\tilde{x}) = 0$. It now must be proven that this is the only point where this is so. Note that as both terms on the right-hand side of (4.88) are negative semi-definite, it follows that both must be independently zero for $\dot{v}(\tilde{x}) = 0$; that is,

$$\begin{aligned}
0 &= -\tilde{x}'C'QC\tilde{x} && (4.89)\\
0 &= \tilde{x}'PB\left(sat(-R(x,r)B'P\tilde{x} + F\tilde{x} - Jr) - F\tilde{x} + Jr\right) && (4.90)
\end{aligned}$$

Note that for (4.90) to hold either $P\tilde{x} \in \mathcal{N}(B)$, which implies $\tilde{x} = 0$ as $P > 0$ and B has full column rank; or that $sat(-R(x,r)B'P\tilde{x} + F\tilde{x} - Jr) - F\tilde{x} + Jr = 0$. As one is interested in the case that $\tilde{x} \neq 0$ (it has already been mentioned that $\tilde{x} = 0$ is the trivial equilibrium point) assume the latter . Now, from equation (4.40), it follows that in this case the closed loop system dynamics are simply $\dot{\tilde{x}} = A_c\tilde{x}$.

Also, for $\dot{v}(\tilde{x}) = 0$, in addition to equation (4.90) holding, equation (4.89) must also hold. Note that as $Q > 0$, this is equivalent to $C\tilde{x} = 0$. Differentiating this $n-1$ times yields

$$\begin{bmatrix} C \\ CA \\ \vdots \\ CA^{n-1} \end{bmatrix} \tilde{x} = 0 \tag{4.91}$$

As it has been assumed that (C, A) is observable, this implies $\tilde{x} = 0$. Thus the only point at which $\dot{v}(\tilde{x}) = 0$ is the origin; hence $v(\tilde{x}) = \tilde{x}'P\tilde{x} = \tilde{x}'\Pi\tilde{x}$ is a valid choice for a Lyapunov function for the system.

It is also possible to deduce information about the stability of the system for fixed $R(x, r)$: with the nonlinear feedback added, the closed loop A-matrix becomes

$$A_c = A - BE^{-1}B'P - BR(x,r)B'P \tag{4.92}$$

$$= A - B(E^{-1} + R(x,r))B'P \tag{4.93}$$

which, for each fixed $R(x, r)$ is Hurwitz.

Essentially, an LQR output regulation approach has been used to make sure that there are minimal directionality problems with the nonlinear feedback, but other ARE based techniques could have a similar effect (e.g. $\mathcal{H}^\infty$ state feedback, the low-gain control in [46]).

Remark. Note that without a procedure similar to this it is difficult to preserve decoupling properties, because even if $R(x, r)$ is chosen very small in the steady state, as $B'P\tilde{x}$ and $F\tilde{x}$ are unlikely to have the same direction, significant cross coupling may be observed.

Riccati Synthesis when $D \neq 0$

The LQR method for this case is not as straight-forward, but will be illustrated for completeness, and to point out the difficulties encountered in this case.

Ideally one would like to choose our Lyapunov function P, so that a diagonal property is preserved in our control law. That is one would like (in the $\tilde{x}$ co-ordinates)

$$u = -(R(x,r) + W)B'P\tilde{x} + (-WB'P + G)r \tag{4.94}$$

where W is a diagonal positive definite matrix. Following a similar rationale to the strictly proper case, the functional to be minimised is

$$\frac{1}{2}\int_0^\infty (Cx+Du)'Q(Cx+Du)+u'Eu \quad dt = \frac{1}{2}\int_0^\infty \begin{bmatrix} x \\ u \end{bmatrix}' \begin{bmatrix} C'QC & C'QD \\ D'QC & D'QD+E \end{bmatrix} \begin{bmatrix} x \\ u \end{bmatrix} dt \tag{4.95}$$

which has cross terms present. It is well known that the control, u, which minimises this functional and provides internal stability is given by

$$u = -(D'QD+E)^{-1}(D'QC+B'\Pi)x \tag{4.96}$$

where $\Pi > 0$ satisfies the ARE

$$(A+BV^{-1}D'QC)'\Pi+\Pi(A+BV^{-1}D'QC)-\Pi BV^{-1}B'\Pi+C'(Q+QDV^{-1}D'Q)C=0 \tag{4.97}$$

where $V = D'QD+E$ and $C'(Q+QDV^{-1}D'Q)C > 0$. To enforce the diagonal structure above, it is desirable to choose

$$(D'QD+E)^{-1}(D'QC+B'\Pi) = WB'\Pi \tag{4.98}$$

Note that $\Pi > 0$ is nonsingular so equation (4.98) can be re-arranged as

$$(D'QC+B'\Pi)\Pi^{-1} - D'QDWB' = EWB' \tag{4.99}$$

As $B' = [0 \quad \bar{B}]$ and $\bar{B} \in \mathbb{R}^{m\times m}$ is nonsingular, multiplying on the right by $\begin{bmatrix} 0 \\ \bar{B}^{-T} \end{bmatrix}$ (which is a right inverse of B') yields

$$E = (I+D'QY)W^{-1} - D'QD \tag{4.100}$$

where $Y := (C_1\tilde{\Pi}'_{12}\bar{B}^{-T} + C_2\tilde{\Pi}_{22}\bar{B}^{-T})$, given that Π^{-1} is partitioned as

$$\Pi^{-1} := \begin{bmatrix} \tilde{\Pi}_{11} & \tilde{\Pi}_{12} \\ \tilde{\Pi}'_{12} & \tilde{\Pi}_{22} \end{bmatrix} \tag{4.101}$$

Inserting this value of E into the ARE (4.97) gives the quadratic term

$$B(I+D'QY)^{-1}WB' \tag{4.102}$$

which can be solved, by standard methods, if and only if this quadratic term is symmetric, which requires either $D = 0$, in which case it reduces to the situation discussed in the main text, or $Y = D$ and $W = \alpha I_m$, where α is a constant. If this is the case our control will have a diagonal structure, but generally this will not be the case and therefore when $D \neq 0$ it may be difficult to obtain good decoupling with the additional nonlinear term. This is an area left open for future research.

4.6 Examples

4.6.1 Helicopter Pitch Control

Initially the effectiveness of the technique is demonstrated on systems of dimensions greater than two. The example considered is the pitch attitude control for a helicopter. The model used is a residualised 5th order model, obtained from a simplified 20 knot linearisation of a modified Bell 205 helicopter (see the UK Defence Evaluation and Research Agency (DERA) report, [73]). The objective is to control the pitch attitude of the aircraft without exceeding the control limits of $+/-14^o$ in longitudinal cyclic.

Assuming full state-feedback, a linear feedback gain which places the closed loop eigenvalues at

$$\{-0.8889 + 0.5666i, -0.8889 - 0.5666i, -0.00008, -0.3, -2.5786\} \tag{4.103}$$

and one which does not exceed the control constraints for the flight condition of interest is given by

$$F = [0.1791 \quad 0.2158 \quad 0.0006 \quad 0.0005 \quad -3.4008] \tag{4.104}$$

Figure 4.1 shows the nominal linear response to a step of 5 degrees. This is a rather slow step response, but one which does not exceed actuator limits for the flight condition; the aim is to improve it by using the nonlinear gain.

To calculate P, Q was set $Q = I$, and after several simulations, the (scalar), nonlinear parameter was chosen as

$$R(x, r) = 10^{-10} \exp\{-|30y|\} \tag{4.105}$$

This is similar to the manner in which the nonlinear parameter was chosen in Lin *et al.*'s paper ([44]), except there the exponential of $|y - r|$ is used instead of just $|y|$ here. The reason for this

is that in [44], as only second order systems are considered, stronger mathematical conditions are obtained on the nonlinear parameter. In particular, a small damping ratio is guaranteed. Here no such guarantees can be given and it was found that by using $|y - r|$ instead of only $|y|$, some peculiar overshooting behaviour could be observed.

Using the control $u = u_L + u_N$, with the parameters just defined, resulted in an improved transient response. Figure 4.2 shows the responses of the system with and without the nonlinear parameter at the same flight condition subject to a step demand of 5^o. Note that the response is significantly faster with the nonlinear control added, although the control action is much higher with a large initial surge of actuator activity. Note that the actuator still saturates briefly, as this scheme does not attempt to prohibit actuator saturation, but rather seeks to ensure that the actuators saturate in a benign manner.

In this case $R(x, r)$ was chosen to be a monotonically decreasing function of y in order to ensure a fast transient response for small demands, but to avoid excessive actuator saturation for high demands. Figure 4.3 shows the responses of linear and nonlinear controls for a step demand of 20^0 for comparison. Here the response with the addition of u_N is much closer to the linear one. Note that this monotonicity property of $R(x, r)$ is not required, but simulations have indicated that, at least for some systems, this is desirable.

4.6.2 MIMO Missile Control

This example is taken from the paper by [11] who in turn took it from [95] and considers the two axis control of the linearised lateral dynamics of an air-air missile. Originally eigenstructure assignement was used to design a static output feedback controller; here the Riccati based synthesis procedure of the previous section is used to compute a state feedback controller. The aim is to achieve a fast, well damped response with little coupling and without exceeding the control constraints (which are artificially set at $+/-20^o$ for demonstration purposes).

For the nominal linear design, Q was chosen as $Q = diag(5, 0.1)$ and $R = I_2$. Using these in the ARE synthesis procedure the linear state feedback was obtained as

$$F = \begin{bmatrix} -0.8469 & 0.0959 & 0.0093 & 0.3131 & -0.1445 & -0.0439 \\ 0.6130 & -0.1086 & 0.0144 & 0.0443 & -0.439 & -0.1091 \end{bmatrix} \tag{4.106}$$

Figures 4.4 and 4.5 show the nominal linear responses using linear controls which respect actuator limitations. Notice that, to avoid saturation in Channel 1, the gain used is low and thus significant cross coupling occurs into Channel 2. The response to a step in Channel 2 is better, but the low gain means that the transient response is not ideal.

Figures 4.6 and 4.7 depict the system's response using the control law $u = u_L + u_N$, where the matrix $P = \Pi$ was synthesised using the Riccati technique above, and the nonlinear parameter $R(x, r)$ was chosen as

$$R(x,r) = diag\left\{500\exp(0.1|y_1 - r_1|), 500\exp(0.1|y_2 - r_2|)\right\} \tag{4.107}$$

It is immediately clear that the cross-coupling has been dramatically reduced by the addition of the nonlinear term when a step in Channel 1 is demanded. The damping of this channel is also improved, although the speed of response is slowed slightly. The transient response to a step in Channel 2 has also been improved: a slightly faster response with better damping is quite evident. Note that the actuators in both figures saturate briefly, but that this does not have a detrimental effect on the system's performance.

Remark. Initially it was attempted to use the feedback gain designed in [11] as the F matrix and the nonlinear design was tried to be tailored around this. Unfortunately, as aforementioned, it is difficult to pick an $R(x, r)$ which does not degrade the linear performance in some way. This prompted the development of the Riccati approach, which seems to enable one to pick the nonlinear parameter with greater ease and intuition. Some early investigations on this example also highlighted the fact that a poorly designed F tends to mean that the nonlinearly augmented system behaves poorly; that is, the choice of the linear gain F is of paramount importance.

◇◇

4.7 Conclusion

The results of [44] have been extended to the case of a more general class of linear systems with input saturations. Some restrictions are imposed, such as a right invertibilty condition on $\tilde{C}$ and the use of a particular realisation for the system; these are in, in many practical cases, satisfied. Examples have demonstrated the engineering pertinence of these results and have shown that the nonlinear tracking scheme gives better performance than pure linear feedback, while also adhering to the control constraints.

Future research is likely to concentrate on how some of the restrictions imposed by the methodology presented here can be removed. The question of the scheme's robustness also needs serious investigation, although it is hoped that by a suitable robust linear design method, the system's robustness will not be impaired by the nonlinear term. Ideally, for any actual implemetation, the scheme should be able to function with output feedback rather then the state-feedback which is advocated here.

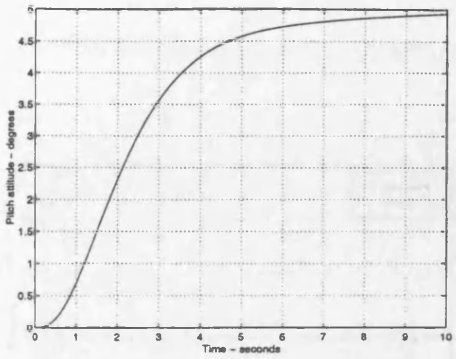

Pitch Response

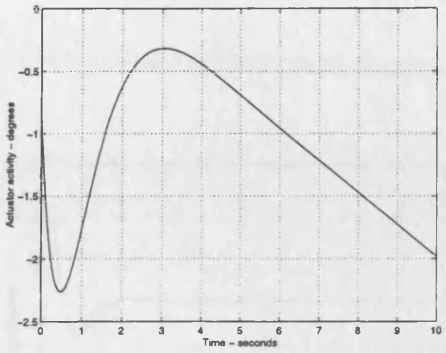

Actuator Reponse

Figure 4.1: Response to Step demand of 5^o

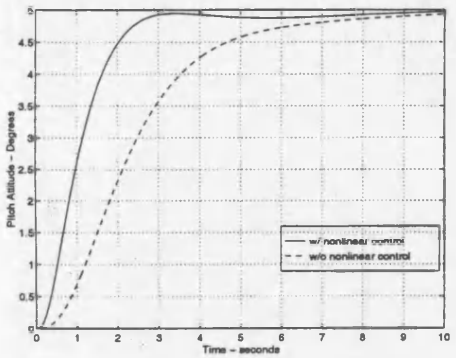

Pitch Response

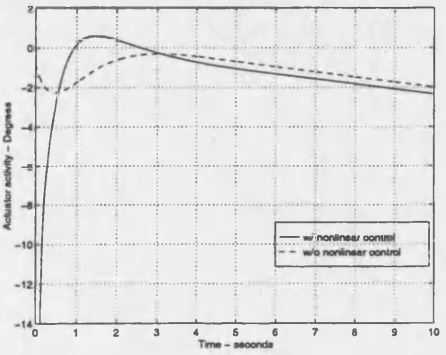

Actuator Reponse

Figure 4.2: Response to Step demand of 5^o

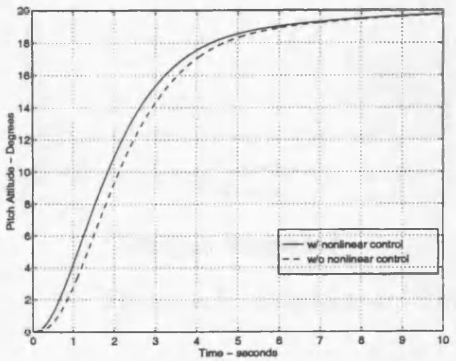

Pitch Response

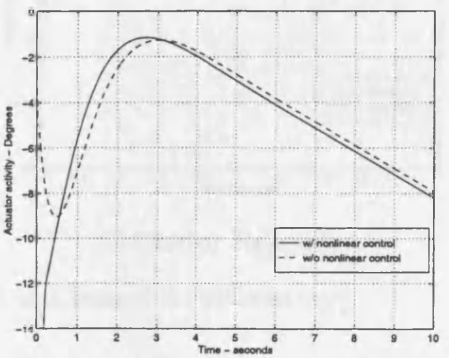

Actuator Reponse

Figure 4.3: Response to Step demand of 20^o

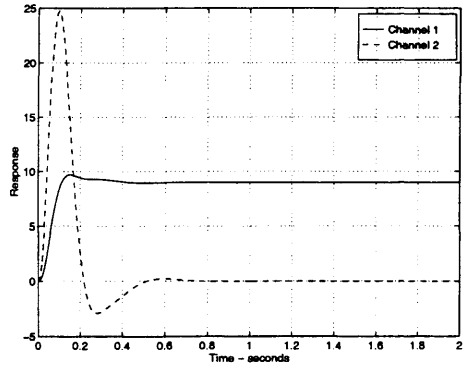

Output Response

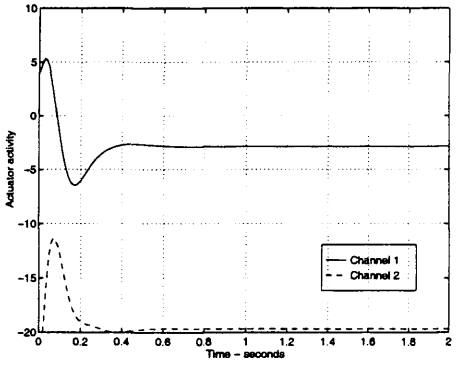

Actuator Reponse

Figure 4.4: Response to Step demand of 9^o in Channel 1 (without u_N)

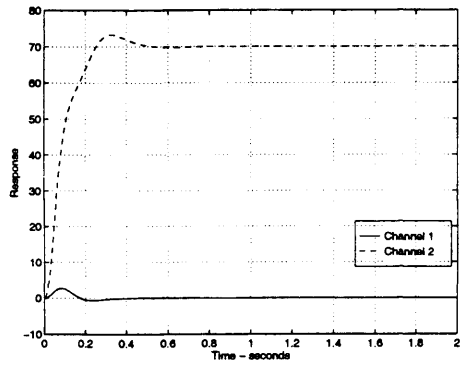

Output Response

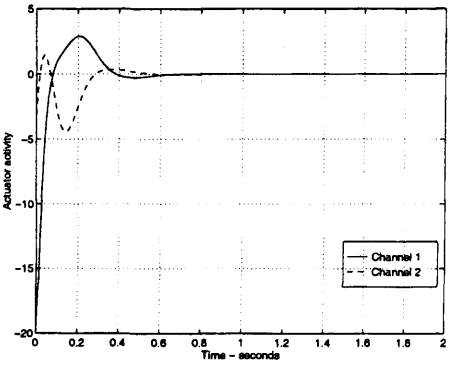

Actuator Reponse

Figure 4.5: Response to Step demand of 70^o in Channel 2 (without u_N)

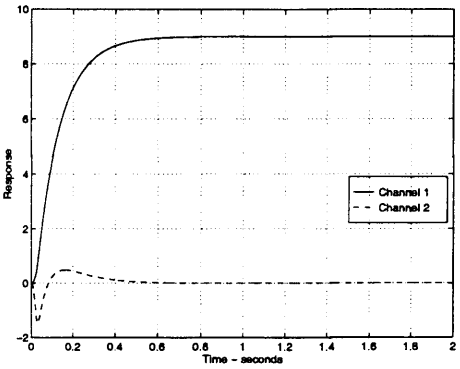

Output Response

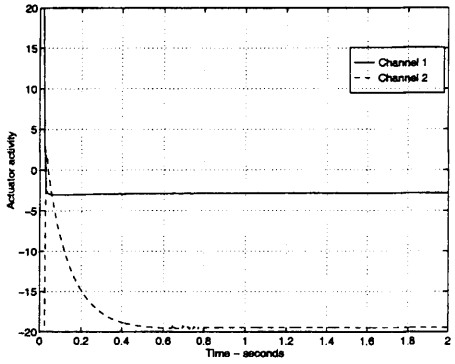

Actuator Reponse

Figure 4.6: Response to Step demand of 9^o in Channel 1 (with u_N)

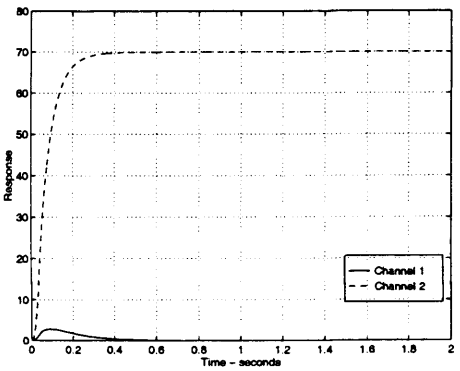

Output Response

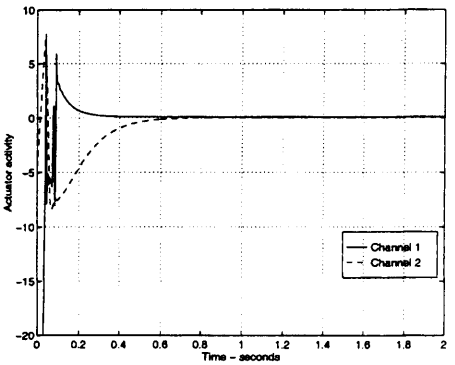

Actuator Reponse

Figure 4.7: Response to Step demand of 70^o in Channel 2 (with u_N)

Chapter 5

The Helicopter Control Problem

5.1 Overview

This chapter introduces the main application of the thesis: helicopter control. This is a problem which, in its various guises, draws upon the thesis' central themes: robustness to model uncertainty and saturation constraints. Later chapters will discuss the two applications, namely limited authority control of a Westland Lynx helicopter and robust control of the decoupled longitudinal and lateral dynamics of the Bell 205 fly-by-wire helicopter.

5.2 Introduction

Helicopter control is a problem which has been studied by control engineers virtually since the aircraft's inception. Indeed, one of the major reasons for the helicopter's slow advent in the aircraft world was due to control problems - see chapter 1 of [38] or Chapter 23 of [58]. Today one of the major challenges is to improve the handling qualities of the aircraft, such that they meet stringent requirements for desired task performance, and also to ease pilot workload.

Helicopter control has received significant attention in the past fifteen years or so due partly to the aforementioned drive to increase handling qualities, but also partly due to the advent of robust multivariable control techniques. These enabled researchers such as [96] and [88] to apply advanced robust control techniques to decouple the responses and robustify the system to the uncertainty notorious in mathematical models of helicopters.

Until relatively recently, these studies were confined to nonlinear and piloted simulation, which, while being an important part of the research in the field, could not yield any concrete results about the performance of these control laws in a real environment. Several years ago, [68] demonstrated the first fully functional example of an $\mathcal{H}^\infty$ controlled helicopter, which actually behaved in an acceptable manner on the first flight.

The aim of this part of the thesis is to develop these recent advances in helicopter control in novel ways, with particular regard to the robustness and constrained input concepts discussed in the first part.

This thesis is not centered around either aerodynamics or modelling and for such the reader is referred to, for example, [54], [38], or for a more control related point of view, [96]. For a more detailed description of the workings of the control linkages, a good reference is chapter 23 of [58].

The discussion in this chapter pertains particularly to the high-performance Lynx and modified Bell 205 rotorcraft, but is also roughly true for most single main rotor helicopters. Generally speaking the theory remains the same, but the details will change for different types of rotorcraft.

5.3 Review of Previous Helicopter Control Work

Although the control problem has been around for the aircraft's history, only relatively recently has serious attention been devoted to the design of novel control laws to improve the helicopter's responses to pilot commands. Initially, control engineers, in line with the tools available at the time, applied classical control to the problem; this still accounts for the majority of the control laws implemented. However, when considering a multivariable plant such as the helicopter, classical control can encounter difficulties and hence attention shifted to emerging areas of advanced control. Following some of the successes on fixed-wing aircraft, various optimal control techniques were applied to the problem (see [77]), although few of these designs went beyond the simulation stages.

When papers such as [12] exposed the lack of robustness of LQG-type compensators, some attention was devoted to ways of synthesising robust control laws; modelling uncertainty was known to be significant in the case of the helicopter. Researchers such as [77] and [96] devoted their attention to the then new $\mathcal{H}^\infty$ method, with some success. Through singular value analysis and desktop simulation they were able to show the potential of $\mathcal{H}^\infty$ as a control strategy for the helicopter.

This research was continued by [88] and [89], who proposed using the then novel $\mathcal{H}^\infty$ loop-shaping design procedure to synthesise controllers. This not only allowed some classical ideas to be used in the design but also the choice of uncertainty, being perturbations of the plant's normalised coprime factors, was known to be a type of optimal robustness cost function in terms of the gap metric. This approach was different to the mixed sensitivity designs of [97], and [88] was able to demonstrate promising results. Later [89] took the designs one step further and

conducted a series of ground-based piloted simulations in collaboration with DERA, Bedford.

Up to this point all work was either ground-based testing or simulation and directed specifically at the high-performance Lynx helicopter. In [68], the first successful flight test of an $\mathcal{H}^\infty$ controlled helicopter was recorded on the NRC's modified Bell 205 airborne simulator. This was followed by repeat tests in [66] where improved performance was demonstrated. For these tests the $\mathcal{H}^\infty$ loop-shaping procedure was used but for tests conducted by [90], mixed sensitivity procedures, in the vein of [96], were used. One of the chapters in the thesis is based on this work and has already been partially reported in [90] and [91].

Other research into helicopter control has also been conducted, and the literature review has neglected the important work on eigenstructure assignment, favoured by many fixed-wing engineers; and work such as the recent gain-scheduling approach, reported in [55]. For a more detailed summary of some of this work, the reader should consult, for example, [67].

5.4 The Plant

5.4.1 General Description

There are a wide variety of helicopters in use in the world today, of which the single main rotor and tail rotor version is the most common (others are discussed in [96]). These also exist in different forms, but have many aspects in common. The characteristic which sets the helicopter apart from most other aircraft is its ability to hover efficiently. This is achieved through its most salient feature: the main rotor. This airfoil provides lift to the helicopter and can be tilted, by cyclically changing the individual blades' inclinations, to provide pitching and rolling moments.

This perhaps gives some insight into one of the reasons that helicopter control is a challenging problem. The fact that the main rotor is responsible for height, pitch and roll control suggests the plant exhibits significant cross-coupling. Indeed this is the case; the helicopter is an overtly multivariable machine with a high degree of cross-coupling in all axes. Disregard for this can have detrimental effects.

Furthermore, the nature of the aircraft's dynamics is not benign. The highly nonlinear nature of the vehicle causes considerable variation in behaviour at different flight conditions, which emphasizes the importance of robust control for such a model. Apart from the fact that at most of these flight conditions one or more of the modes are unstable, the complexity of the flight mechanics makes the helicopter a difficult plant to model accurately. In fact most mathematical models of the helicopter suffer from a variety of uncertainty, resulting in poor

behavioural prediction, with particular problems in predicting off-axis response - in both sense and magnitude (see [73]).

Considering these factors, it is not difficult to see why most helicopters currently perform below their desired level. The main objectives for the control problem are:

1. Stabilise the aircraft
2. Decouple the responses
3. Enable sufficient performance to be achieved under the existing uncertainty

The last point is particularly difficult to achieve as high performance is assocaited with high bandwidth which has the potential to cause stability and performance problems if uncertainty is present. Furthermore, as the vehicle's rigid body and rotor dynamics are coupled around the bandwidth, the difficulty of the problem is further exacerbated.

5.4.2 Input-Output Structure

The helicopter is a complex vehicle with many different flight configurations. Some of these are explained in [54], but as only one of these configurations is considered attention is restricted to that alone.

Pilot Inceptors

These are the cockpit controls which the pilot moves to influence the motion of the helicopter. In conventional helicopters these directly influence the actuators, possibly with the addition of a small amount of feedback. In fly-by-wire control systems, the inceptors are responsible for providing reference signals to the control system.

Essentially the pilot has three inceptors:

1. The cyclic stick: Conventionally this controls the lateral and longitudonal cyclic actuators and is mainly responsible for pitching (moving the stick fore and aft) and rolling (moving the stick left and right) the rotorcraft.
2. The collective stick: Conventionally this controls the main rotor collective actuator and is responsible for controlling the vertical motion of the helicopter. When this stick is pulled up, the pilot commands increased height / height rate; when it is pushed down, the pilot commands decreased height / height rate.

3. Pedals: These control the tail rotor collective and hence influence the yawing of the vehicle. Right pedal down makes the vehicle yaw to the right; left pedal down gives a left yawing motion. Some pedals are spring-balanced, others are not; the basic operation remains the same, but pilots have individual preferences.

Actuators

The helicopter has four sets of actuators which control movement about three body axes, pitch, roll and yaw, and also motion in the vertical plane. Their relationship with the pilot inceptors for conventional helicopters has already been pointed out; this will remain broadly the same for a fly-by-wire aircraft as the helicopter has an approximate diagonal structure.

1. Main rotor collective: mainly influences vertical motion.
2. Longitudinal Cyclic: mainly influences pitching motion.
3. Lateral Cyclic: mainly influences rolling motion.
4. Tail rotor collective: mainly influences yawing motion.

Note that there are two types of actuation: collective and cyclic. Roughly speaking collective actuation alters the inclination of the rotor blades in the horizontal plane (with reference to the helicopter body) simultaneously. This increases their angle of attack and induces an increase in lift (main rotor collective) or thrust (tail rotor collective). The cyclic type of actuation again increases the angle of attack of the rotor blades, but only once per cycle. This gives an additional longitudinal or lateral thrust which causes the aircraft to pitch or roll.

Controlled Outputs

There are several response types sought after in helicopter control, chiefly attitude-command-attitude-hold, rate, and translational rate. All have their merits, but a discussion of such is not the subject of this thesis. We shall be content to describe the one used in the case studies, namely ACAH, but for discussions of the other types see [59] or [54].

The ACAH response type is as its name suggests; the pilot's inceptors command an attitude and then the aircraft is held at that attitude until another demand is given. More informally, movement of the main stick commands an attitude change, which is held while the stick is in a given position. To return to the trim point, the stick is then be re-centered. The ACAH response type is commanded in pitch and roll, but in yaw a rate command is sought, partly

ϕ	Roll attitude
θ	Pitch attitude
ψ	Heading
r	Yaw rate
p	Roll rate
q	Pitch rate
u	Longitudinal velocity
v	Lateral velocity
w	Vertical velocity

Table 5.1: Helicopter aerodynamic variables

due to the fact that confusion arises when executing full turns as 360 degrees is identical to zero [1].

Table 5.1 shows the main outputs of interest, which are usually featured as states in most mathematical models. The last six variables describe the *rigid body* dynamics and are a feature of virtually all state-space descriptions of aircraft.

These variables are included as states in all the mathematical models considered here, but others are sometimes included as well. Relevant discussion regarding the states of the various models will be given when required.

Control Authority

In a *full authority* control system either the pilot, through the mechanical control linkages, or the control system has complete influence over the total range of the actuators. That is, movement of the stick and / or sensor feedback influences directly the position of the actuators.

A *limited authority* control system only gives the control system partial authority over the actuator positions. Basically the stick drives the actuators directly, and also acts as a reference signal for a control system which also drives the actuators, but only has a limited capacity. This type of control will be elaborated on later in the thesis.

[1] In virtually all helicopters, yaw is the only axis where a full turn is allowed, although occasionally a pilot may barrel-roll a Lynx helicopter

5.5 Sources of Uncertainty

One of the primary reasons robust control has been targetted at the helicopter control problem is due to the high degree of uncertainty present in most mathematical models. This uncertainty varies in the two applications and more will be said about this subject later. However, helicopters have broadly similar sources of uncertainty, even though its specific structure will be peculiar to the particular aircraft. Some of these sources will now be described:-

- **Inter-axis Uncertainty**. Although the various control channels are known to have interactions with one another, the precise form of these interactions is often modelled poorly, and is not even completely understood in the theoretical sense. In fact empirical adjustments are often made to the mathematical models to make them more representative of the real aircraft (see [49]), as commonly the sense and magnitude of the interactions are modelled erroneously (see [73]).

- **Neglected Rotor Dynamics.** In many models the rotor dynamics, which encompasses the coning and flapping of the flexible main rotor, are neglected completely, partially modelled, or modelled erroneously. Often they can be approximated as a time delay, which in turn can be approximated in the manner of Pade. Experimental evidence has suggested that poorly modelled rotor dynamics can have a calamitous effect on the rotorcraft's stability (see [90], for example). In addition, the rotor is usually over-simplified to be a rotating disc, (which is equivalent to modelling it with an infinite number of blades) which introduces more uncertainty.

- **Nonlinearities.** The main control system in both of the applications considered here is linear and hence will have been designed around an operating point in the helicopter's flight envelope. Due to the highly nonlinear nature of the helicopter's aerodynamics, there is significant difference in the model at one flight condition to another. In fact, those eigenvalues which are unstable at hover may migrate to stable regions at higher forward speeds (and vice versa). Thus, for satisfactory performance, the controller must be able to robustify the closed loop over a range of uncertainty in the parameters.

- **Miscellaneous Unmodelled Dynamics.** In addition to the main sources of uncertainty outlined above there are various other areas which add uncertainty to the model. For example, engine dynamics are virtually always modelled independently of the airframe dynamics, even though it is accepted that interactions exist between the two systems. Actuator dynamics are often known imprecisely and sensor noise and uncertainty is also a cause for concern.

5.6 Handling Qualities

The success of a particular control strategy is judged finally upon the handling qualities returned by the pilot. Although simulations and collected data gives a guide to the controller's performance, a handling qualities evaluation gives a clearer picture of the controller's performance in the real world.

The major criteria for handling qualities of helicopters can be found in the U.S. Army's ADS-33D document ([59]), which sets out both qualitive and quantitive tests, as well as defining levels of performance in a fairly rigorous way. Essentially the ADS-33 criteria fall into two categories: pilot opinion and data evaluation. The first, not surprisingly, entails the pilot answering structured questions about the performance of the helicopter under a given controller; the second enables tests to be conducted either on simulation data, which serves as a prediction or warning, or on test data which can be used as verification and validation of the pilot's comments.

It would be tedious and unnecessary to give a complete description of the ADS-33 document; the interested reader is encouraged to consult this for more information. The important features from it which are particularly pertinent to this thesis are summarised below.

5.6.1 Handling Qualities Ratings

The scale on which a pilot judges the performance of the aircraft under a given controller is known as the Cooper-Harper scale and associated with it are several handling-qualities ratings (HQRs). These, in turn, correspond to different levels of performance. It is normally the case that an HQR rating is given for each manoeuvre the pilot carries out, to explicitly identify a controller's strengths or weaknesses.

Table 5.2 summarises the handling qualities ratings and their corresponding performance level (a more detailed description and table can be found in [59] or [72]).

As a rough guide, the object of active control laws is to achieve Level 1 capabilities where possible; this indicates good vehicle performance. Few, if any, helicopters in service attain this level of performance. Level 3 indicates ineffective control system design, and Level 2 performance gives a measure of control laws between the two extremes.

5.6.2 Quantative Measures of Performance

Within the ADS-33 document, there exist various quantative measures which, as mentioned already, can help assess the performance of a controller. They again correspond to one of the

Aircraft Characteristic	Demands on the pilot in Selected Task / Operation	HQR	Level
Excellent Highly Desirable	Pilot compensation not a factor for desired performance	1	1
Good Negligible deficiencies	Pilot compensation is not a factor for desired performance	2	1
Fair - mildly unpleasant deficiencies	Minimal pilot compensation required for desired performance	3	1
Minor but annoying deficiencies	Desired performance requires moderate pilot compensation	4	2
Moderately objectionable deficiencies	Adequate performance requires considerable pilot compensation	5	2
Very objectionable but tolerable deficiencies	Adequate performance requires extensive pilot compensation	6	2
Major deficiencies	Adequate performance not attainable with maximum tolerable pilot compensation. Controllablity not in question	7	3
Major deficiencies	Considerable pilot compensation is required for control	8	3
Major deficiencies	Intense pilot compensation is is required to retain control	9	n/a
Major deficiencies	Control will be lost during some portion of the operation	10	n/a

Table 5.2: Handling Qualities Summary

three performance levels, but can be used on predicted and simulated responses as well as actual data.

A complete guide to these measures can be found in the ADS-33 document, but two of the more important, which are used in this thesis, are *bandwidth* and *phase delay.* These are useful in evaluating the handling qualities in response to low amplitude pilot demands, and their combination gives a handling quality rating (HQR).

Their definition is somewhat at odds with conventional control literature, but is thought to offer a more realistic assessment set of criteria (experiments have indicated that bandwidth and phase delay, as defined by in [59] are more in agreement with what the pilot experiences, than traditional definitions). A brief explanation of these two criteria is given here. Calculation is done either by inspection or with the useful DERA Matlab Toolbox [35]. More detail about both the bandwidth and phase delay can be found in [59].

Bandwidth

The ADS-33 Bandwidth of a closed loop system, ω_{BW} is defined, for attitude command type responses discussed here as the point where the phase response of the closed loop individual channel frequency response intersects the -135 degrees line. The phase response of the closed loop system is taken on an individual channel basis and is the phase relationship between one of the attitudes (θ, ϕ, ψ) and the corresponding control inceptor.

For rate response-types, the definition is slightly different, but will not be discussed here as this response type is not considered. The yaw rate response is integrated to obtain - approximately - heading, and the bandwidth is calculated from that.

Phase Delay

Let ω_{180} be the frequency at which the closed loop phase response intersects the -180 degrees line, then the quantity $\Delta\Phi 2\omega_{180}$ is defined as the difference between the -180 degrees line and the phase of the closed loop at $2\omega_{180}$. The phase delay is then defined as

$$\tau_p := \frac{\Delta\Phi 2\omega_{180}}{57.3(2\omega_{180})} \tag{5.1}$$

Again the phase delay is an individual channel measure and is found using the closed-loop transfer function between a pilot control inceptor and its primary output (e.g. pedals and heading).

5.6.3 Manoeuvres

It is often the case that, due to the multivariable nature of the rotorcraft and frequent modelling errors and uncertainties, the helicopter will have different performance levels in each of its axes. An overall handling qualities rating can thus be misleading and it is more usual for the pilot to 'rate' the performance of the vehicle by carrying out simple manoeuvres. These manoeuvres are specifically designed to test certain axes and to expose cross-coupling and anomalous behaviour. More details of these can be found in, for example, [67], but below is a summary of the ones used in this thesis.

1. **Quick Hop**. This primarily examines the pitch axis and involves the pilot pitching the helicopter forward, from hover, to gain longitudinal speed rapidly. The pilot then, after a certain distance, attempts to stop the vehicle at a pre-specified point.

2. **Side Step**. This manoeuvre is designed to assess the roll axis of the helicopter and involves the pilot rolling the vehicle to one side sharply from hover, to increase lateral air-speed. Then, at a pre-specified point, the pilot will attempt to stop the aircraft.

3. **Turn to Target**. Aimed at examining the yaw axis, this manoeuvre takes place at hover. The pilot sharply yaws the vehicle around, stopping after 180 degrees change in heading has been achieved.

4. **Pirouette**. This is a fairly demanding manoeuvre that requires control inputs in most axes. The task involves the pilot circling a central point while ensuring the helicopter's nose faces the central point at all times. This manoeuvre requires a fair amount of precision in most channels and can expose cross couplings.

5. **Precision Hover**. This is a fairly easy manoeuvre and the object is for the pilot to keep the helicopter flying over a given point on the ground for a certain amount of time. This is useful for examining cross couplings and any minor instabilities or oscillatory characteristics of the controller.

During the evaluation of the Lynx's limited authority control system, the following non-standard manoeuvres were also used to further evaluate the control system.

1. **Accel/Deccel**. This can be best thought of as an extended quick-hop and entails the pilot pitching down to accelerate the aircraft to a given speed. Then the pilot cruises at this speed for a certain distance until decelerating to stop at a given certain point.

2. **Slalom**. Designed to test the rolling and yawing movement of the helicopter, this manoeuvre also can test outer-loop functions such as the co-ordinated turn function. It involves the pilot guiding the helicopter above a meandering road with quite sharp bends, while keeping within a certain height range. When flown aggressively, this can be a demanding manoeuvre.

3. **Hurdles**. This task primarily tests the pitch and heave axes and can highlight interactions between the two. Essentially it requires the pilot to pitch the helicopter forward and fly at a constant speed, while adjusting the helicopter's height to fly over hurdles of various heights above the ground. There are two different ways of performing this task, as, in a 3-axis control system, both the pitch control and the heave control can be used to adjust height. Normally, when the task is being flown slowly, the heave is primarily used, and when flown aggressively, the pitch control is used.

5.7 Control System Design Objectives

Based on the matters discussed so far the objectives for a controller are to:-

- Stabilise the helicopter.
- De-couple the responses.
- Ensure sufficiently agile manouvres are achievable.
- Try to ensure that ADS-33 performance measures such as bandwidth and phase delay meet Level 1 requirements.

These issues will be addressed for the Lynx and Bell 205 aircraft in the two subsequent chapters.

Chapter 6

Limited Authority Control of Helicopters

6.1 Overview

This chapter explores an avenue in the area of robust input-nonlinearity control, namely that of *limited authority* control. This area of control is relatively unknown in the academic control community, but in the helicopter control world is widely used; examples of helicopters currently using this configuration are the Longbow Apache AH64 and the Westland Mk7 Lynx which we consider here. Possibly one of the reasons for the academic aversion to this problem is the fact that it is difficult to obtain strong theoretical results, given the levels of authority which are allowed.

Roughly speaking limited authority control is a controller configuration whereby both the pilot and the controller are allowed to directly influence the vehicle's actuators, but the signal produced by the controller is subject to hard limits. The difficulty of the problem is exacerbated by the common limit on control amplitude being only 10-20 per cent of the total actuator deflection. For unstable systems, such as the helicopter, this can cause not only performance degredation but severe stability problems. Directionality is also affected, and multivariable controllers, which would normally offer attractive time responses, can perform poorly in such a situation.

The aim of this chapter is to explore more fully the area of limited authority control in the context of helicopter control; the aim is to meld together some of the lessons learned from the previous chapter in helicopter control and some of the developments in constrained input control which have been covered earlier. Note that this chapter is part of on-going research into helicopter control and is based on the paper [82] and also draws on material from [96], [90] and [68].

6.2 The Control Problem

6.2.1 The Westland Lynx Mk7

The Lynx Mk7 is a highly agile multi-purpose combat helicopter which exhibits charateristics, described in more detail in the previous chapter, common to most conventional helicopters: open-loop unstable modes, substantial inter-axis coupling, and highly nonlinear behaviour. A high degree of agility can be obtained due to the four bladed semi-rigid rotor system imparting greater moments to the fuselage than would be the case with teetering or articulated rotor systems, albeit at the expense of a more malevolent instability characteristic at high speeds.

As pointed out in Chapter 5, the complexity of the phenomena at work during helicopter flight, make it a difficult machine to model. The Lynx is no exception and the model used in this study assumes rigid rotor blades with sprung hinges at the hub, which, for a semi-rigid rotor, only serves as a crude representation.

Although intrinsically a four axis system, with inceptors as described in the previous chapter, this chapter concentrates on a three axis ACAH design for the Lynx: the roll, pitch and yaw axes. The heave axis is left open-loop, partly because it is stable and easy to control and partly because pilots prefer to control this axis manually - see [90] and references therein for example. This configuration also allows the controller designed here to be compared with the standard Lynx control system.

For more information on the Lynx aircraft and helicopter dynamics, the interested reader should consult [54] or [96] for example.

6.2.2 The Rationale Behind Limited Authority Control

It is generally accepted that full authority control systems are able to out-perform limited authority systems and, from an architectural point of view, their implementation is more straightforward. This provokes the question as to why *limited authority* control is of any interest and, moreover, if it has any advantages. In fact there are several answers to this question:

- It is easier and cheaper to outfit existing service helicopters with limited authority systems than completely converting them to full authority.
- Limited authority systems are preferable from a safety/reliability perspective. They do not have to be manufactured to the same degree of reliability as full authority systems

as, if the control system fails, the pilot still maintains control over the aircraft via the direct mechanical linkages.

- There are arguments to suggest that the limited authority configuration can give 'desirable' handling qualities in low/moderate aggression manoeuvres; this will be elaborated on later in the chapter.

- In certain parts of the flight envelope, where the helicopter exhibits severely nonlinear behaviour (for example the chaotic *vortex ring* state), it is difficult to know how a full authority controller will perform, and in this situation a limited authority controller may well be preferable.

However, limited authority controllers suffer from the distinct disadvantage that their control signal magnitudes are limited to only a certain, often small, percentage of the actuators' full scale deflection. This restricts the set of controllable states to a subset of the state-space, as the Lynx is an unstable plant, and, unless a large authority is used, results in there being states to which the pilot wants to drive the aircraft, but which are not controllable. Stability analysis is difficult for the Lynx, as its open loop instability prevents classical results from being applied (see appendix).

Currently, there has been little research into advanced control used in such configurations and so far the control laws have relied on classical methods and a substantial knowledge of the vehicle itself. However, due to their reliance on heuristics, one might expect these to be inferior to modern techniques which are more precise in their controller synthesis.

6.3 Limited Authority Control System Architecture

The Lynx limited authority control configuration is somewhat more complex than one would find on a conventional full-authority aircraft. It allows strictly limited control signals to be passed into the plant, while allowing the pilot to directly influence the vehicle's behaviour through his cockpit inceptors. This increase in complexity is due partly to the two types of actuation employed (series and parallel), and also due to the, often necessary, inclusion of some compensation to modify the system's behaviour in the event of saturation limits being reached.

6.3.1 System Operation

The basic diagram of the limited authority control configuration used in this paper is shown in Figure 6.1. Although complex, the basic idea is this: for small pilot inputs (and hence small manoeuvre commands) the series actuators have authority to significantly decrease or increase

(in relative terms) the pilot's direct control signal, thus enabling the aircraft to exhibit a wide range of manoeuvre responses. When large pilot inputs are applied, the series actuators will not have the authority (they will saturate) to alter the pilot's command significantly and the aircraft will tend to have a more 'open-loop' type of behaviour.

From the diagram note that the helicopter's total input (swash plate deflection) is affected by three distinct operations.

- **Series Actuators**. The pilot's stick deflections, relative to their datum positions, are interpreted as manoeuvre commands and are fed into the controller along with measurements of the helicopter's response. The blade angle commanded by the pilot is subtracted from the control signal generated by the controller, before being fed into the series actuators. Hence the limited authority system attempts to transiently match the total blade angle demand with the controller's output - if the series actuators do not saturate, the net input from the control linkages is zero. The series actuators have only a small percentage influence over the total blade angle demand and hence may saturate during aggressive manoeuvering.

- **Direct Pilot Input**. The pilot influences the behaviour of the control system independently of the control system through the mechanical linkages. The absolute stick positions (stick deflections added to datum positions) directly command blade angles via the full authority mechanical control system. These commands can be partially modified by the series actuators as described above.

- **Parallel Actuators**. These devices whose behaviour is dominated by very low rate limits (15 seconds end-to-end), are responsible for driving the stick's datum. As the datum moves, the blade angles, via the full authority mechanical control system, will be modified. The limited authority system uses the parallel actuators to drive the mechanical linkages so that its commanded blade angles matches those generated by the controller. In the long term, this will drive all series actuator commands to zero and prevents long term series actuator saturation.

Table 6.1 shows the total actuator displacement, the series actuator limits and the resulting control authority.

During extensive series actuator saturation, instability may well occur, but as the pilot also "closes the loop" around the aircraft, control is not lost. Furthermore previous research has suggested that this may actually improve the handling qualities of the aircraft: open-loop the helicopter has a more 'rate' type of behaviour, which can be desirable for aggressive manoeuvres.

Channel	Total Actuator Displacement	Series Actuator Limits	Control Authority
Pitch	-18.6/+13.7 deg	+/-2.99 deg	18.5 per cent
Roll	-9.4/+10.2 deg	+/-1.84 deg	18.9 per cent
Yaw	-9.2/31.5 deg	+/- 3.61 deg	17.7 percent

Table 6.1: Actuator Limits and Control Authority

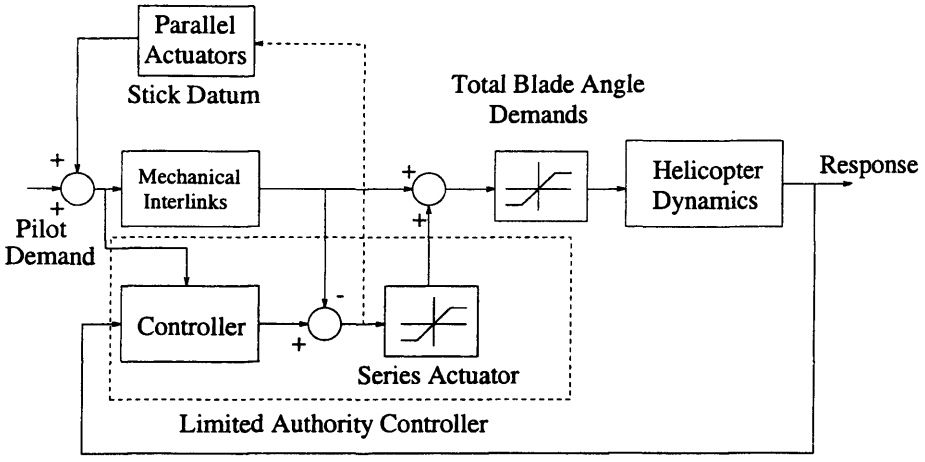

Figure 6.1: Limited Authority Control Configuration

The control system design is also complicated by the fact that the mechanical interlinks are not modelled as simple linear gains, but as coupled quadratic equations which depend upon on the absolute position of the pilot inceptors, which in turn depends on the helicopter's position in the flight envelope. Thus for linear simulation, the best one can hope for is to linearise the mechanical linkages about a certain operating point, even though this can give misleading results for large inputs.

6.3.2 Trimmed Flight

The changes in trim blade angle which are required to trim the aircraft in a given flight condition are often more than can be accomodated within the relatively low authority limits of the series actuators. Thus the parallel actuators, via the mechanical linakges generate the trim blade angels required. A trim command from the pilot causes the parallel actuators to move the stick datum to be consistent with the required blade angle demands for a given trim position. This then allows the series actuators to modify the helicopter's transient response.

6.3.3 Anti-windup Compensation

As noted earlier, due to the tight limits on series actuator authority, when large inputs are applied we can expect saturation to occur. Saturation can seriously degrade performance, cause integrator wind-up, and, particularly with unstable plants, compromise closed-loop stability.

Most anti-windup schemes available to date assume that the control system is full authority; that is the input to the plant can be directly manipulated by the anti-windup compensator [1]. For this situation, various schemes have been put forward which can guarantee stability of the closed-loop system. The situation here is not as straightforward as we have a plant where we can only control the 'smaller' of the two inputs and have no control over one of them (the direct pilot input). We can expect, from simple root-locus ideas, that the pilot can, as he has the greater authority negate the stabilising effect of the controller and force the system into instability if his input is large enough. In other words, the pilot can apply an input directly, which forces the system to a state beyond the closure of the set of states controllable by the controller.

However, recognising that no global stability guarantees can be made, it is still desirable to preserve performance and have as large a stabilty domain as possible. It is hard to calculate this explicitly and meaningfully, but it is known that anti-windup compensators can go some way toward enlarging this. Some anti-windup compensation of the *direct model* type (as discussed in Chapter 2) is thus included on the series actuators to improve stability and performance. The resulting more complicated diagram is shown in Figure 6.2

6.3.4 Outer Loop Functions

In addition to the basic stabilisation and crude functionality of the three controlled axes, it is desirable to give the pilot some extra features in the control system, which further reduce the burden of flying. These are generally referred to as *outer-loop* or *auto-pilot* functions and are enabled using simple logic which is either controlled by the pilot or implemented automatically.

The standard Lynx is fitted with three outer-loop functions, which were also included in the limited authority design during piloted simulation, so that the pilot has a less arduous task in familiarising himself with the new control system. These functions are:-

- Heading Hold - This is automatically engaged when the pilot removes his feet from the pedals, and ensures that the aircraft's heading does not deviate from that originally commanded by the pilot.

[1] A good summary of these can be found in [10]

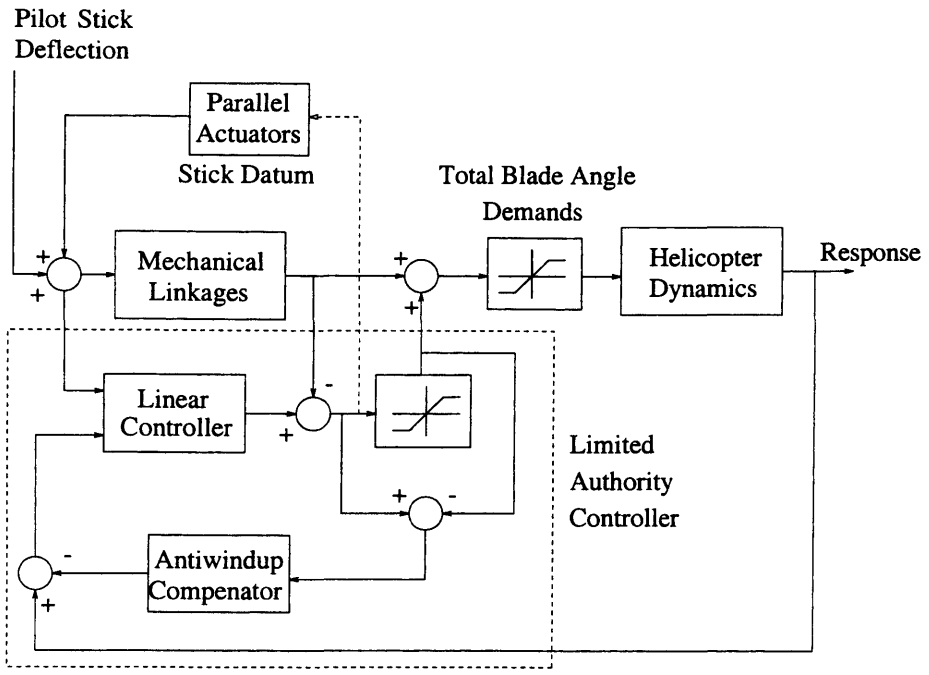

Figure 6.2: Limited Authority System with Direct Model Anti-windup Compensation

- Height Hold - This is an extra control loop around the heave axis, which ensures the vehicle maintains its current height. This can be switched in and out by the pilot.
- Turn Co-ordination - This enables the aircraft to turn neatly without side-slipping and is blended in when the helicopter flying at 55-62 knots i.e below 55 knots there is no turn co-ordination; above 62 knots there is full turn co-ordination.

6.4 $\mathcal{H}^\infty$ Controller Design

6.4.1 Design

The design approach used was 2 DOF mixed sensitivity $\mathcal{H}^\infty$ optimisation, as reviewed briefly at the beginning of the thesis. The calculations for the design were carried out with the aid of the Mu-Tools Toolbox in MATLAB ([4]).

The design was treated as a full authority design due to the structure of our system, and also because this allows us to work purely with linear [2] transfer functions and so commercially available packages can be used to compute results.

The controller was designed near hover (10 knots longitudonal equivalent airspeed) using a 13 state linearisation from the GKN Westland nonlinear flight mechanic model. The command type which was aimed for was attitude-command-attitude-hold (ACAH) in pitch and roll, and rate in yaw. Specifically the following outputs were controlled

[2]Nonlinear $\mathcal{H}^\infty$ (or more accurately $\mathcal{L}_2$ induced gain) control is still in its infancy

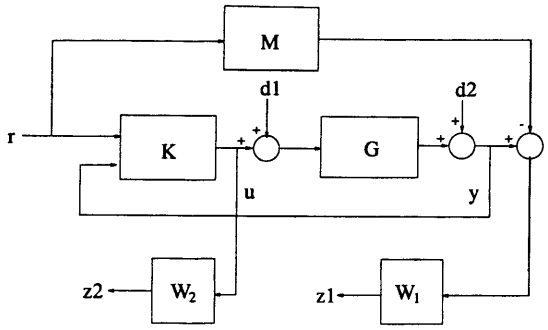

Figure 6.3: System for $\mathcal{H}^\infty$ Controller Design

- ϕ - roll angle
- θ - pitch angle
- r - yaw rate

and, to improve performance, the following were fed back

- p - roll rate
- q - pitch rate

Extracting the nonlinear elements and adding appropriate weighting functions, we obtain the following system in Figure 6.3, where $\mathbf{K}$ and $\mathbf{G}$ represent the controller and the plant respectively. The 2DOF mixed sensitivity approach, as described in Chapter 2 with $\mathbf{M}$ as the ideal model, was used for design. That is, a controller, $K(s)$, was sought to enforce, for a sufficiently small value of γ,

$$\left\| \begin{bmatrix} \mathbf{W}_1(\mathbf{M} - \mathbf{S}_o G \mathbf{K}_1) & \mathbf{W}_1 \mathbf{S}_o \mathbf{G} & \mathbf{W}_1 \mathbf{S}_o \\ \mathbf{W}_2 \mathbf{S}_i \mathbf{K}_1 & \mathbf{W}_2 \mathbf{T}_i & \mathbf{W}_2 \mathbf{S}_i \mathbf{K}_2 \end{bmatrix} \right\|_\infty \leq \gamma \tag{6.1}$$

$\mathbf{W}_1$ was chosen as an approximate integrator to ensure good low-frequency model following and disturbance rejection, as well as tolerance to output feedback uncertainty.

$$\mathbf{W}_1 = \frac{1}{s + 10^{-4}} \times I_3 \tag{6.2}$$

To ensure low high frequency control activity and robustness to high frequency unmodelled dynamics $\mathbf{W}_2$ was chosen in a similar way as suggested in [96], except our second breakpoint is slightly lower to reduce further high frequency control activity.

$$\mathbf{W}_2 = \frac{0.5s + 0.0005}{s + 7} \times I_3 \tag{6.3}$$

The ideal reference model was chosen as a decoupled diagonal transfer function matrix of second order ideal models.

$$\mathbf{M} = diag\{\mathbf{W}_{mr}, \quad \mathbf{W}_{mp}, \quad \mathbf{W}_{my}\} \tag{6.4}$$

where the roll, pitch and yaw ideal models are respectively

$$\mathbf{W}_{mr} = \frac{1}{0.15s^2 + 0.5s + 1} \tag{6.5}$$

$$\mathbf{W}_{mp} = \frac{1}{0.15s^2 + 0.5s + 1} \tag{6.6}$$

$$\mathbf{W}_{my} = \frac{1}{0.1s^2 + 0.35s + 1} \tag{6.7}$$

It is also worth noticing that our saturation element which models the series actuator limits may be decomposed as a linear term and a dead-zone element; that is

$$sat(u) = u - Dz(u) \tag{6.8}$$

and the dead-zone element can be treated as input multiplicative uncertainty. Thus using the *Small Gain Theorem* we can ascertain that the system will tolerate uncertainty of that form if

$$\|Dz(u)\|_{i,2} < \frac{1}{\|\mathbf{T}_i\|_\infty} \tag{6.9}$$

As $\|Dz(u)\|_{i,2} = 1$, the requirement is that $\|\mathbf{T}_i\|_\infty < 1$. As proved in the appendix, this is not possible, as T_i contains the open-loop unstable plant. As expected this implies no guarantees regarding global stability can be made (unstable systems are not globally null-controllable with bounded controls). However, as $Dz(u)$ is a monotonically increasing function of u, it attains its supremum at the supremum of u. Thus if u is restricted to a compact subset of the control space, say $\mathcal{U} \in \mathbb{R}^m$, then $\|Dz(u)\|_{i,2} < 1, \forall u \in \mathcal{U}$, which implies $\|\mathbf{T}_i\|_\infty \geq 1$ will give a region of local stability. The conclusion which may be drawn from this is that, even though global stability is not possible, the smaller $\|\mathbf{T}_i\|_\infty$ is, the larger the domain of local stability. In the $\mathcal{H}^\infty$ design, the shape of $\|\mathbf{T}_i\|_\infty$ is directly influenced by $\mathbf{W}_2$, so some control over local stability is obtained.

6.5 Anti-Windup Compensator Design

6.5.1 Restrictions on Compensators

Due to the low authority of the control system, one would intuitvely expect that, at moderate to high levels of aggression, the control signal would be saturated by the series actuators. Hence the choice of anti-windup strategy would be influential in the overall controller's performance.

Many methods of anti-windup compensation have been put forward in the literature, particularly in recent years. Unfortunately many of these methods require some conditions to be met before they can be applied. The chief difficulty with the situation here is that a large proportion of the existing anti-windup schemes assume that the controller is essentially *full authority*; many also assume that the anti-windup compensator can directly manipulate the plant input, whereas in this case it certainly cannot.

A quite viable class of the existing anti-windup schemes which can be used is the *model based* type, which was described in Chapter 2: the objective here is to introduce a *direct model* into the controller feedback loop when the control signal saturates - see figure 6.4 for this scheme in the limited authority format. One of the restrictions of this type of anti-windup compensators is that to ensure boundedness of certain signals, the direct model must be stable.

In this work use is made of the $\mathcal{H}^\infty$ -optimisation based direct model anti-windup compensation suggested in [15], which is convenient for several reasons.

- It fits into the direct model framework and hence only modifies the controller input.
- It is an inherently multivariable compensation method, and is thus well suited to the original multivariable controller
- It requires no additional assumptions on the plant or controller, which many anti-windup schemes stipulate (e.g. bi-properness, stablity etc.)
- Convenient to alter and re-design.

The one problem with this methodology is that the $\mathcal{H}^\infty$ optimisation procedure does not guarantee that $\mathbf{G}_m$ will be stable, although no problem has been found in achieving this in practice (see [15])

6.5.2 The $\mathcal{H}^\infty$ Anti-windup Method

As already mentioned this approach is a variant of the model-based type of anti-windup compensators, and has several features which make it attractive for our anti-windup problem. The

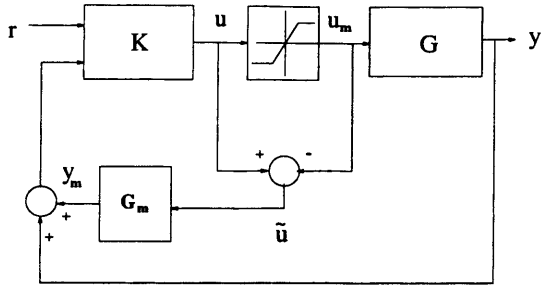

Figure 6.4: Model Based Anti-windup Scheme for the Limited Authority Configuration

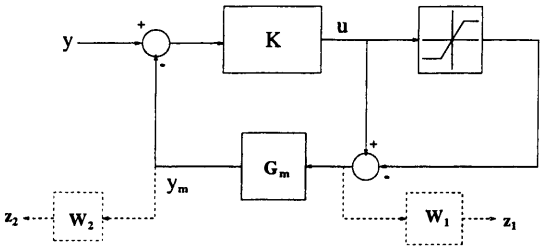

Figure 6.5: Additional Loop around Controller

method considers designing a direct-model which forms a loop around the feedback part of the controller only when saturation occurs. This is shown in Figure 6.5

Note that when saturation does not occur, the loop around the controller is not active as $sat(u) = u$ and hence $u - sat(u) = 0$.

The objective is to minimise two sets of signals in the $\mathcal{L}_2$ sense:

- $u - sat(u)$ - The difference between the control signal produced and that which will actually be fed into the plant. The smaller this signal is, the closer u and $sat(u)$ will be. To this end, $sat(u)$ is replaced by a *fictitious* disturbance signal, u_m.
- y_m - The signal, y_m, produced by the direct model. Ideally this should be as small as possible so not to corrupt the nominal behaviour of the controller too much.

Note that these two requirements are conflicting if the plant saturates as, to attenuate saturation as quickly as possible (making $u - sat(u)$ small), requires a large reaction from $\mathbf{G}_m$ and hence y_m will be large. It has been found that weighting $u - sat(u)$ with approximate integral action, or with a low pass filter, and using a constant weight on y_m can give satisfactory results: this tends to attenuate the effects of saturation fairly swiftly, and make the signal y_m gradually decay.

For the Mk7 Lynx helicopter it was observed that appoximate integral action with very slow poles ($s = -.01$) was not appropriate: although this type of weighting ensured a 'gracefully degraded' transient response, the system took a relatively long time (tens of seconds) to return

to nominal linear behaviour. This affected the outer loop responses detrimentally, as functions such as turn co-ordination did not function satisfactorily. Instead, the transient response was allowed to deteriorate more by using faster poles, which tended to introduce a more 'peaking' type of transient response. However these faster poles also tended to return the system to its linear regime more quickly, which had the knock-on effect of causing no degradation to the outer-loop functions.

Consequently, the weighting on $u - sat(u)$ was chosen as

$$\mathbf{W}_u = \frac{3}{s+1} \times I_3 \tag{6.10}$$

The weigthing on y_m was chosen as a constant, specifically

$$\mathbf{W}_y = 0.25 \times I_5 \tag{6.11}$$

6.6 Desktop Simulation

The resulting controllers were tested for both performance and robustness using linear and nonlinear models. The linear based tests were useful in assessing nominal performance and robustness to certain types of uncertainty; the nonlinear tests were useful for time domain tests which could determine a given controller's performance over different parts of the flight envelope, and also in evaluating the system's behaviour during series actuator saturation.

6.6.1 Linear-based Testing

Performance

Due to series actuator saturation limits, linear simulation could only accurately indicate performance for small reference demands. These reference inputs were normalised in the three controlled axes, with -1 indicating that the pilot inceptor was fully displaced in one direction, and $+1$ indicating full displacement in the opposite direction, assuming a centrally located stick datum, parallel actuator.

Figures 6.6, 6.7 and 6.8 show the linear responses and actuator demands for steps of 0.1 in all controlled channels. This level of demand was sufficiently small to ensure that series actuator saturation was avoided. It can be seen that fast response times are obtained with little off-axis coupling. The sensitivity function is shown in Figure 6.9. The sensitivity function approximately defines the low frequency tracking capability and we can see that for all channels our bandwidth is between 3 and 6 rad/s.

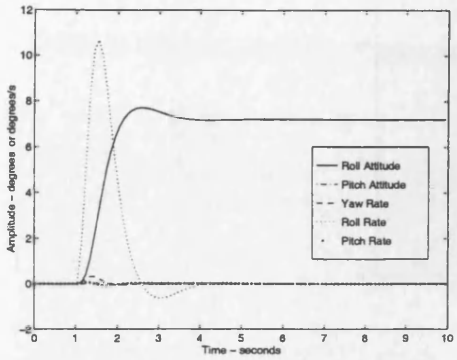

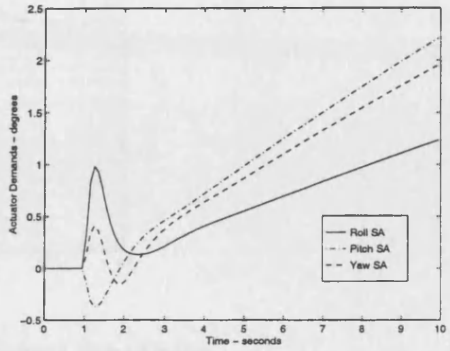

Output Response Series Actuator Reponses

Figure 6.6: Linear Response Due to Step in Roll Attitude

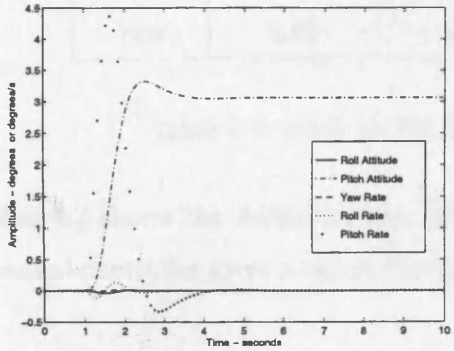

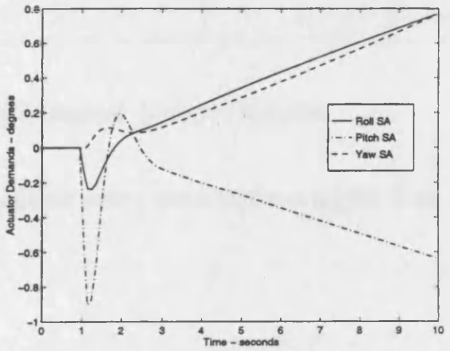

Output Response Series Actuator Reponses

Figure 6.7: Linear Response Due to Step in Pitch Attitude

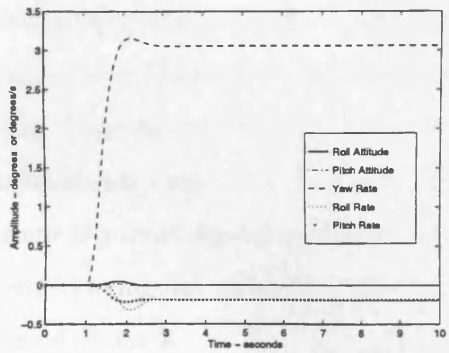

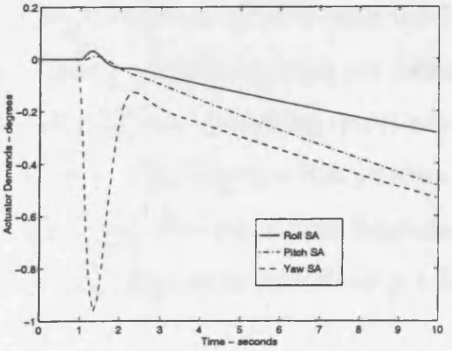

Output Response Series Actuator Reponses

Figure 6.8: Linear Response Due to Step in Yaw Rate

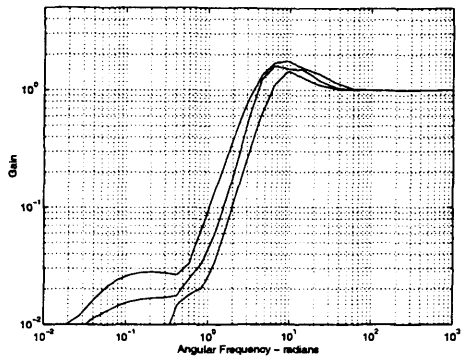

Figure 6.9: Singular Values of Input Sensitivity

Channel	Bandwidth	Phase Delay	HQ Level	
			Target Accquisistion	Other MTEs
Pitch	3.35	0.14	1	1
Roll	3.82	0.12	1/2	1
Yaw	5.87	0.02	1	1

Table 6.2: ADS-33 Handling Qualities of Nominal Linear Designs

Table 6.2 shows the ADS-33 bandwidths and phase delays; note that these suggest that the nominal controller gives a desired level of performance.

Robustness

For implementation on real aircraft, robustness is a required virtue of any control system, as modelling errors and omissions will inevitably occur. Figure 6.10 shows the closed-loop linear system's input *co-sensitivity* function, $\mathbf{T}_i$ and the function $\mathbf{S}_i\mathbf{K}_2$ plotted against angular frequency. These give indiciations of the system's robustness to input multiplicative and additive uncertainty respectively (for more detail see [27]). Note that the system in both cases is robust against these types of uncertainties at high frequencies, where modelling errors are likely to occur. Considering the graph of $\mathbf{T}_i$, the system is most vulnerable to modelling errors around the bandwidth where the frequency response peaks at about 2. The function $\mathbf{S}_i\mathbf{K}_2$ shows the system is robust against additive uncertainty at high frequncies, but not at low frequencies, where the singular values are fairly large [3]. Once again, close to the bandwidth there is a local peak of about 2.

The sensitivity function also imparts robustness information and in fact its peak defines the smallest output-feedback multiplicative uncertainty which can destabilise the closed loop sys-

[3]Note that is normally the case that modelling errors are not large at low frequencies

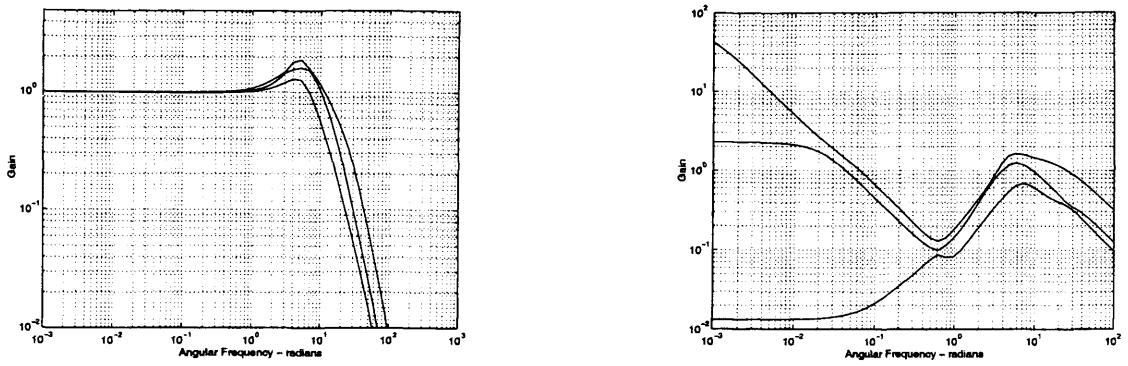

Input Co-Sensitivity S_iK_2

Figure 6.10: Singular Values of Input Co-Sensitivity and S_iK_2

tem. By perusing Figure 6.9 it can be seen that this appears around the bandwidth and thus there exists a perturbation of $\|\Delta\|_\infty = \|\Delta(j\omega_{bw})\| = \frac{1}{1.9}$ will de-stabilise the system. As this value is quite large, at this frequency it is unlikely.

6.6.2 Nonlinear Based Testing

Performance

Due to the presence of the stick-input dependent mechanical linkages, the parallel actuators and the saturating series actuators, as well as the actual flight-mechanic model nonlinearities, nonlinear simulation was considered the better way to assess performance: both of the controller and also of the anti-windup compensator.

Figures 6.11, 6.12 and 6.13 show the response, series actuator demand and total actuator demand for 8 second pulses of 0.35, 0.35 and 0.6 in the pitch roll and yaw axes respectively, with the aircraft near its nominal operating point of 10 knots. In all axes there is little inter-axis coupling and the responses are similar to those predicted in linear simulation. Notice that the series actuators saturate, quite extensively, but that the anti-windup scheme attenuates the effects well, suggesting that this functions correctly.

Robustness

The Lynx Mk7 has a flight envelope ranging from hover up to 160 knots over a wide variety of altitudes. Although one would expect a different behaviour from the aircraft at different speeds (one would not expect the helicopter to suddenly yaw 90 degrees at 150 knots), the controller should still impart a good level of functionality at those speeds distant from the nominal operating point.

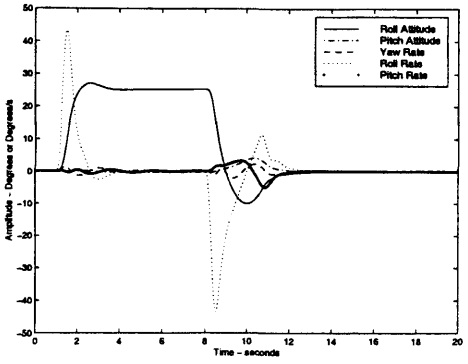

Output Response (10 knots)

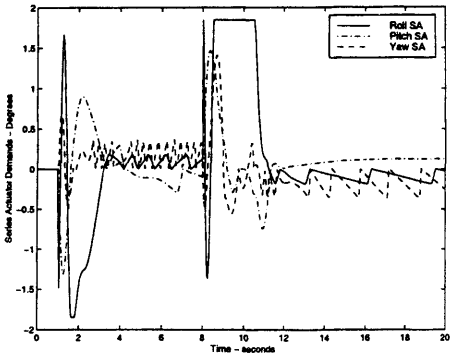

Series Actuator Reponses (10 knots)

Figure 6.11: Nonlinear Response Due to Pulse in Roll Attitude

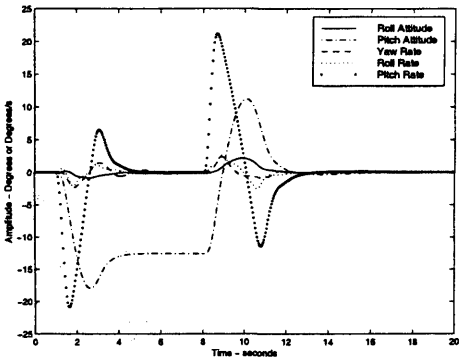

Output Response (10 knots)

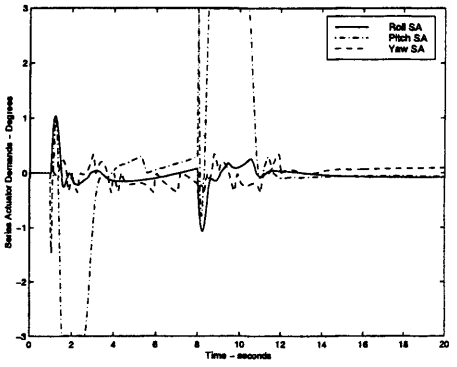

Series Actuator Reponses (10 knots)

Figure 6.12: Nonlinear Response Due to Pulse in Pitch Attitude

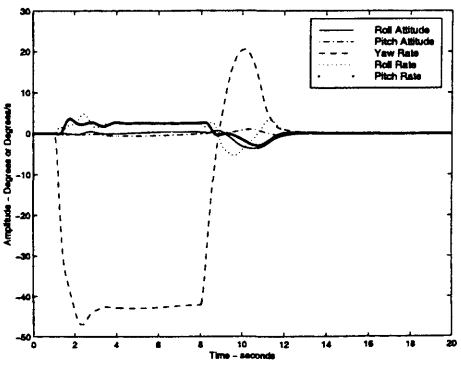

Output Response (10 knots)

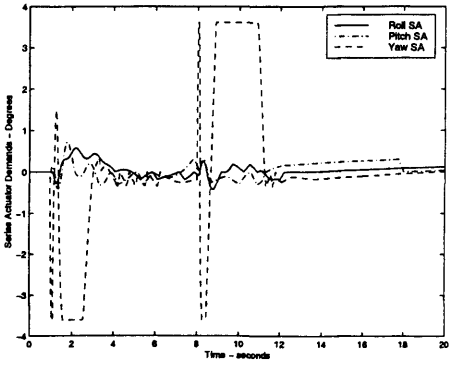

Series Actuator Reponses (10 knots)

Figure 6.13: Nonlinear Response Due to Pulse in Yaw Rate

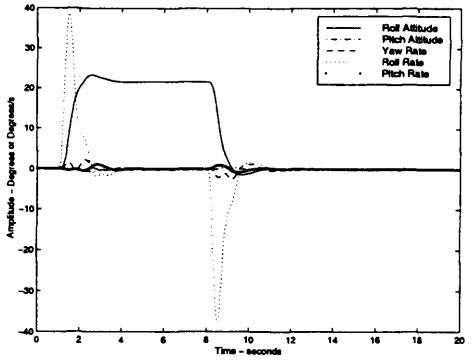

Output Response (160 knots)

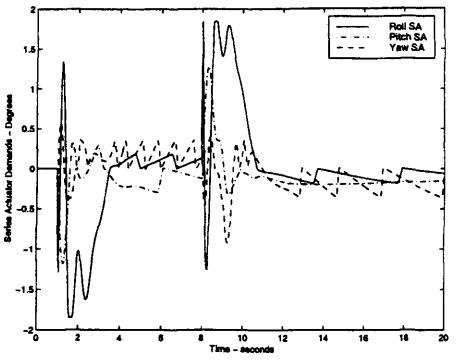

Series Actuator Reponses (160 knots)

Figure 6.14: Nonlinear Response Due to Pulse in Roll Attitude

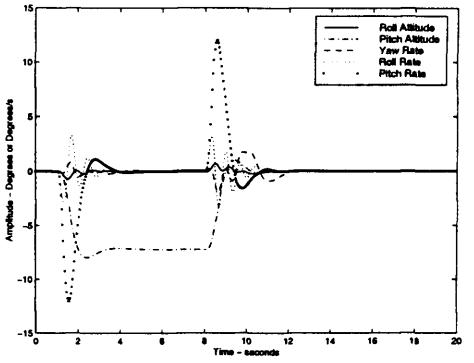

Output Response (160 knots)

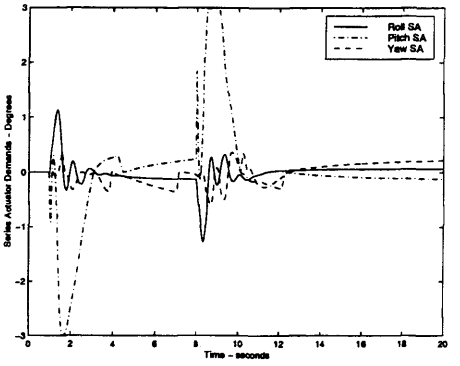

Series Actuator Reponses (160 knots)

Figure 6.15: Nonlinear Response Due to Pulse in Pitch Attitude

Figures 6.14, 6.15 and 6.16. show the aircraft behaviour at 160 knots, using the 10 knot controller and accepting steps of 0.3, 0.2 and 0.1 in roll, pitch and yaw respectively. It is apparent that even at this extreme point in the envelope that the system's performance remains close to that at the design point. This suggests that the controller has good robust stability and robust performance properties.

Series Actuator Saturation

As mentioned earlier, it is difficult to assess the impact of actuator saturation accurately on a linear model, due to the dependance on flight condition of the mechanical linkages. However, with a limited authority system, this assessment is clearly necessary, as the series actuators are expected to saturate during aggressive flight.

Figures 6.17, 6.18 and 6.19 show the responses of the system during actuator saturation in all three channels (8 second pulses of demands of 0.4, 0.3 and 0.7 in roll, pitch and yaw respectively). This nonlinear simulation did not have any anti-windup scheme fitted and it is evident that the system behaves poorly in all three cases. Although initially, the system's behaviour seems satisfactory, in both the roll and yaw axes it is evident that stability is actually

lost; in the pitch axis an undesirable oscillatory characteristic can be seen.

Figures 6.20, 6.21 and 6.22 show the system's responses to the same levels and duration of pulse inputs, but this time with the proposed anti-windup scheme fitted. In this case the system's behaviour degrades somewhat less, and although a deviation from linear behaviour is noticeable, it is considered tolerable. In fact, the system with the anti-windup scheme can tolerate substantially larger inputs than without, although it is not expected it will able to maintain stability for all pilot inputs due to the low authority of the controller and the fact that the helicopter has open-loop unstable modes [4]

As the helicopter is *not* globally null-controllable with bounded controls (see Chapter 2), there are states from which *any* controller - linear or nonlinear - cannot stabilise the system.

[4]If a system has open-loop unstable modes, it's null-controllable set is the Cartesian product of its anti-stable and semi-stable controllable sets - see [36].

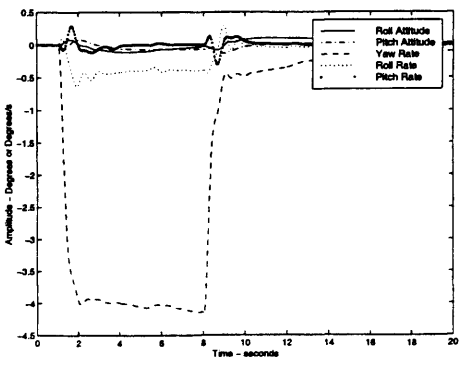

Output Response (160 knots)

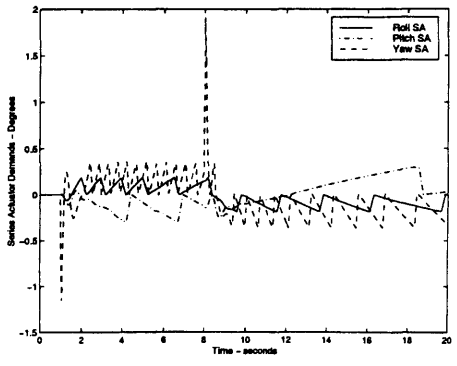

Series Actuator Reponses (160 knots)

Figure 6.16: Nonlinear Response Due to Pulse in Yaw Rate

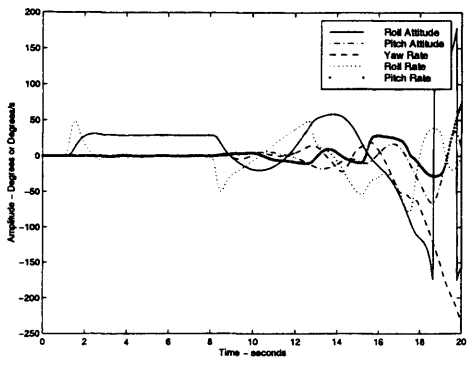

Output Response (10 knots)

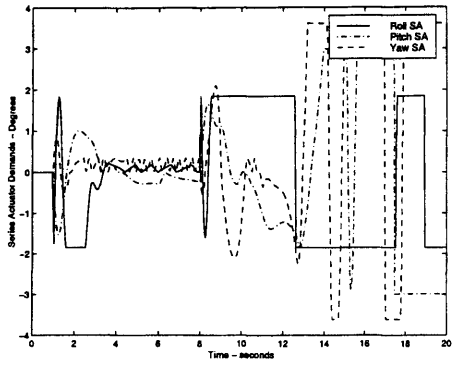

Series Actuator Reponses (10 knots)

Figure 6.17: Nonlinear Response Due to Pulse in Roll Attitude, without Anti-windup Compensation

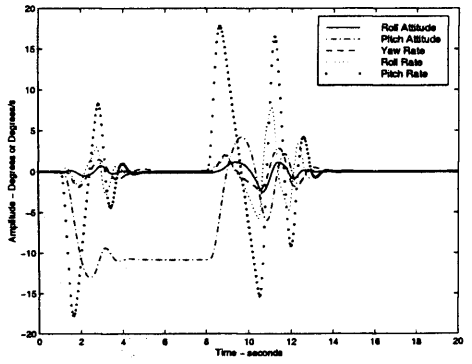

Output Response (10 knots)

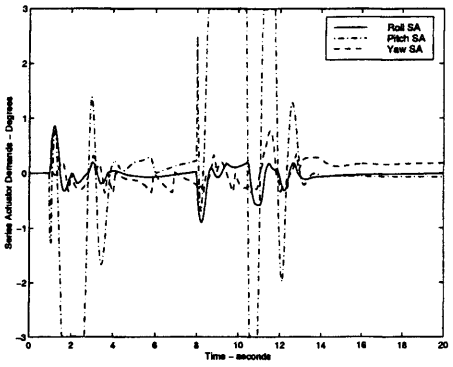

Series Actuator Reponses (10 knots)

Figure 6.18: Nonlinear Response Due to Pulse in Pitch Attitude, without Anti-windup Compensation

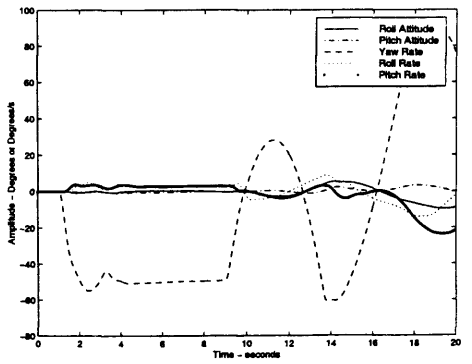

Output Response (10 knots)

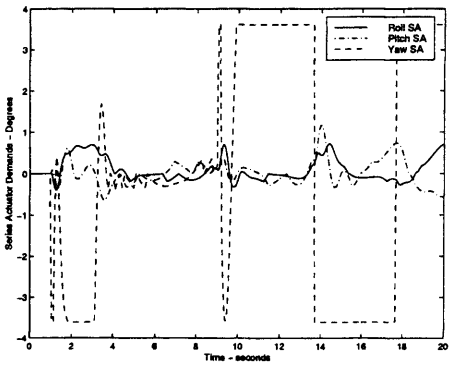

Series Actuator Reponses (10 knots)

Figure 6.19: Nonlinear Response Due to Pulse in Yaw Rate, without Anti-windup Compensation

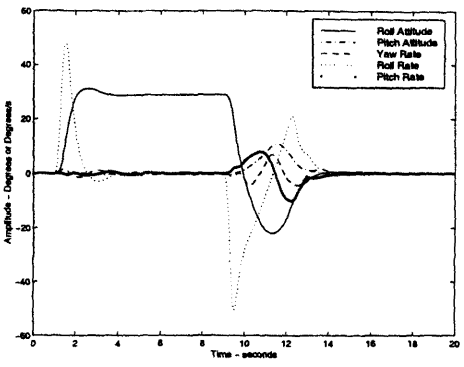

Output Response (10 knots)

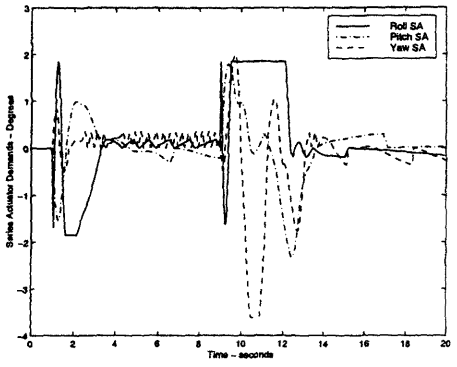

Series Actuator Reponses (10 knots)

Figure 6.20: Nonlinear Response Due to Pulse in Roll Attitude, with Anti-windup Compensation

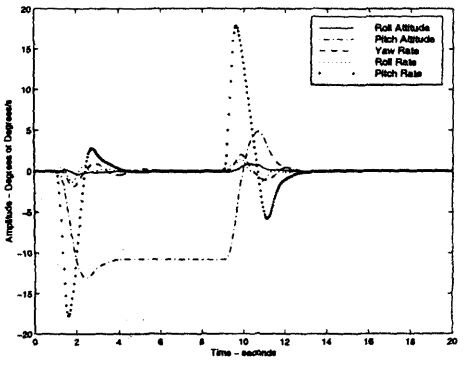

Output Response (10 knots)

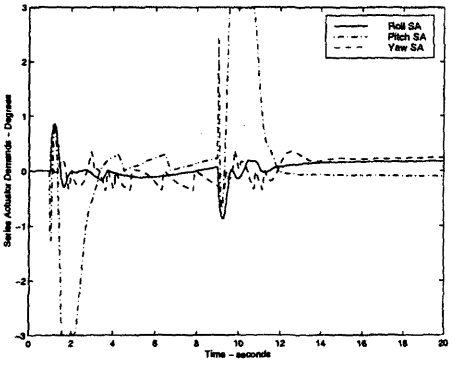

Series Actuator Reponses (10 knots)

Figure 6.21: Nonlinear Response Due to Pulse in Pitch Attitude, with Anti-windup Compensation

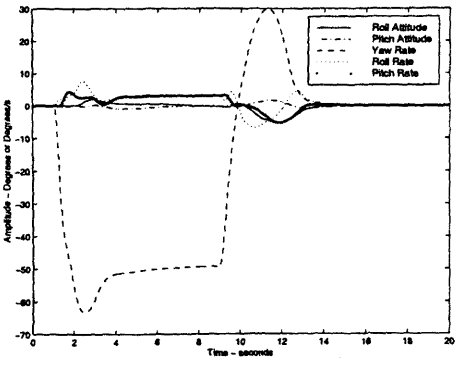

Output Response (10 knots)

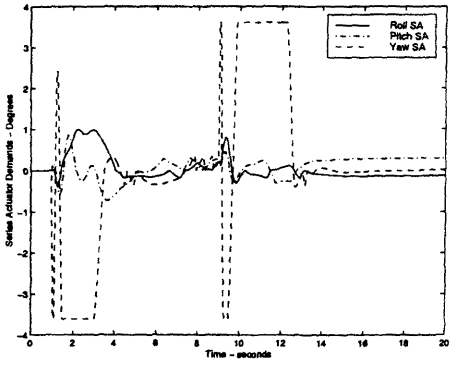

Series Actuator Reponses (10 knots)

Figure 6.22: Nonlinear Response Due to Pulse in Yaw Rate, with Anti-windup Compensation

6.7 Piloted Simulation

6.7.1 The Westland Simulator

The Advanced Engineering Simulation Facility (AESF) at GKN Westland Helicopters is a fixed-base real-time research flight simulator that attempts to emulate the behaviour of an actual aircraft through the use of visuals which, in conjunction with a mathematical model of the helicopter, allow the pilot to fly around in a virtual environment.

The simulator itself consists of a cockpit, containing all the usual helicopter controls, a display of the primary flight instrumentation, and a concave screen, onto which is projected the virtual outside world. Pilot inceptor movement produces a signal which is fed into a network of Silicon Graphics computers; these then use the mathematical models of the helicopter and controller to derive an apparent movement of the helicopter, which is then displayed on the screen or delivered to the cockpit display. All flying controls have parallel actuators (like a real Lynx) so they can, if desired, have their spring datums driven either manually or automatically.

No motion is featured, but the large visual display and fairly faithful (at low aggression) reproduction of an actual helicopter's movement, does instill in the pilot the partial belief of flying in a real aircraft. Nevertheless, the AESF does tend to be better at reproducing certain helicopter manouevres than others: its 45 degrees vertical field of view restricts the severity of pitch manoeuvres; and the 30Hz visual system causes the projected terrain/objects to move in an unsmooth fashion during high angular/translational rates.

6.7.2 The Tasks

In order to point out the controller's merits or deficiencies several mission task elements (MTEs) were performed. Due to some of the simulator's short comings, it was decided against doing a full ADS-33 evaluation, but several of the tasks were taken from that document and assessed. The Lynx Mk7's current limited authority control system was also tested concurrently, to enable a comparison (also tested was a gain-scheduled full authority controller, the results of which will be reported elsewhere). The tasks chosen are the same as in Chapter 4, but are elaborated on slightly below

Accel/Decel	The Pilot accelerated from hover to 80 knots, at a height 17m above a straight road, for 500m; cruising for another 500m; then decelerating to hover over the next 500m
Pirouette	Helicopter pirouetted around a circle of radius 60m
Pedal Turn	equivalent to ADS-33 turn to target
Side Step	500m lateral translation at 17m above ground level
Hurdles	flying helicopter along straight road alternating between heights of 14 and 32 metres. Hurdles 210m apart and flown at 70 and 140 knots
Slalom	Pilot follows meandering road while maintaining height between 14 and 20m above ground. Flown at 70 and 140 knots.

6.7.3 Task Results

The pilot carried out the tasks several times for each controller, and was asked to rate, objectively, the best completion of each task for each controller. By no means conclusive, this enabled an impression of the performance of the limited authority controller and also enabled a comparison with the standard Mk7 Lynx.

Rating	Task Cues	Level of Aggression	Performance	Workload
1	Inadequate	Minimal	Adequate performance not achievable	Minimal
2	Poor	Low	Adequate performance marginally achievable	Moderate
3	Fair	Moderate	Clearly within adequate performance limits	Considerable
4	Good	High	Desired performance marginally achievable	Extenisve
5	Excellent	Maximum	Clearly within desired performance limits	Intolerable

Table 6.3: Key to ratings

Task	Rating							
	Cues		Agression		Performance		Workload	
	$\mathcal{H}^\infty$	Mk7	$\mathcal{H}^\infty$	Mk7	$\mathcal{H}^\infty$	Mk7	$\mathcal{H}^\infty$	Mk7
Accel/Decel	3	3	4	4	4	4	3	3
Pirouette	2	2	3	3	4	4	2	2
Pedal Turn	3	3	4	4	3	5	2	2
Side-step	2	2	4	4	4	4	2	2.5
Hurdles (70 knots)	4	4	3	4	5	5	2	2
Slalom (70 knots)	4	4	4	4	4	5	3	3
Hurdles (140 knots)	4	4	4	3	4	3	2	2
Slalom (140 knots)	4	4	4	4	4	3	3	3

Table 6.4: Piloted Evaluation Results

Tables 6.3 and 6.4 show the results for all tasks performed for both the novel $\mathcal{H}^\infty$ limited authority controller and the standard Lynx mk7. By perusing the table, the results suggest that

- The pilot's conception of the two controllers does not appear to be vastly different
- In certain tasks, notably those at high agression, the $\mathcal{H}^\infty$ controller out-performed the standard controller; in other tasks the standard controller out-performed the $\mathcal{H}^\infty$ controller
- Care has to be taken when interpreting the results of the first four manouevres; the relatively poor cues could easily affect the ratings given.

It should be noted that this table of results is fairly crude. Certain anomallies ocurred during the trial, which were not objectively rated. In particular, during some informal flying, the pilot stated that he preferred the yaw handling of the $\mathcal{H}^\infty$ controllers - a result which did not manifest itself during the evaluation, as from the pedal turn ratings, it is plain that he preferred the standard Lynx. Also, as the controllers were tested back-to-back, the pilot was arguably not given enough time to completely familiarise himself with the $\mathcal{H}^\infty$ controller, and so was expecting it, subconsciously, to perform identically to the standard Lynx. When the differences did occur, he may have been unsettled by them and consequently rated the $\mathcal{H}^\infty$ controller lower than it may have deserved.

The overall conclusion from the piloted simualtions is that they represent an impression of the type of handling qualities achievable with $\mathcal{H}^\infty$ optimisation, and that the comparisons with the standard Lynx should not be taken as definitive.

As aforementioned, it was not really possible to rigorously test the controllers at high levels of aggression due to the limitations of the simulator, so no conclusions can be drawn about the $\mathcal{H}^\infty$ control system's performance under these conditions, or how it compares with the standard Lynx. Note that at high levels of aggression, the control system loses some of its ability to stabilise the loop, and thus the stabilisation is performed by the pilot in an "outer-loop".

6.8 Conclusion

This chapter has discussed the design, desktop testing and piloted simulation of a limited authority control system for the Lynx helicopter based on $\mathcal{H}^\infty$ optimisation. The controller was linear-time-invariant, yet offered a high degree of robustness over a wide range of flight conditions. In particular, it showed the ability to suppress some of the undesirable behaviour caused by saturation, which is inevitable in such a configuration.

Piloted simulation was successful in the sense that, for relatively un-aggressive manoeuvres, the pilot reported favourable handling qualities ratings for $\mathcal{H}^\infty$ controller. What is less clear, and in need of future research, is how the $\mathcal{H}^\infty$ controller performs during highly aggressive manoeuvering. The comparisons to the standard Lynx control system are considered a useful excercise, but fairly inconclusive. Future work should also include a more thorough comparison, with ample time for the pilot to accustom himself to the non-standard $\mathcal{H}^\infty$ control system.

Chapter 7

Bell 205: Control Law Design and Implementation

7.1 Overview

This chapter describes the control law design for and subsequent flight test of the NRC modified Bell 205-A fly-by-wire helicopter. Documented here are the results of linear simulations and robustness tests, together with extracts from analysis of some of the actual data collected during some of the flight tests. The outcome of the flight test is described and compared with the predictions made by various pre-flight desk-top tests. This chapter describes part of an on-going investigation into robust control of helicopters and additional material can be found in [90] and [91].

7.2 Introduction

In Chapter 5 it has already been mentioned that the Bell 205's timely availability as a test-bed for $\mathcal{H}^\infty$ control laws allowed an up-tempo movement in the study of robust control for helicopters. This began with controllers, designed using NASA linearisations and the $\mathcal{H}^\infty$ loopshaping methodology, being tested on the modified Bell 205 helicopter. The outcome of these tests are described in [67] but, in summary, although stability and rudimentary functionality was achieved with such control laws, performance was still some way from 'desirable'.

Even when new, supposedly higher fidelity, models of the helicopter were provided by DERA, the performance achieved in the resulting flight tests was still less than expected. It seemed to be the case that, even though the DERA model predicted coupling somewhat more faithfully than the NASA version, its ability to predict this accurately was severely limited. This inability to predict cross-couplings, together with the multivariable nature of the controller design, made the iterative design of controllers, which gave rise to a de-coupled response in the air, problematic.

This chapter builds on lessons learned in the three previous $\mathcal{H}^\infty$ control law flight tests on the NRC Bell 205, and attempts to use a different structure for controller design and implementation. The results have been partially reported in [90] and [91], although many ideas are new and some are inherited from [96]. The work here departs from the work of [68] in several key respects:

- The longitudinal and lateral dynamics are *decoupled* during the design phase: the resultant controller is actually two separate $\mathcal{H}^\infty$ controllers.
- Although the models used contained rotor dynamics, they were *residualised* [1] and the residualised model used as a design linearisation.
- Rather than use the normalised coprime factor approach to design, the synthesis algorithm used the S/KS procedure, more akin to that of [96].

The reason for some of the approaches will become clearer throughout the discussion, but as the results demonstrated, they lead to arguably the best performing $\mathcal{H}^\infty$ controllers tested in-flight to date.

The chapter is organised as follows. First the Bell 205 is briefly described, followed by a description of the control law design. Various simulation results are then presented before a summary of flight test results and an analysis are given. The chapter ends with some concluding remarks and suggestions for future work.

7.3 The NRC Bell 205

The Bell 205 helicopter operated by the NRC, Canada is an advanced experimental fly-by-wire helicopter which allows the testing of various advanced control techniques through use of a flight control computer. It is not the objective of this thesis to exhaustively describe this complex machine and several texts such as [67] and [73] describe it in more detail. In particular, the reader interested in technical detail regarding the helicopter is referred there.

The NRC Bell 205 is a multi-purpose helicopter, with a top speed of around 150 knots and the ability to operate in a wide variety of flight conditions. The NRC version of the aircraft has several important modifications which standard versions lack. From an aerodynamic point of view the major difference is the absence of the stabiliser bar on the fuselage; this makes the helicopter more unstable, but allows it to perform more agile maneouvres.

[1] Replaced with their DC values

To facilitate the implementation of advanced control features, the helicopter is fully fly-by-wire: movement of the pilot inceptors affects a hydraulic actuator via electrical signals. The centre of the fly-by-wire system is the flight control computer which enables advanced control laws to be used and several control strategies stored for evaluation. The computer allows in-flight alteration of the control laws, and also allows a 'manual' mode, where the actuators behave as in a purely mechanical system.

Being an experimental test-bed, the NRC Bell 205, also is equipped with a wide range of sensors - some which are used for feedback in the controller - and recording equipment which enables the logging of data and monitoring of the helicopter's flight condition. Some of these sensors are known to be unreliable, in some parts of the flight envelope, and (see later) various strategies have been devised to overcome this.

Mixed Rate Feedback

A unique feature of the NRC's Bell 205 is the option of 'mixed rate' feedbacks. Practical experience has shown that the use of mixed rates rather than the purely measured rates imparts greater stability and performance potential to the helicopter - see [3].

The Bell's rotor can be modelled as a pure time delay of 120-180mS between control input and aircraft response. In addition the measured rates are not pure and when used as feedback can transmit unwanted structural modes to the controller. This large time delay and significant model uncertainty restricts the amount of bandwidth achievable; the idea of mixed rates was introduced to remedy the problem.

The mixed rate is a composite signal consisting of low frequency components from the measured rate, together with high frequency components constructed a model of the helicopter. It is described below

$$p_{mix} = p_{measured}\frac{\alpha}{s+\alpha} + p_{model}\frac{s}{s+\alpha} \tag{7.1}$$

The high pass filter is driven by a first order on-axis control prediction model response to the appropriate actuator input

$$p_{model} = \frac{a}{s+b}\delta_{act} \tag{7.2}$$

This process results in a clean signal, which is essentially the result of prediction at frequencies beyond approximately 11.5 radians/s. All designs described here were not robust enough to

function without mixed angular rates (i.e. the q and p signals used were actually q_{mix} and p_{mix}).

7.3.1 Mathematical Models

DERA Models

The work described in this thesis makes use of the mathematical models of the NRC Bell 205 described in [73]. These are models derived from flight-test data and inserted into the DERA generic HELISIM helicopter model; a nonlinear flight-mechanic model based primarily on the rigid-body equations of motion, but with the ability to incorporate extra dynamics such as those of the rotor, for example. Linearisations were extracted from this nonlinear model, and the 20 knot version formed the basis of the control law design.

The full nonlinear model had the following states, ordered the same as given in the nonlinear model:

$\psi, \theta, \phi, u, v, w, p, q, r, x_{\delta_0}, x_{\delta_{1s}}, x_{\delta_{1c}}, x_{\delta_{tr}}$, +6 rotor states

However due to prior experience it was thought prudent to take the following steps to alter these models. The idea was to improve the likelihood of a controller yielding better performance being designed.

1. **Residualisation**. HELISIM is largely a rigid-body based flight mechanic model and previous experience had shed doubt on whether it was able to predict accurately the rotor dynamics. It was therefore decided to *residualise* these dynamics (replace them with their steady-state value), although it was accepted that this could also have a detrimental effect, as it would remove the 'transport-delay' type of prediction in the model.

2. **Decoupling**. Again, experience had shed doubt on the DERA models' ability to correctly indicate off-axis coupling which is so important in helicopter control law design. In fact in the report [73], there is acknowledgement of the poor coupling predicted in some axes. Yaw-pitch coupling is cited as being particularly bad. In an effort to remedy this, the lateral and longitudinal dynamics were thus decoupled, so that the overall control law consisted of one SISO longitudinal controller and one MIMO lateral controller.

Thus the design linearisations consisted of two parts: the residualised lateral dynamics and the residualised longitudinal dynamics. The states, inputs and outputs are shown below.

States	θ	Pitch Attitude	radians
	q	Pitch Rate	radians/s
	u	Longitudinal Velocity	ft/s
	w	Vertical Velocity	ft/s
	$x_{\delta_{1s}}$	Long. cyclic actuator	radians
Outputs	θ	Pitch Attitude	radians
	q	Pitch Rate	radians/s
Inputs	δ_{1s}	Longitudinal Cyclic	radians

Table 7.1: Longitudinal DERA Model

States	ϕ	Roll Attitude	radians
	p	Roll Rate	radians/s
	r	Yaw Rate	radians/s
	v	Lateral Velocity	ft/s
	w	Vertical Velocity	ft/s
	$x_{\delta_{1c}}$	Lat. cyclic actuator	radians
	$x_{\delta_{tr}}$	Tail rotor actuator	radians
Outputs	ϕ	Roll Attitude	radians
	r	Yaw Rate	radians/s
	p	Roll Rate	radians/s
Inputs	δ_{1c}	Lateral Cyclic	radians
	δ_{tr}	Tail Rotor Collective	radians

Table 7.2: Lateral DERA Model

NASA Models

Also available were a set of NASA linearisations, described in [32]. These were generally regarded as of inferior quality (although this is by no means certain) to those supplied by DERA, and included only rigid body dynamics. Furthermore, they were based on a version of the Bell 205 which did not have its stabiliser bar removed. However, they represented a comparison to the DERA models and were routinely used to validate control laws at the NRC Flight Research Lab. Comparisons will be made with these models at the appropriate point.

The inputs, outputs and states of the NASA models are given in Table 7.3.

The units used in the models vary, but generally speaking a reasonably robust controller designed using the DERA models, as a rule works on the NASA models, although the converse

States	ϕ	Roll Attitude	radians
	θ	Pitch Attitude	radians
	p	Roll Rate	radians/s
	q	Pitch Rate	radians/s
	r	Yaw Rate	radians/s
	u	Longitudinal Velocity	ft/s
	v	Lateral Velocity	ft/s
	w	Vertical Velocity	ft/s
Outputs	ϕ	Roll Attitude	radians
	θ	Pitch Attitude	radians
	r	Yaw Rate	radians/s
	p	Roll Rate	radians/s
	q	Pitch Rate	radians/s
Inputs	δ_{1c}	Lateral Cyclic	cm
	δ_{1s}	Longitudinal Cyclic	cm
	δ_{tr}	Tail Rotor Collective	cm

Table 7.3: NASA Model

tends not to be true.

7.4 Control Law Design

As aforementioned, the controllers designed were based on the $\mathcal{H}^\infty$ mixed sensitivity design paradigm, which, in the author's opinion is a fairly flexible design procedure. While possibly not having the same enviable robustness properties of so-called $\mathcal{H}^\infty$ loopshaping controllers, flexibility is given by the ability to *explicitly* weight *closed loop* transfer functions, rather than merely to frequency shape open loop ones in the LSDP. In other words, the cost-function minimised in the $\mathcal{H}^\infty$ optimisation procedure can be moulded quite easily to fit robustness *and* performance design criteria directly.

There are however a number of pitfalls to $\mathcal{H}^\infty$ mixed sensitivity controllers such as inability to cope with zeros on the imaginary axis and a tendency to cancel the plant zeros, which can sometimes give rise to undesirable lightly damped modes. However, generally speaking these effects were not observed, although remarks about these will be made later.

The specific type of $\mathcal{H}^\infty$ mixed sensitivity we chose to use was the S/KS procedure, where a (suboptimal) controller K was sought, such that

$$\left\| \begin{array}{c} \mathbf{W_1 S} \\ \mathbf{W_2 KS} \end{array} \right\|_\infty \leq \gamma \tag{7.3}$$

where γ is some small number close to the minimal; $\mathbf{W}_1$ and $\mathbf{W}_2$ are some frequency dependent weighting functions; and where the minimisation is performed over all stabilising $\mathbf{K}$. Generally speaking, as described in Chapter 2, one tries to choose $\mathbf{W}_1$ as a low pass filter to ensure good tracking, disturbance rejection and robustness to output multiplicative uncertainty at low frequency; and $\mathbf{W}_2$ as a high-pass filter to ensure resistance to noise and robustness against high-frequency unmodelled dynamics.

7.4.1 Longitudinal Controller

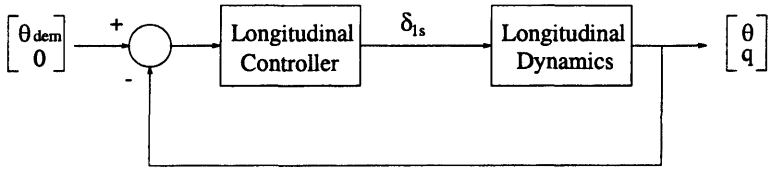

Figure 7.1: Longitudinal Control System

The longitudinal controller was essentially a SISO design: the controlled output was pitch attitude, with longitudinal cyclic being the input. To enhance the performance, pitch rate was also fed back to increase the damping. The configuration used for design is shown in Figure 7.1.

The origins of the type of weighting functions used can be traced back to [97], who also considered the S/KS design procedure. Specifically, the $\mathbf{S}$ weight was chosen to be of the form

$$\mathbf{W}_1 = \begin{bmatrix} \mathbf{W}_{1p} & 0 \\ 0 & \mathbf{W}_{1\dot{p}} \end{bmatrix} \tag{7.4}$$

$$\mathbf{W}_{1p} = k_1 \frac{s + \alpha_1}{s + \beta_1} \tag{7.5}$$

$$\mathbf{W}_{1\dot{p}} = k_{1\dot{p}} \frac{s}{s + \beta_1} \tag{7.6}$$

where β_1 was chosen very small to enforce approximate integral action (a true integrator would not satisfy the standard assumptions laid out in the Chapter 2). The bandwidth of this weight determines the approximate tracking bandwidth of the nominal closed loop system. The combination of k_1 and α_1 was used to limit the magnitude of the sensitivity peak, which is known to impair robustness (see [27] for a discussion of the waterbed effect).

$\mathbf{W}_2$ was chosen to be of the form

$$\mathbf{W}_2 = k_2 \frac{s+\alpha_2}{s+\beta_2} \tag{7.7}$$

As noted before this was chosen as a high pass filter to enforce robustness to unmodelled or poorly modelled dynamics at high frequency. Again, in order to satisfy the standard assumption, it was chosen as proper rather than stricly proper, by making β_2 level off its response at high frequencies.

Several iterations were performed on this controller, before the following final choices were made for the weights:

$$\mathbf{W}_{1p} = \frac{0.5}{s+0.01} \tag{7.8}$$

$$\mathbf{W}_{1\dot{p}} = \frac{s}{s+0.01} \tag{7.9}$$

$$\mathbf{W}_2 = 2\frac{s+0.001}{s+5} \tag{7.10}$$

In addition, for design the rate and attitude outputs were both scaled by a diagonal matrix $diag\,\{0.2, 0.2\}$. A diagram of the design procedure is shown below in Figure 7.1. The resulting controller was of 8th order and was implemented in discrete-time using a zero-order-hold.

7.4.2 Lateral Controller

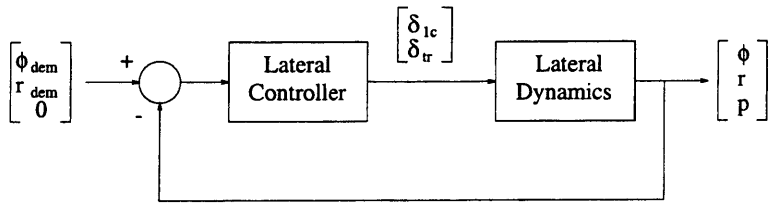

Figure 7.2: Lateral Control System

The lateral controller was a MIMO system: its controlled outputs were roll attitude and yaw rate, and its inputs were lateral cyclic and tail rotor collective. Also, the roll rate was fedback to improve performance as with the longitudinal case. The system used for design is shown in Figure 7.2.

The sensitivity weight was chosen to be of the form

$$\mathbf{W}_1 = \begin{bmatrix} \mathbf{W}_{1r} & 0 & 0 \\ 0 & \mathbf{W}_{1y} & 0 \\ 0 & 0 & \mathbf{W}_{1\dot{r}} \end{bmatrix} \tag{7.11}$$

where

$$\mathbf{W}_{1r} = k_{1r}\frac{s+\alpha_{1r}}{s+\beta_{1r}} \tag{7.12}$$

$$\mathbf{W}_{1\dot{r}} = k_{1\dot{r}}\frac{s}{s+\beta_{1r}} \tag{7.13}$$

$$\mathbf{W}_{1y} = k_{1y}\frac{s+\alpha_{1y}}{s+\beta_{1y}} \tag{7.14}$$

The diagonal nature of the weight was intended to ensure decoupling for frequencies below the bandwidth. The components of $\mathbf{W}_{1r}$ and $\mathbf{W}_{1y}$ were chosen with the same rationale as the $\mathbf{W}_1$ weight for the longitudinal design.

Similarly, the **KS** weight, $\mathbf{W}_2$, was chosen as

$$\mathbf{W}_2 = \begin{bmatrix} \mathbf{W}_{2r} & 0 \\ 0 & \mathbf{W}_{2y} \end{bmatrix} \tag{7.15}$$

where

$$\mathbf{W}_{2r} = k_{2r}\frac{s+\alpha_{2r}}{s+\beta_{2r}} \tag{7.16}$$

$$\mathbf{W}_{2y} = k_{2y}\frac{s+\alpha_{2y}}{s+\beta_{2y}} \tag{7.17}$$

with the diagonal nature reflecting the decoupling required. These transfer functions were chosen in the same manner as for the longitudinal controller.

The final choices for the weights was

$$\mathbf{W}_{1r} = 0.3\frac{s+0.5}{s+0.01} \tag{7.18}$$

$$\mathbf{W}_{1y} = 0.3\frac{s+0.5}{s+0.01} \tag{7.19}$$

$$\mathbf{W}_{1\dot{r}} = \frac{s}{s+0.01} \tag{7.20}$$

$$\mathbf{W}_{2r} = 2\frac{s+0.001}{s+4} \tag{7.21}$$

$$\mathbf{W}_{2y} = 2\frac{s+0.001}{s+4} \tag{7.22}$$

In addition, the outputs, roll attitude, yaw rate and roll rate, were scaled, respectively, by the matrix $diag\{0.2, 0.2, 0.4\}$.

7.4.3 Pole-Zero Cancellations

One of the possible problems with $\mathcal{H}^\infty$ mixed sensitivity design is that pole-zero cancellations are likely to occur. The controller often approximately cancels stable plant zeros with some of its poles. This can lead to problems if lightly damped zeros are present, as this approximate cancellation can, in practice, allow lightly damped modes to be observed in the resulting closed loop.

The model of the longitudinal dynamics had two minimum-phase zeros located at $s = -0.5719$ and $s = -0.0304$, which were duly cancelled by longitudinal controller poles at the same locations (to four decimal places). Zeros located at $s = -0.5402$ and $s = -0.0055$ were present in the model of the lateral dynamics and were cancelled by lateral controller poles at the same locations (to three decimal places).

In both cases, as the cancellations took place on the real axis, undesirable effects caused by light damping were thought to be unlikely.

7.5 Simulation Results

The vital simulation part of the design procedure took essentially two forms: linear simulation and nonlinear simulation. Due to the known uncertainty of the model, more notice was taken of information from the linear simulations - which can give important information such as stability margins, bandwidths and phase delays - than the nonlinear simulations, whose contribution is really only time history plots.

7.5.1 Linear DERA Simulations

These simulations provided, along with pilot comment, the cornerstone of the post-design analysis. As aforementioned, the linear analysis of designs contributes information such as stability margins and bandwidths, which allows the engineer to make important judgements about robustness and performance. In particular, the ADS-33 definitions of 'bandwidth' and 'phase delay' were used to assess the likely performance of the aircraft.

The controller being used for the time domain simulations is the discretised version (using a zero-order-hold and sample period of 1/64 second) of the controller designed using the continuous time $\mathcal{H}^\infty$ optimisation procedure. The frequency response plots were obtained using the purely continuous time controllers and plants.

Residualised Simulation

This consisted of separate simulations for longitudinal and lateral axes on residualised models. This represented the nominal design point and intuitively the expectation is that the responses should be relatively 'good'. The frequency responses of both the longitudinal and lateral controllers look acceptable (Figures 7.3 and 7.6) with the singular value plots of the co-sensitivities suggesting good robustness to high frequency unmodelled dynamics and uncertainty. Similarly the sensitivity plots suggest good disturbance rejection characteristics and the small peak in both cases means good tolerance of output multiplicative feedback uncertainty.

The step responses are not as encouraging as shown in Figures 7.5 - 7.7. Although the approximate integrator used in the $\mathbf{W}_1$ weight ensures approximately zero-steady state error to step inputs, the transient response does not look particularly well damped and the rise-time is quite slow. This is explained by the iterative way in which the weights were chosen. Using a higher gain $\mathbf{W}_1$ gave better responses in simulation, but often lead to an unstable aircraft in practice! This suggested that the open-loop gain on the real helicopter was greater than that predicted by the DERA model, which caused the weights above to be chosen.

The ADS-33 bandwidths and phase delays predicted at the nominal design point are shown in Table 7.4. Along with the time responses, these values suggest performance which is below level 1, although the severe model uncertainty - discussed later - meant that in pitch and roll, the obtained bandwidths were actually well into level 1.

Coupled Simulation

This consisted of a combined simulation of lateral and longitudinal controllers on a coupled residualised model, obtained from the DERA nonlinear flight-mechanic model. The simulation attempted to replicate the real implementation, which is shown in Figure 7.8

Figure 7.9 shows the frequency responses plots for this simulation. Note that the co-sensitivity plot is relatively good, with broad agreement with the de-coupled version. Again the low gain at high frequency suggests that the closed loop has certain robustness properties. The sensitivity plot is not as encouraging as at very low frequency (below 10^{-3} rad/s), one of the singular values actually lies above the zero dB point, which represents poor low frequency disturbance rejection and vulnerability to output feedback multiplicative uncertainty.

Indeed this is reinforced by inspecting the time responses (Figures 7.10 - 7.11), in particular the response to a step in yaw results in severe steady state error both the yaw and roll channels. Generally the step responses are not adequate in this simulation, with poorly damped and poorly decoupled responses resulting. However, as aforementioned, heavy doubt was placed on

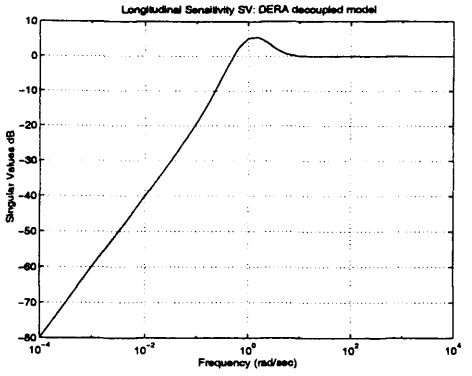

Sensitivity Singular Value Plot

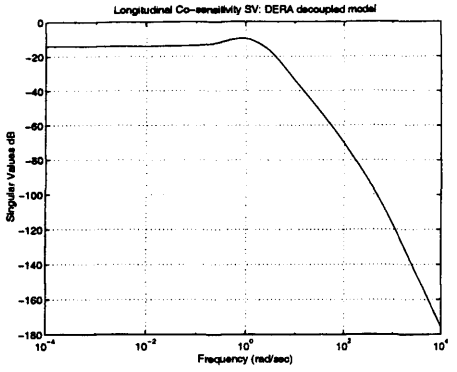

Co-sensitivity Singular Value Plot

Figure 7.3: Longitudinal Frequency Responses - Decoupled Model

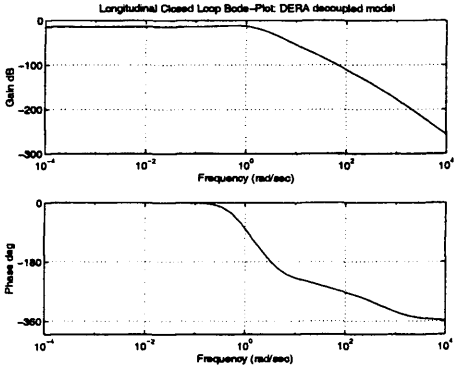

Figure 7.4: Longitudinal Axis Bode Plot - Decoupled Model

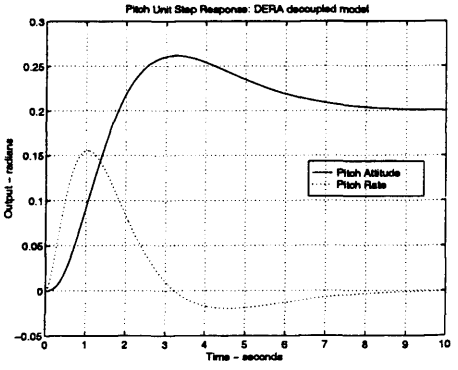

Figure 7.5: Longitudinal Unit Step Response - Decoupled Model

Channel	Bandwidth	Phase Delay	HQ Level	
			Target Accquisistion	Other MTEs
Pitch	1.8924	0.0981	2	2
Roll	2.3403	0.0545	2	1
Yaw	2.0190	0.0418	2/3	1/2

Table 7.4: ADS-33 Handling Qualities predicted by Decoupled Model

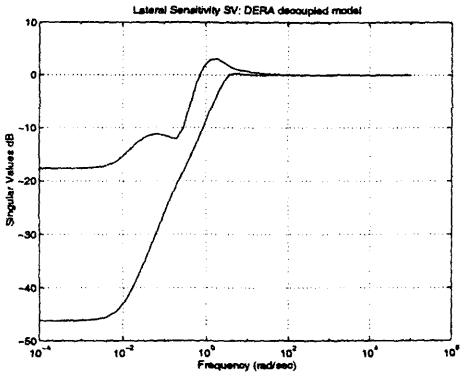

Sensitivity Singular Value Plot

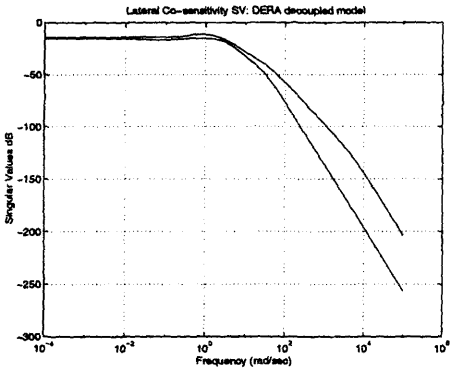

Co-sensitivity Singular Value Plot

Figure 7.6: Lateral Frequency Responses - Decoupled Model

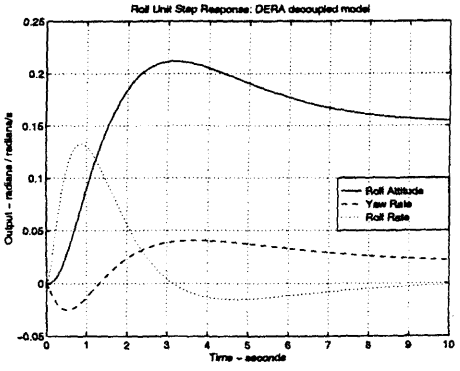

Roll Channel

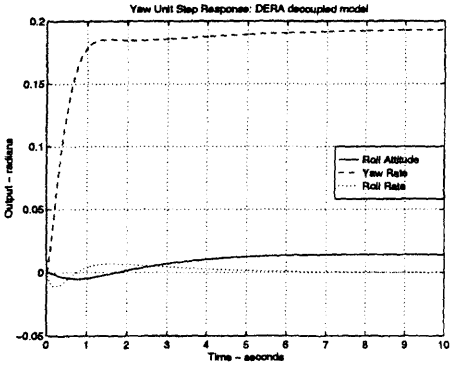

Yaw Channel

Figure 7.7: Lateral Unit Step Responses - Decoupled Model

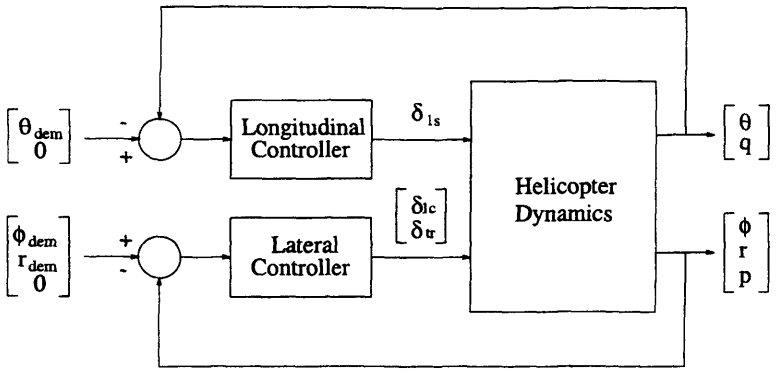

Figure 7.8: Control System Implementation

the ability of the model to predict these cross-couplings.

Surprisingly the ADS-33 predictions made by this model (Table 7.5) show a strong agreement with those predicted by the de-coupled models, although this is at odds with those actually obtained in flight.

7.5.2 NASA Simulations

The NASA models were generally regarded as inferior to those constructed by DERA, although as they formed the basis of the NRC's controller assessment procedure, it was felt that they had some relevance to the desktop evaluation of the controllers. It should be noted that in open-loop analysis it was found that the NASA linearisations' singular values were significantly higher than the DERA equivalents - as much as 20dB around the bandwidth.

The simulations here are produced by closing the loop around a coupled eight-state NASA model at twenty knots with the controller *mix12* (i.e. the two de-coupled DERA-based controllers), using appropriate scaling factors.

Figure 7.12 depicts the frequency response of the closed loop system. Both the sensitivity and co-sensitivity plots suggest good performance and robustness properties, with the co-sensitivity having low gain at high frequency and sensitivity having low gain at low frequency.

The step responses are also significantly better than those produced with the DERA model (due to the higher gain present in the NASA linearisations). Faster, well damped responses with little cross-coupling and zero steady-state error are shown in all axes - see Figures 7.13 - 7.14. Likewise, the predicted ADS-33 handling qualities are level 1 in all channels: although these are unrealistic when compared to in-flight results.

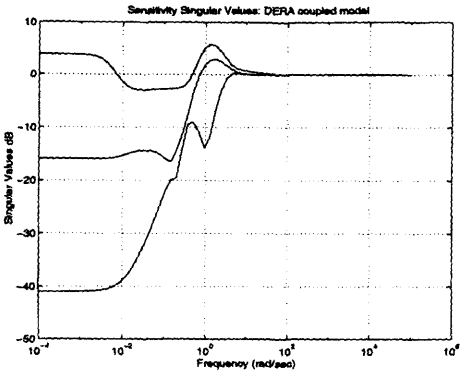

Sensitivity Singular Value Plot

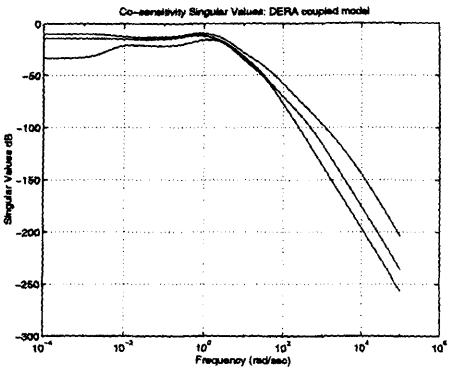

Co-sensitivity Singular Value Plot

Figure 7.9: Frequency Responses - Coupled Model

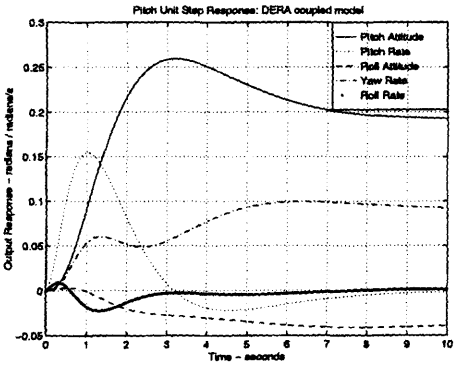

Figure 7.10: Step Response to Longitudinal Unit Step - Coupled Model

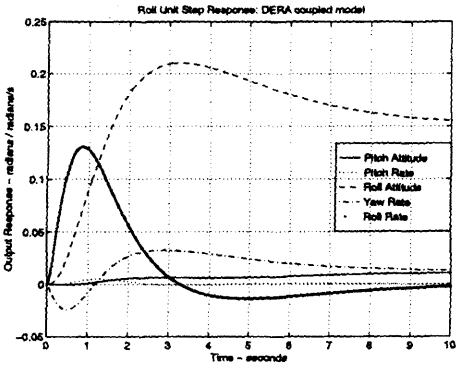

Step in Roll

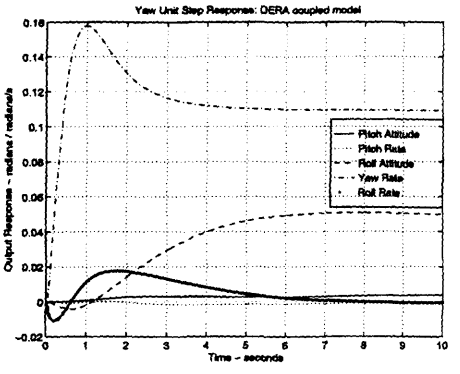

Step in Yaw

Figure 7.11: Response to Lateral Unit Steps - Coupled Model

Channel	Bandwidth	Phase Delay	HQ Level	
			Target Accquisistion	Other MTEs
Pitch	1.9714	0.0981	borderline 1/2	borderline 1/2
Roll	2.3832	0.0547	2	1
Yaw	2.3496	0.0419	2	1

Table 7.5: ADS-33 Handling Qualities predicted by Coupled Model

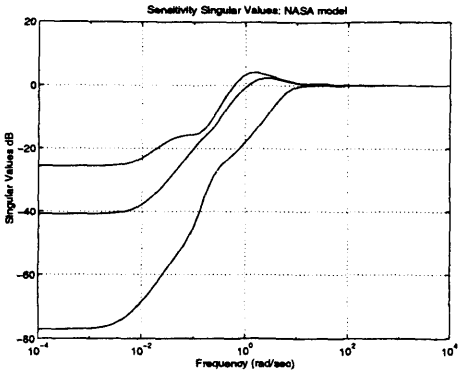

Sensitivity Singular Value Plot

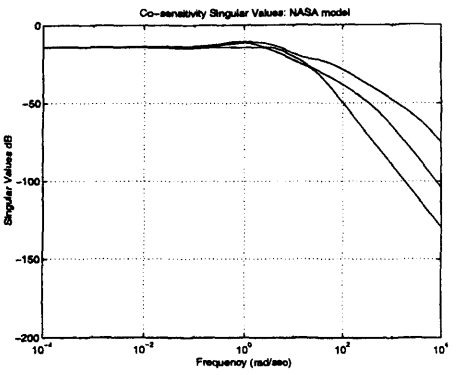

Co-sensitivity Singular Value Plot

Figure 7.12: Frequency Responses - NASA model

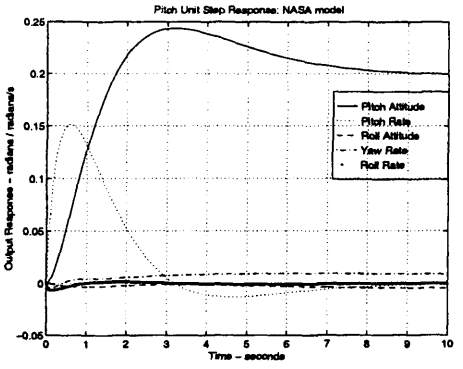

Figure 7.13: Step Response to Longitudinal Unit Step - NASA Model

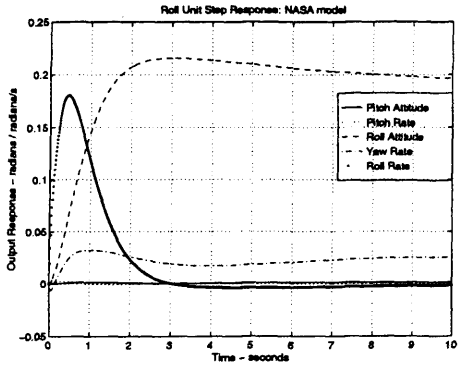

Step in Roll

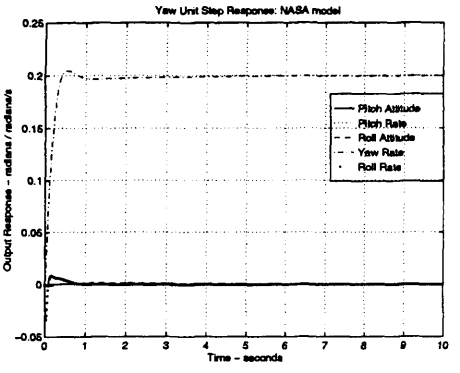

Step in Yaw

Figure 7.14: Response to Lateral Unit Steps - NASA Model

Channel	Bandwidth	Phase Delay	HQ Level	
			Target Accquisistion	Other MTEs
Pitch	5.1195	0.0014	1	1
Roll	6.3456	$1.5e^{-4}$	1	1
Yaw	5.6314	0.0100	1	1

Table 7.6: ADS-33 Handling Qualities predicted by NASA Model

7.5.3 Non-residualised Model

The ADS-33 bandwidths and phase delays were also calculated for a non-residualised, coupled DERA model. This was identical to the previous coupled model, except the rotor dynamics were not removed. Although the time responses were similar, as expected the phase delays were significantly greater using this model (the rotor is often represented as a time delay).

Channel	Bandwidth	Phase Delay	HQ Level	
			Target Accquisistion	Other MTEs
Pitch	1.9338	0.2342	2	2
Roll	2.3413	0.1645	2	1
Yaw	2.3031	0.0379	2	1

Table 7.7: ADS-33 Handling Qualities predicted by Non-residualised Model

The yaw channel was 'PIO prone' according to the ADS-33 document as the gain bandwidth was less than the phase bandwidth. Interestingly, yaw was described by the pilot as oscillatory, and certainly as the worst axis, in many of the flight-tests (see next section).

7.5.4 A Note on Tolerance of Time Delays

The rotor, and to a lesser degree the actuators, are known to give rise to a pure time delay (or an effect which is often modelled as such) in the forward path of the control loop. Obviously, this can have a destabilising effect, and as this time delay is of the order of 180ms in each channel, is cause of concern to the designer.

Furthermore as a pure time delay is an *infinite dimensional* system, that is it can only be described by a state-space of infinite dimensions, it is known to be problematic to mixed sensitivity designs, which robustify the closed-loop against additive and multiplicative uncertainties [2]. It was thus decided to conduct additional analysis to guage the level of time delay tolerance the designed controller gave to the closed loop.

The analysis used was relatively crude: time delays were placed in each loop and increased until the system went unstable. The approximate value of time delay which caused the system to just remain stable was then recorded and tabulated. Two models were used for this purpose: the DERA coupled and residualised model, and the NASA model. Due to the lack of rotor dynamics included in each of these models, the adding of a time delay could be conceived as adding crude rotor dynamics to the loop. Also a third simulation was performed with the

[2]It is however handled relatively easily with the gap metric

DERA coupled model with an extra static gain of 10 added to the loop to make its open-loop singular values correspond to those of the NASA model.

Model	Time Delay		
	Pitch	Roll	Yaw
DERA coupled	350ms	350ms	350ms
NASA coupled	100ms	70ms	180ms
DERA $\times 10$	10ms	20ms	10ms

Table 7.8: Time Delay Tolerance of Different Models with 'mix12' controller

Observe that the closed-loop containing the DERA coupled model appears to be robust to time delays up to about twice the duration of that estimated, which combined with the singular value plots suggests that 'mix12' will deliver a robust closed-loop system. However, the NASA linearisations, having a higher open-loop gain, do not agree and robustness is not guaranteed for time delays of 180ms in all channels. The time delay tolerance is worse still with the DERA model with a ten-fold increase in gain, which shows alarmingly little resistance to relatively small time delays.

If the open-loop singular values of the helicopter are indeed significantly higher than predicted by the DERA linearistions, this could help to explain why stability problems were encountered without mixed rate feedback.

In continuous time, it is difficult to explicitly cater for pure time delays using standard $\mathcal{H}^\infty$ methods, as a time delay is an infinite dimensional system. The conventional solution to this problem is to use Pade approximations to time delays, but for accurate approximations, this can lead to higher order controllers. An alternative is to use discrete time methods, where time delays can be handled without resorting to approximations as they are just delays (providing the time delay is close to an integer multiple of the sampling period T).

7.6 Flight Test Results

The flight test results are presented for the 'best' controller tested during the eight days available - *mix12*. It is stressed that other controllers did not perform as well, although the design procedure generally seemed able to give one the ability to relate pilot comment and flight test data to the design parameters (weights) chosen. Thus there was a definite iterative procedure and the 'best' controller was arrived at on the fifth of the eight days.

The controllers used in flight-testing were implemented in the same manner as in the coupled simulations (see Figure 7.8).

The flight test results are split into two distinct parts: analysis of the data collected and pilot comment and ADS-33 rating.

7.6.1 Pilot Comment

One of the most immediate and simplest methods of evaluating a given controller, is the pilot's opinion of how the helicopter performs when flown with that controller. Some caution must exercised when listening to pilot comment of course; human factors such as personal preference, ability to be mistaken, and inconsistency are all factors to be aware of when interpreting the pilot's opinions. Moreover, as the pilot essentially forms another feedback loop around the helicopter, human-machine interactions may cause anomalous behaviour; one common example is pilot-induced-oscillations (PIO), which can be caused by closed-loops with sluggish responses and significant phase-lag.

Ideally, more than one pilot should be used for testing, but limits on time and money prevented this; hence the results of this section are based purely on the opinions of one pilot, albeit an experienced one. Although this at first may seem imprudent, experience showed that the one pilot's comments gave a fairly accurate evaluation of the resulting controllers performance - this is borne out by results obtained from the flight test data, given later in this section.

In the iterative design procedure, one of the main tools used for controller re-design, along with resulting linear responses, was pilot comment. This was possibly because man-machine interactions are not exposed in simulation, and also partly due to the degree of inaccuracy present in the models.

Manoeuvres

Table 7.9 shows the pilot evaluation of the helicopter's performance, under the influence of *mix12*, while performing various manoeuvres.

Manoeuvre	HQR	Additional Comment
Quick Hop	4	"Pitch rate not quite brisk enough. Small yaw excursion"
Side Step	4	"Good pitch/roll capture. Small variations in yaw rate"
Turn-to-target	5	"Yaw too slow/unpredictable"
Precision Hover	4	"Small excursions in yaw aft - every 1/4 second"
Pirouette	4	"Small yaw excursions. Constant long. inputs"

Table 7.9: Helicopter Performance Using $\mathcal{H}^\infty$ Controller (Flight y99022)

From Table 7.9, it is clear that, overall, the controller yielded an ADS-33 rating of border-line Level 1/Level 2 handling qualities. The pilot's chief complaint was the yaw axis, which seemed quite oscillatory, possibly too responsive. Roll was deemed "about right" and pitch in one informal flight was considered "about right", but in another slightly too sluggish. Throughout the controller evaluation the pilot did not notice any cross-coupling; from previous results, designed using wholly multivariable methods, this suggested it was a feature of the methdology - the de-coupled architecture particularly - which gave rise to the de-coupled responses. The flights from which these results are taken are Flights y99021 and y99022.

7.6.2 Data Analysis

An important complement to the pilot comment is the analysis of the data recorded with the helicopter's on-board equipment. This enabled a more objective assessment of the flight to be conducted, and also enabled a quantative comparison of time and frequency domain responses obtained in simulation to those obtained during flight.

Step Responses

The step response data plotted shows the demand and the primary response. As the actual reference given to the control system was given in *cm* of inceptor deflection and scaled by cockpit instrumentation located on the pilot's stick, the demands have been adjusted to a value consistent with the response. The sense of the input has also been adjusted: for the pitch and roll axes this means the addition of 180 degrees of phase, as for example, stick forward (positive movement), corresponds to nose down (negative movement). The responses are all given in degrees or degrees/s.

Pitch Axis. Figure 7.15 shows the helicopter's response to a pilot "step" demand in pitch attitude. Note how the response follows the demand closely, with a rise time of approximately 1 second and a damping ratio of approximately 0.7-0.8.

Roll Axis. Figure 7.16 depicts the helicopter's response to a step in roll attitude. The dynamic response has similar characteristics to the pitch axis: close tracking of the demand, with rise time slightly less than 1 second, and damping ratio around 0.8.

Yaw Axis. This axis undoubtedly performed the poorest during the flight tests. Figure 7.17 shows the step response in this axis. It can be seen that, while tracking of the demand can be seen, the response is highly oscillatory - even when the pedal input is virtually zero.

The step response plots essentially tally with pilot comment. The roll axis which was deemed the best has the fastest rise time and greatest damping ratio, and exhibits close tracking of

the demand. The pitch axis, which the pilot also rated favourably but complained slightly of "sluggishness", appeared to have a slightly slower rise time. Finally the yaw axis, which was the chief source of pilot complaint, was clearly excessively oscillatory from the time response plot.

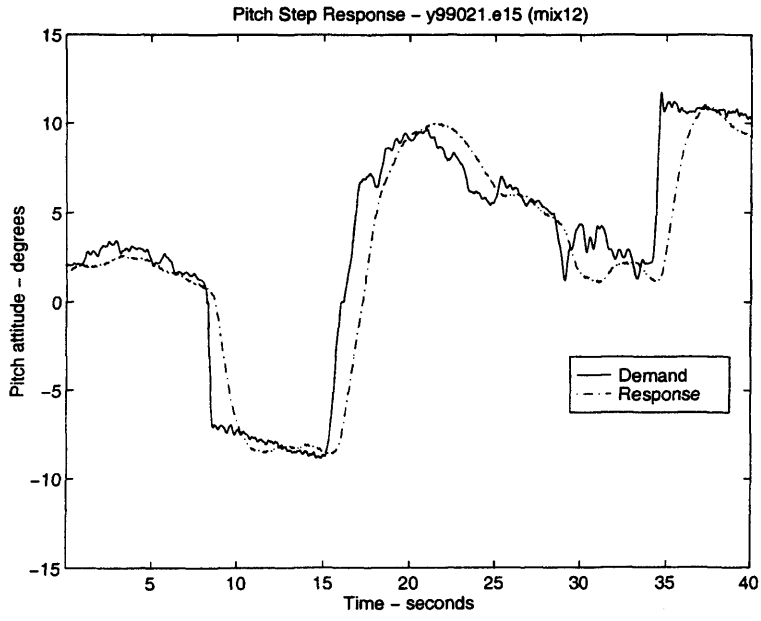

Figure 7.15: In-flight Pitch Axis Response

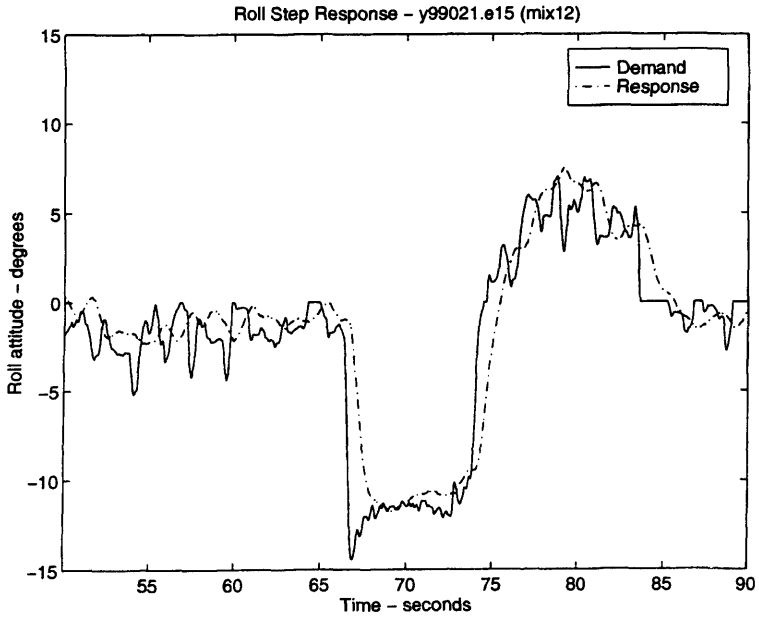

Figure 7.16: In-flight Roll Axis Response

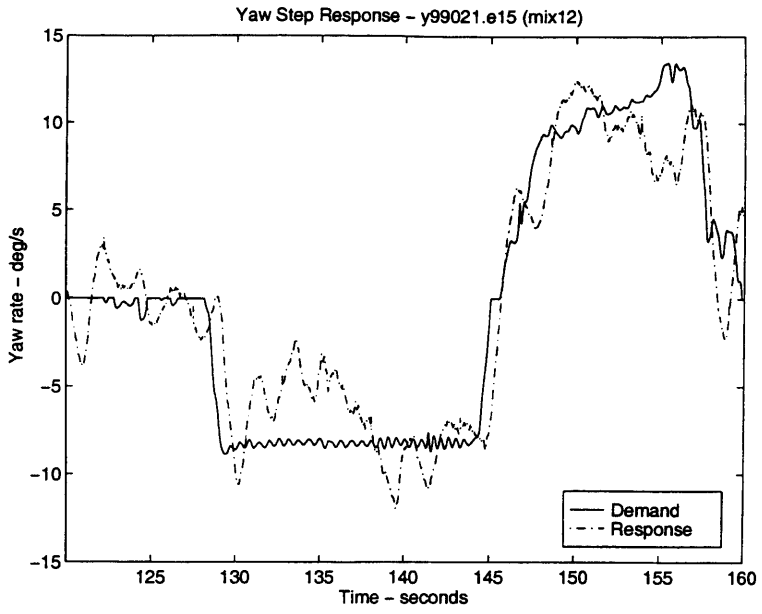

Figure 7.17: In-flight Yaw Axis Response

Frequency Response

Crude estimates of the helicopter's single-loop frequency response can be obtained by comparing the response to a pilot frequency sweep. Such a sweep is obtained by the pilot "oscillating" his inceptor in a given axis while keeping the remaining inceptors neutral. The oscillation starts slowly and increases frequency over a number of seconds.

The frequency response estimate is obtained by comparing the discrete Fourier Transform (DFT) of the pilot demand to the DFT of the output. The crudity of such an estimate is evident from the fact that the pilot has difficulty in putting in an exact "chirp" signal and in reality the low and high frequency responses are poorly determined. The fundamental limit is given by Shannon's Sampling Theorem, which in this case lead to an absolute maximum accuracy of 32Hz (the data was logged at 64Hz).

However, estimates of fair accuracy can be made in the frequency band between about 0.5 radians/s to about 10 radians/s. Depending on the precise method used to compute the DFT comparison (i.e. Window type, length of DFT, method of data de-trending), slightly different results can be obtained in this frequency band, but the general shape is similar using most methods. For the analysis here, the data was linearly de-trended and windowed using a Hanning window; the DFT had as many points as there were samples.

Figures 7.18 - 7.20 show the frequency response estimates of the closed loop in the pitch, roll and yaw channels respectively. Note that, in the mid frequency range, the pitch and roll channels have broadly similar response shapes to those predicted by the model (the gain increase is

due to the different units used in the references and the adjustable pilot controls). The yaw response is not as good and it is questionable as to whether this estimate is indicative of the true frequency response.

The ADS-33 bandwidths and phase delays calculated from the frequency responses are given in Table 7.10 . The bandwidths are read direct from the bode plots and are only given to one significant figure due to the uncertainty inherent in the estimation. The phase delays calculated should be considered with some caution as the frequency at which they are calculated (twice the frequency at which the phase crosses 180 degrees) is poorly determined and is calculated by extrapolating the phase present in the mid frequency band to this frequency.

Channel	Bandwidth	Phase Delay	HQ Level	
			Target Acquisition	Other MTEs
Pitch	2.4	0.11	1	1
Roll	3.5	0.11	1	1
Yaw	2.5	0.14	2	1

Table 7.10: ADS-33 Handling Qualities calculated from Flight Test Data

Note that, with the exception of yaw, the bandwidths and phase delays obtained from the flight test data all meet Level 1 performance. The yaw bandwidths and phase delays also suggest good performance, but doubt is placed on the accuracy of the yaw frequency response estimate.

Comparison with those predicted by the various models reveals that, in agreement with pilot comment, the performance obtained in flight was better than predicted by both the coupled and decoupled DERA models, but worse than that predicted by the NASA model. In fact, if the yaw channel was not as poor, it is conjectured that Level 1 performance would be obtained.

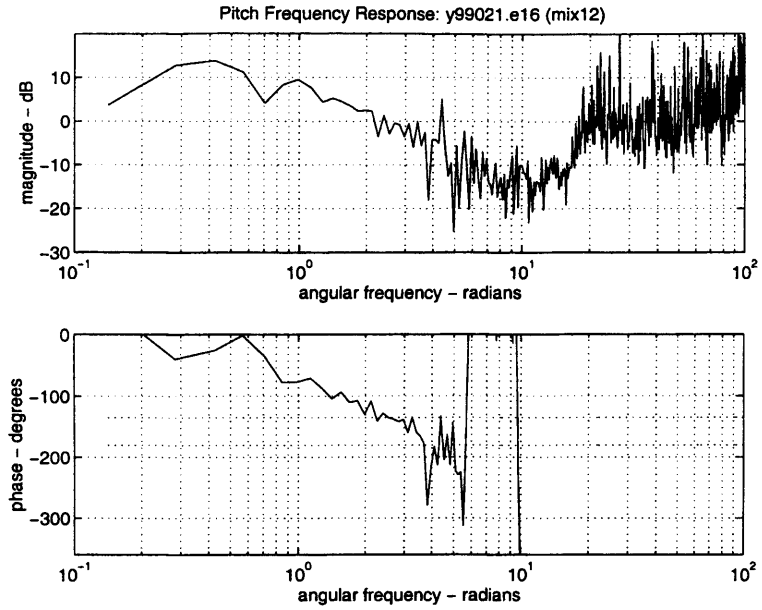

Figure 7.18: Pitch Axis Frequency Response Estimate

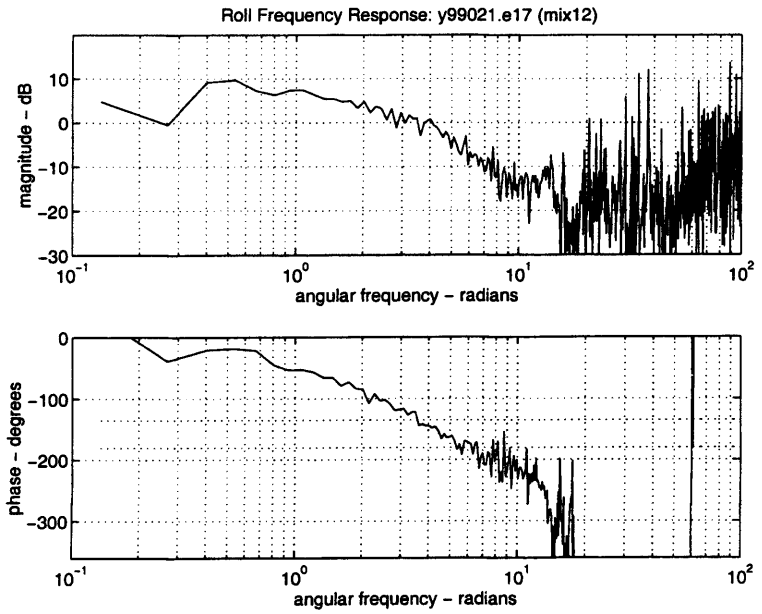

Figure 7.19: Roll Axis Frequency Response Estimate

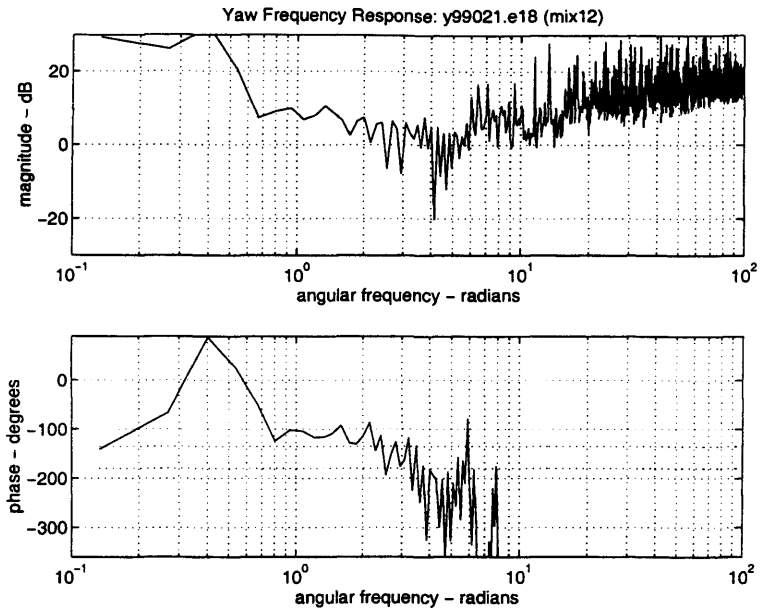

Figure 7.20: Yaw Axis Frequency Response Estimate

7.7 Conclusion

The following summary can be drawn from the desk-top simulation and flight testing of the *mix12* $\mathcal{H}^{\infty}$ controller:-

- The strategy used allowed the synthesis of a controller giving upper Level 2 performance to be synthesised within strict time limits (8 days).
- The semi-de-coupled structure allowed de-coupled responses to be obtained.
- Adjustment of the various weighting functions in response to pilot comment and simulation appeared fairly straight-forward, with a generally clear correlation between the choice of weights and in-flight behaviour.
- The resultant controller was not robust enough to function without mixed-rate feedback; it is thought that this is at least partially due to the relatively poor fidelity of the model.

In addition to these primary conclusions, the weakness of the model was also high-lighted. In particular:-

- Suspicions about the model's inability to predict off-axis couplings were largely confirmed.
- The DERA model tended to *under-predict* ADS-33 bandwidths when compared to the flight-test data; the NASA model tended to *over-predict*. It is likely that the actual aircraft's open-loop gain lies somewhere between these two extremes.

- Mixed rates were needed in order for the controller to stabilise the helicopter. This is probably partly due to the inability of the de-coupled DERA linearisations and NRC linearisations to predict time-delay tolerances and phase lags accurately.
- The yaw axis appeared to be especially poorly modelled. Evaluation of the flight-test data suggests that if it were not for the poor yaw performance, Level 1 performance would have been attained in some manouevres (the roll and pitch bandwidths and phase delays indicated Level 1 behaviour).

This chapter has by no means described all that is achievable in the field of $\mathcal{H}^\infty$ control of helicopters. While it is thought that successful achievements have been made, there are a number of recommendations for future research:-

- Experience in the flight trials described here suggests that improvement of model fidelity is highly desirable. This would make the design process easier and would increase the correlation between desk-top simulation and flight-test results.
- The poor time-delay tolerances predicted by some models, combined with the need for mixed rates leads one to believe that increasing the controller's robustness to larger dead-times would enhance the stability of the aircraft; possibly negating the need for mixed rates.
- The yaw axis, it was felt, seemed to be a major deficiency of the system. In order to attain Level 1 handling qualities it is vital that the response of this axis be improved.
- In the event of a more accurate model becoming available it would be interesting to compare the results obtained using the decoupled and residualised approach used here, with that of a truly multivariable full-order approach.
- Although a long and arduous task, data collected from the flight tests described here needs to be analysed and compared with data collected from the flight tests described in [57] and [67].

Chapter 8

Conclusion

The main contributions of the thesis are now summarised:-

- A new method for achieving bumpless transfer was proposed and promising results demonstrated. The main advantage of the proposed scheme is its wide applicability, unlike others in the literature.
- A modification to this scheme was made, which allows controllers with fast dynamics to be handled more effectively. This is achieved through a low pass filter in each control channel, which increases the order of the bumpless transfer compensator.
- The problem of tackling, *a priori*, the control of linear systems subject to input saturation has been considered and a technique already existing in the literature has been extended to include high-order and multivariable systems. Preliminary results using the extended method have been encouraging.
- An $\mathcal{H}^\infty$ limited authority control system was designed for the Mk7 Lynx helicopter. Characteristics of the resulting controller were high uncertainty tolerance which allowed one linear controller to be used throughout the flight envelope, and acceptable performance in the event of input saturation. In the limited piloted simulations performed, the pilot rated the $\mathcal{H}^\infty$ controller's performance highly.
- $\mathcal{H}^\infty$ control of the Bell 205 was studied and an $\mathcal{H}^\infty$ mixed sensitivity controller was designed, which was the best performing $\mathcal{H}^\infty$ controller to have been tested in-flight to date. The choice of weighting functions appeared to affect the aircraft's behaviour in the air in a relatively straightforward manner.
- Analysis of the flight test results seemed to suggest that, were it not for the yaw axis, Level 1 handling qualities would be achievable (upper Level 2 were achieved in the tests).

Areas in need of future research are identified as being:-

- The choice of weighting matrices in the bumpless transfer scheme needs further investigation. So far only rough guidelines have been established.
- The state feedback nature of the nonlinear tracking scheme for constrained input systems is restrictive. An observer based scheme would be preferable, in conjunction with some robustness analysis. The choice of the nonlinear parameter also needs further research.
- Only low aggression manouvres were performed with the Lynx helicopter in the trial of the limited authority system. An assessment of high aggression manoeuvres, over an extended period of time, needs to be conducted to enable more concrete conclusions about its viability to be drawn.
- Modelling issues are thought to lie at the heart of the problems with the Bell 205. Ideally a repeat test using higher fidelity models should be carried out. This has the potential to yield Level 1 handling qualities.

Appendix A

Classical Results Do Not Apply to Open-loop Unstable Systems

A.1 Problem

In Chapter 1 it was stated that classical stability results such as the Popov and Circle Criteria and even the Small Gain Theorem cannot give *global* stability predictions about open-loop unstable linear systems with bounded inputs. Here this statement is confirmed through the use of a quite general exposistion. Although the exposure is new, the concept is not and a result similar to this for the case of the Small Gain Theorem can be found in [52]. For the Circle and Popov criteria, the weakness of these tests has been alluded to in [51], although no detailed analysis was been given.

A.2 System Decomposition

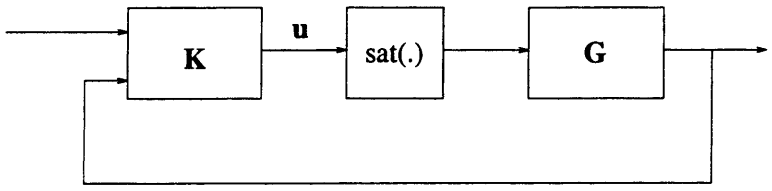

Figure A.1: Linear System with Saturation Nonlinearity

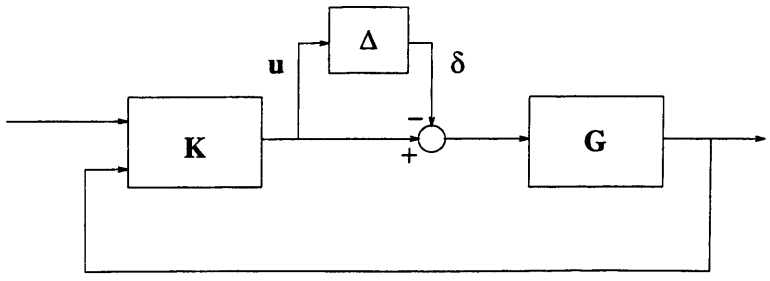

Figure A.2: Linear System with Deadzone 'perturbation'

In order to demonstrate the inapplicability of the classical results we shall make a standard decomposition, which was pointed out in Chapter 1; this has been used extensively in the anti-windup literature - see [93].

Consider the system in Figure A.1, where $sat(.)$ is the standard symmetric saturation operator with unity saturation limits. Note that as $sat(.) = I - Dz(.)$ allows this to be re-drawn as Figure A.2. In turn this can be re-drawn as Figure A.3, where $\mathbf{T}_{u,\delta}$ denotes the transfer function from the deadzone output to the control signal.

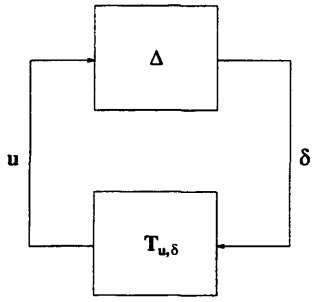

Figure A.3: Small Gain Connection of Stable closed loop and perturbation

Let the plant be unstable with right coprime factorisation $\mathbf{G} = \mathbf{N}\mathbf{M}^{-1}$ where $\mathbf{M}, \mathbf{N} \in \mathcal{RH}^{\infty}$ and thus $\mathbf{M}$ contains non-minimum phase zeros. Let the controller be partitioned as $[\mathbf{K}_1 \quad \mathbf{K}_2]$ in which $\mathbf{K}_2$ has left coprime factorisation $\mathbf{K}_2 = \mathbf{V}^{-1}\mathbf{U}$. Furthermore, let these coprime factors be chosen such that the following *Bezout* identity holds

$$\mathbf{V}\mathbf{M} - \mathbf{U}\mathbf{N} = I \tag{A.1}$$

and as before $\mathbf{U}, \mathbf{V} \in \mathcal{RH}^{\infty}$.

A.3 Classical Results do not Hold

A.3.1 Small Gain Theorem

To demonstrate that the Small Gain Theorem does not predict stability for open-loop unstable systems, consider the $\mathcal{L}_2$ induced norm version of the theorem. Note that the $\mathcal{L}_2$ induced norm of the deadzone is unity so a sufficient condition for stability is (see Chapter 1)

$$\|\mathbf{T}_{u,\delta}\|_{\infty} < 1 \tag{A.2}$$

Next it will be shown that, for open-loop unstable plants this is impossible (this proof follows along similar lines to [52], except that reference considers the system in the presence of an anti-windup compensator).

$$\begin{aligned}
\mathbf{T}_{u,\delta} &= \mathbf{K}_2\mathbf{G}(I-\mathbf{K}_2\mathbf{G})^{-1} && \text{(A.3)}\\
&= \mathbf{V}^{-1}\mathbf{U}\mathbf{N}\mathbf{M}^{-1}(I-\mathbf{V}^{-1}\mathbf{U}\mathbf{N}\mathbf{M}^{-1})^{-1} && \text{(A.4)}\\
&= \mathbf{V}^{-1}\mathbf{U}\mathbf{N}\mathbf{M}^{-1}(\mathbf{V}^{-1}\mathbf{V}\mathbf{M}\mathbf{M}^{-1}\mathbf{V}^{-1}\mathbf{U}\mathbf{N}\mathbf{M}^{-1})^{-1} && \text{(A.5)}\\
&= \mathbf{V}^{-1}\mathbf{U}\mathbf{N}(\mathbf{V}\mathbf{M}-\mathbf{U}\mathbf{N})^{-1}\mathbf{V} && \text{(A.6)}\\
&= \mathbf{V}^{-1}\mathbf{U}\mathbf{N}\mathbf{V} && \text{(A.7)}
\end{aligned}$$

Now from A.1, $\mathbf{U}\mathbf{N} = \mathbf{V}\mathbf{M} - I$, so

$$\mathbf{T}_{u,\delta} = \mathbf{M}\mathbf{V} - I \qquad \text{(A.8)}$$

Now, as $\mathbf{M}$ contains right-half plane zeros it is evident that $\|\mathbf{M}\mathbf{V} - I\|_\infty \geq 1$ and thus the Small Gain Theorem does not predict stability.

A.3.2 Popov and Circle Criteria

It shall be shown that the Popov criterion does not predict stability, and thus, as the Circle criterion, in the context considered here, is a special case of this, it will follow that this does not predict stability either.

With reference to Chapter 1, recall that according to the Popov criterion given a nonlinearity in the sector $[0, \bar{V}]$, then stability results if a certain transfer function is strictly positive real. Note that for the deadzone we have $Dz(.) \in$ Sector$[0, 1]$ and hence for stability a sufficient condition is

$$\begin{aligned}
\mathbf{Z} &= I + (1+\eta s)\mathbf{T}_{u,\delta} = \mathbf{M}\mathbf{V} + \eta s(\mathbf{M}\mathbf{V} - I)\\
&= -I\eta s + (1+\eta s)\mathbf{M}\mathbf{V}
\end{aligned}$$

is strictly positive real. Now as $-I\eta s \Rightarrow -I\eta j\omega + (-I\eta j\omega)^* = 0$, then $-I\eta s$ does not affect the strict positive realness of $\mathbf{Z}$. Hence for $\mathbf{Z}$ to be strictly positive real $(1+\eta s)\mathbf{M}\mathbf{V}$ must be strictly positive real; as $(1+\eta s)\mathbf{M}\mathbf{V}$ contains right half plane transmission zeros this is impossible. Thus the Popov criterion does not predict stability.

That the circle criterion does not predict stability follows by noting that in this case, $\eta = 0$. Then the argument follows along the same lines as before.

Appendix B

Discrete-time Modified Linear Quadratic Bumpless Transfer

B.1 Derivation of Formulae

For completeness, formulae for the 'modified' method of linear quadratic bumpless transfer are derived for discrete time systems. the treatment will be brief due to the consideration given to discrete time LQ bumpless transfer and continuous time modified LQ bumpless transfer in the main text.

The configuration is that described in Figure 3.2, where it is sought to minimise the difference between the on and off-line control signals, with regard also to the size of the additional signal α. The off-line controller is described by the following discrete-time state-space equations

$$x_{k+1} = Ax_k + B_1(r_k + \tilde{\alpha}_k) + B_2 y_k \tag{B.1}$$

$$u_k = Cx_k + D_1(r_k + \tilde{\alpha}_k) + D_2 y_k \tag{B.2}$$

where (A, B_1, C) is assumed controllable and observable. The low pass filter ($L(s)$ is replaced by $L(z)$) is assumed to have the strictly proper minimal realisation

$$x_l(k+1) = A_l x_l(k) + B_l \alpha_k \tag{B.3}$$

$$\tilde{\alpha}_k = C_l x_l(k) \tag{B.4}$$

The performance index to be minimised is

$$J = \frac{1}{2}\sum_{k=0}^{T-1}[z_u'(k)W_u z_u(k) + \alpha_k' W_e \alpha_k] + \frac{1}{2}z_u'(T)P z_u(T) \tag{B.5}$$

where $z_u(k) = u_k - \tilde{u}_k$.

Combining equations (B.2) and (B.4) results in the following expression

$$\tilde{x}_{k+1} = \tilde{A}\tilde{x}_k + \tilde{B}_1 w_k + \tilde{B}_2 \alpha_k \tag{B.6}$$

$$u_k = \tilde{C}\tilde{x}_k + \tilde{D}_1 w_k \tag{B.7}$$

where

$$\tilde{A} = \begin{bmatrix} A & B_1 C_l \\ 0 & A_l \end{bmatrix} \quad \tilde{B}_1 = \begin{bmatrix} B_1 & B_2 \\ 0 & 0 \end{bmatrix} \quad \tilde{C} = [C \quad D_1 C_l] \quad \tilde{D}_1 = [D_1 \quad D_2] \tag{B.8}$$

$$\tilde{x}_k = \begin{bmatrix} x_k \\ x_l(k) \end{bmatrix} \quad w_k = \begin{bmatrix} r_k \\ y_k \end{bmatrix} \quad \tilde{B}_2 = \begin{bmatrix} 0 \\ B_l \end{bmatrix} \tag{B.9}$$

The *Hamiltonian* can be formed as

$$H_k = \frac{1}{2}[z_u'(k) W_u z_u(k) + \alpha_k W_e \alpha_k] + \lambda_{k+1}'(\tilde{A}\tilde{x}_k + \tilde{B}_1 w_k + \tilde{B}_2 \alpha_k) \tag{B.10}$$

where $\lambda_{k+1} \in \mathbb{R}^{n+n_l}$ is a dynamic Lagrange multiplier. Using B.7, the Hamiltonian can be expanded as

$$H_k = \frac{1}{2}\left\{(\tilde{C}\tilde{x}_k + \tilde{D}_1 w_k - \tilde{u}_k)' W_u (\tilde{C}\tilde{x}_k + \tilde{D}_1 w_k - \tilde{u}_k) + \alpha_k' W_e \alpha_k\right\} + \lambda_{k+1}'(\tilde{A}\tilde{x}_k + \tilde{B}_1 w_k + \tilde{B}_2 \alpha_k) \tag{B.11}$$

Evaluating the first order necessary conditions as described in Chapter 3, yields

$$\tilde{x}_{k+1} = \tilde{A}\tilde{x}_k + \tilde{B}_1 w_k + \tilde{B}_2 \alpha_k \tag{B.12}$$

$$\lambda_k = \tilde{C}' W_u \tilde{C}\tilde{x}_k + \tilde{C}' W_u \tilde{D}_1 w_k - \tilde{C}' W_u \tilde{u}_k + \tilde{A}'\lambda_{k+1} \tag{B.13}$$

$$\alpha_k = -W_e^{-1}\tilde{B}_2'\lambda_{k+1} \tag{B.14}$$

Using (B.14) in (B.12), one obtains

$$\tilde{x}_{k+1} = \tilde{A}\tilde{x}_k - \tilde{R}\lambda_{k+1} + \tilde{B}_1 w_k \tag{B.15}$$

$$\lambda_k = \tilde{Q}\tilde{x}_k + \tilde{A}'\lambda_{k+1} + \tilde{C}' W_u \tilde{D}_1 w_k - \tilde{C}' W_u \tilde{u}_k \tag{B.16}$$

where $\tilde{Q} := \tilde{C}' W_u \tilde{C}$ and $\tilde{R} := \tilde{B}_2 W_e^{-1} \tilde{B}_2'$. Assuming the affine relationship

$$\lambda_k = \Pi_k \tilde{x}_k - g_k \tag{B.17}$$

$$\lambda_{k+1} = \Pi_{k+1} \tilde{x}_{k+1} - g_{k+1} \tag{B.18}$$

one can obtain

$$\lambda_{k+1} = -\tilde{A}^{-T}[(\tilde{Q} - \Pi_k)\tilde{x}_k + g_k + \tilde{C}' W_u \tilde{D}_1 w_k - \tilde{C}' W_u \tilde{u}_k] \tag{B.19}$$

From (B.18) and (B.15) it follows that

$$\lambda_{k+1} = (I + \Pi_{k+1}\tilde{R})^{-1}[\Pi_{k+1}\tilde{A}\tilde{x}_k + \Pi_{k+1}\tilde{B}_1 w_k - g_{k+1}] \tag{B.20}$$

Equating coefficients of $\tilde{x}$ in (B.19) and (B.20) gives the discrete Riccati difference equation

$$\tilde{A}'(I + \Pi_{k+1}\tilde{R})^{-1}\Pi_{k+1}\tilde{A} + \tilde{Q} - \Pi_k = 0 \tag{B.21}$$

Equating the remaining coefficients yields

$$-g_k = \tilde{C}' W_u \tilde{D}_1 w_k - \tilde{C}' W_u \tilde{u}_k + \tilde{A}'(I + \Pi_{k+1}\tilde{R})^{-1}[\Pi_{k+1}\tilde{B}_1 w_k - g_{k+1}] \tag{B.22}$$

These can be used in equation (B.18) and λ_{k+1} used in (B.14) to yield α_k. The difference equations (B.21) and (B.22) are solved backwards in time from the terminal conditions, which are found from the first order necessary conditions as

$$\Pi_T = \tilde{C}' P \tilde{C} \tag{B.23}$$

$$-g_T = \tilde{C}' P \tilde{D}_1 w_T - \tilde{C}' P \tilde{u}_T \tag{B.24}$$

To extend this to the infinite horizon, let $P \geq 0$ and assume that $(\tilde{A}, \tilde{R}, \sqrt{\tilde{Q}})$ is stabilisable and detectable (which actually follows from controllability and observability of (A, B, C) and $W_u, W_e > 0$). Then it follows, in a similar manner to Theorem 3.1 that

$$\lim_{T \to \infty} \Pi_{k+1} = \Pi_k := \Pi \tag{B.25}$$

So in the infinite horizon, the difference Riccati equation becomes the discrete ARE:

$$\tilde{A}'(I + \Pi\tilde{R})^{-1}\Pi\tilde{A} + \tilde{Q} - \Pi = 0 \tag{B.26}$$

Also if it is assumed that w_k and $\tilde{u}_k$ are constant, as in the main text, then

$$\lim_{T\to\infty} g_k = g_{k+1} \tag{B.27}$$

Thus in the infinite horizon we have

$$g_k = M \begin{bmatrix} [\tilde{C}'W_u\tilde{D}_1 + \tilde{A}'(I+\Pi\tilde{R})^{-1}\Pi\tilde{B}_1]' \\ -(\tilde{C}'W_u)' \end{bmatrix}' \begin{bmatrix} w_k \\ \tilde{u}_k \end{bmatrix} \tag{B.28}$$

where $M := [I + \tilde{A}'(I+\Pi\tilde{R})^{-1}]^{-1}$, which exists as $\tilde{A}'(I+\Pi\tilde{R})$ is Schur stable (from the stabilising solution of the discrete ARE) and hence $\mathbf{spec}[\tilde{A}'(I+\Pi\tilde{R})] < 1$. Note also that as $\tilde{R} > 0, \Pi \geq 0$, the inverse of $(I+\Pi\tilde{R})$ exists. Then the expression for α_k, in the infinite horizon becomes

$$\alpha_k = F \begin{bmatrix} \tilde{x}_k \\ w_k \\ \tilde{u}_k \end{bmatrix} \tag{B.29}$$

where F is given as

$$F := \tilde{\Delta} \begin{bmatrix} (\Pi\tilde{A})' \\ (\Pi\tilde{B}_1 - M(\tilde{C}'W_u\tilde{D}_1 + \tilde{A}'(I+\Pi\tilde{R})^{-1}\Pi\tilde{B}_1))' \\ -(M\tilde{C}'W_u)' \end{bmatrix}'$$

where $\tilde{\Delta} := -[I + W_e^{-1}\tilde{B}_2'\Pi\tilde{B}_2]^{-1}W_e^{-1}\tilde{B}_2$.

Note that in the infinite horizon, as the solution to the discrete ARE is taken as the postive semi-definite stabilising one, the stability of the off-line control loop is ensured.

Appendix C

General Formulae for Nonlinear Tracking

This appendix describes some alternative formulae for the matrices H and G given in the main body of the thesis. They were suggested by [28] and do not involve the partitioning of the A, B, C and F matrices, unlike the main formulae. However, it is interesting to note that the matrix which dictates the change of co-ordinates, H, given in the main text is independent of the state feedback, F, whereas in these formulae H is actually a function of F [1].

We consider the same linear system as in chapter 4, reproduced for convenience here:

$$\dot{x} = Ax + Bu_L \tag{C.1}$$

$$y = Cx + Du_L \tag{C.2}$$

subject to the control $u_L = Fx + Gr$ where F has been designed such that $A + BF$ is Hurwitz and G is to be determined. The goal is to find a co-ordinate transformation $\tilde{x} = x - Hr$ such that $\lim_{t\to\infty} \tilde{x}(t) = 0 \Rightarrow \lim_{t\to\infty} y(t) = r$ for a constant vector r.

First note that defining $H = -(A + BF)^{-1}BG$ yields the closed loop system

$$\dot{\tilde{x}} = (A + BF)\tilde{x} \tag{C.3}$$

$$y = (C + DF)\tilde{x} + [-(C + DF)(A + BF)^{-1}B + D]Gr \tag{C.4}$$

Providing the matrix $[-(C + DF)(A + BF)^{-1}B + D]$ has full row rank (which requires the number of demands to be less than or equal to the number of control inputs) then choosing

$$G = [-(C + DF)(A + BF)^{-1}B + D]^R \tag{C.5}$$

[1] This is not surprising, since there are an infinite number of co-ordinate systems describing the same model

ensures that $\lim_{t\to\infty} y(t) = r$.

It can be verified that when the system has the structure specified in Chapter 4, these formulae reduce to those given in the main text.

References

[1] K.J. Astrom and B. Wittenmark. *Computer Controlled Systems Theory and Design.* Prentice Hall, New Jersey, 1984.

[2] M. Athans and P.L. Falb. *Optimal Control, An Introduction to the Theory and Its Applications.* McGraw-Hill, New York, 1996.

[3] S.W. Baillie, J. Murray Morgan, and K. Goheen. Practical experiences in control system design using the NRC Bell 205 Airborne Simulator. *Agard Conference Proceedings 560. "Active Control Technology: Applications and Lessons Learned"*, pages 27.1–27.12, 1995.

[4] G. Balas, J.C. Doyle, K. Glover, A. Packard, and R. Smith. *μ analysis and synthesis toolbox.* MUSYN Inc. and The Mathworks Inc., 1991.

[5] D.S. Bernstein and A.N. Michel. A chronological bibliography on saturating actuators. *International Journal of Robust and Nonlinear Control*, 5(5):375–380, 1995.

[6] F. Blanchini. Set invariance in control - a survey. *Automatica*, 35(11):1457–1467, 1999.

[7] S. Boyd, L. El Ghaoui, E. Feron, and V. Balakrishnan. *Linear Matrix Inequalities in System and Control Theory.* SIAM, Philadelphia, 1994.

[8] P.J. Campo and M. Morari. Robust control of processes subject to saturation nonlinearities. *Computing and Chemical Engineering*, 14:343–358, 1990.

[9] P.J. Campo and M. Morari. Multiplier theory and the stability of anti-windup bumpless transfer schemes. *Proceedings of the IEEE Conference on Decision and Control*, 4:3767–72, 1997.

[10] P.J. Campo, M. Morari, and C.N. Nett. Multivariable antiwindup and bumpless transfer: a general theory. *Proceedings of the American Control Conference*, 2:1706–11, 1989.

[11] I. Chouaib and B. Praidin. Eigenstructure assignment with robust root clustering using logarithmic norms. *Proc. 3rd European Control Conference*, 4(2):3400–3405, 1995.

[12] J.C. Doyle. Guaranteed margins for LQG regulators. *IEEE Transactions on Automatic Control*, 23:756–757, 1978.

[13] J.C. Doyle, K. Glover, P.P. Khargonekar, and B.A. Francis. State-space solutions to standard H_2 and H_∞ control problems. *IEEE Transactions on automatic control*, 34(8):831–847, August 1989.

[14] J.C. Doyle, R.S. Smith, and D.F. Enns. Control of plants with input saturation nonlinearites. *Proc. American Control Conference*, pages 2147–2152, 1987.

[15] C. Edwards and I Postlethwaite. Anti-windup and bumpless transfer schemes. *Internal Report, Dept. of Engineering, Leicester Univ.*, 96-5, 1996.

[16] C. Edwards and S.K. Spurgeon. *Sliding Mode Control: Theory and Applications.* Taylor and Francis, New York, 1998.

[17] A.T. Fuller. In the large stability of relay and saturating control systems with linear controllers. *International Journal of Control*, 10:457–480, 1969.

[18] P. Gahinet. Explicit controller formulas for LMI-based $\mathcal{H}^\infty$ synthesis. *Automatica*, 32(7):1007–1014, 1996.

[19] P. Gahinet and P. Apkarian. A Linear Matrix Inequality approach to $\mathcal{H}^\infty$ control. *International Journal of Robust and Nonlinear Control*, 4:421–448, 1994.

[20] Gelfand and Fomin. *Calculus of Variations.* Prentice Hall, New York, 1963.

[21] K. Glover. All optimal Hankel-norm approximations of linear multivariable systems and their $\mathcal{L}_\infty$-error bounds. *International Journal of Control*, 39(6):1115–1193, 1984.

[22] K. Glover and J.C. Doyle. State-space formulae for all stabilising controllers that satisfy an $\mathcal{H}^\infty$ norm bound and relations to risk sensitivity. *Systems and Control Letters*, 11:167–172, 1988.

[23] G.H. Golub and C.F. van Loan. *Matrix Computations.* Johns Hopkins Univeristy Press, Baltimore, 3rd edition, 1996.

[24] S.F. Graebe and A.L.B. Ahlen. Dynamic transfer among alternative controllers and its relation to antiwindup controller design. *IEEE Transactions on Control Systems Technology*, 4(1):92–99, 1996.

[25] M. Green. $\mathcal{H}^\infty$ controller synthesis by J-lossless coprime factorisation. *SIAM Journal of Control and Optimisation*, 28:522–547, 1992.

[26] M. Green, K. Glover, D.J.N Limebeer, and J.C. Doyle. A J-spectral factoristion approach to $\mathcal{H}^\infty$ control. *SIAM Journal of Control and Optimisation*, 28:1350–1371, 1990.

[27] M. Green and D.J.N. Limebeer. *Linear Robust Control.* Prentice Hall, New York, 1990.

[28] D.W. Gu. Private communication. 2000.

[29] P.O. Gutman and P. Hagander. A new design of constrained controllers for linear systems. *IEEE Transactions on Automatic Control*, 30:22–33, 1985.

[30] R. Hanus and M. Kinnaert. Control of constrained multivariable systems using the Conditioning Technique. *Proceedings of the American Control Conference*, 2:1712–1718, 1989.

[31] R. Hanus, M. Kinnaert, and J.L. Henrotte. Conditioning technique, a general anti-windup and bumpless transfer method. *Automatica*, 23(6):729–39, 1987.

[32] R.K Heffley, W.F. Jewell, J.M. Lehman, and R.A. Van Winkle. *A Compilation and Analysis of Helicopter Handling Qualities Data.* NASA Contractor Report 3144, 1979.

[33] D. Henrion, G. Garcia, and S. Tarbouriech. Piecewise linear robust control of systems with input saturation. *European Journal of Control*, 5(1):157–166, 1999.

[34] J. Hespanha and A.S. Morse. Switching between stabilising controllers. *Automatica, submitted*, 2000.

[35] J. Howitt. Handling qualities toolbox. *DERA Internal Report*, 1992.

[36] T. Hu, Z. Lin, and L. Qiu. Null controllability and stabilisability of exponentially unstable linear systems with saturating actuators. *IEEE Transactions on Automatic Control, submitted*, 1999.

[37] R.A. Hyde. *The Application of Robust Control to VSTOL Aircraft.* PhD thesis, Department of Engineering, University of Cambridge, 1991.

[38] W. Johnson. *Helicopter Theory.* Dover Publications Inc., New York, 1994.

[39] P. Kapasouris, M. Athans, and G. Stein. Design of feedback control systems for stable plants with saturating actuators. *Proc. 27th IEEE Conference on Decision and Control*, pages 469–479, 1988.

[40] N. Kapoor, A.R. Teel, and P. Daoutidis. An anti-windup design for linear systems with input saturation. *Automatica*, 34(5):559–574, 1998.

[41] H. Khalil. *Nonlinear Systems.* Prentice Hall, New Jersey, 2nd edition, 1996.

[42] E.B. Lee and L. Markus. *Foundations of Optimal Control Theory.* Wiley, New York, 1968.

[43] F.L. Lewis. *Optimal Control.* Wiley International, New York, 1986.

[44] Z. Lin, M. Pachter, and Siva Banda. Toward tracking improvement - nonlinear feedback for linear systems. *International Journal of Control*, 70(1):1–11, 1998.

[45] Z. Lin and A. Saberi. Semi-global exponential stabilisation of linear systems subject to input saturation via linear feedbacks. *Systems and Control Letters*, pages 225–239, 1993.

[46] Z. Lin and A. Saberi. A semi-global low and high gain design technique for linear systems with input saturation - Stabilisation and Disturbance rejection. *International Journal of Robust and Nonlinear Control*, 5:381–398, 1995.

[47] Z. Lin, A. Saberi, and A.R. Teel. Simultaneous l_p stabilisation and internal stabilisation of linear systems subject to input saturation - state feedback case. *Systems and Control Letters*, pages 219–226, 1995.

[48] Z. Lin, A.A. Stoorvogel, and A. Saberi. Output regulation for linear systems subject to actuator saturation. *Automatica*, 32(1):29–47, 1996.

[49] M.H. Mansur and M.B. Tischler. An empirical correction for improving off-axis responses in flight-mechanics helicopter models. *Journal of the American Helicopter Society*, pages 94–102, 1998.

[50] M. Mariton. *Jump Linear Systems in Automatic Control.* Marcel-Dekker, New York, 1990.

[51] A. Megretski. $\mathcal{L}_2$ BIBO output feedback stabilisation with saturated control. *13th World Congress of IFAC*, D:435–440, 1996.

[52] S. Miyamoto and G. Vinnicombe. Robust control of plants with saturation nonlinearity based on coprime factor representations. *Proc. 35th IEEE Conference on Decision and Control*, pages 2838–2840, 1996.

[53] M. Morari and E. Zafirou. *Robust Process Control.* Prentice Hall, New Jersey, 1989.

[54] G.D. Padfield. *Helicopter Flight Dynamics.* Blackwell Science Ltd., Oxford, 1996.

[55] I. Postlethwaite, I. Konstantopoulus, X.-D. Sun, D.J. Walker, and A. Alford. Design, flight simulation and handling qualities evaluation of an LPV gain scheduled helicopter flight control system. *European Journal of Control, submitted*, 1999.

[56] I. Postlethwaite, R. Samar, B.W. Choi, and D.-W. Gu. A digital mulit-mode $\mathcal{H}^\infty$ controller for the Spey Turbofan engine. *Proceedings of the 3rd European Conference*, 4:3881–3886, 1995.

[57] I. Postlethwaite, A. Smerlas, D.J. Walker, A.W. Gubbells, S.W. Baillie, M.E. Strange, J. Howitt, and R.I. Horton. $\mathcal{H}^\infty$ control: From desk-top design to flight test with handling qualities evaluation. *Proceedings of the 54th Annual Forum American Helicopter Society*, pages 1013–1024, 1998.

[58] R.W. Prouty. *Helicopter Performance Stability and Control.* Krieger Publishing Company, Florida, 1986.

[59] Technical Report. *Handling Qualities Requirements fo Military Rotorcraft, Aeronautical Design Standard ADS-33D.* United States Army ATCOM, St. Louis, MO, 1994.

[60] B. Romanchuk. *Analysis of Saturated Feedback Loops: An input-output Approach.* PhD thesis, Department of Engineering, University of Cambridge, 1995.

[61] E.P. Ryan. *Optimal Relay and Saturating Control System Synthesis.* Peregrinus, London, 1982.

[62] A. Saberi, Z. Lin, and A.R. Teel. Control of linear systems with saturating actuators. *IEEE Transactions on Automatic Control*, 41(3):368–378, 1996.

[63] C. Scherer. $\mathcal{H}^\infty$ control without assumptions on finite or infinite zeros. *SIAM Journal on Control and Optimisation*, 30(1):143–166, 1992.

[64] W.E. Schmitendorf and B.R. Barmish. Null controllability of linear systems with constrained controls. *SIAM Journal of Control and Optimisation*, 18(4):327–345, 1980.

[65] S Skogstad and I. Postlethwaite. *Multivariable Feedback Control: Analysis and Design.* Wiley International, New York, 1996.

[66] A. Smerlas, I. Postlethwaite, D.J. Walker, M.E. Strange, J. Howitt, R.I. Horton, A.W. Gubbells, and S.W. Baillie. Design and flight-testing of an $\mathcal{H}^\infty$ controller for the NRC Bell 205 helicopter. *Proceedings of the AIAA Guidance, Navigation and Control Conference*, pages 1023–1033, 1998.

[67] A.J. Smerlas. *Robust Multivariable Control of Helicopters: From Mathematical Models to Flight Tests.* PhD thesis, Department of Engineering, University of Leicester, 1999.

[68] A.J. Smerlas, I. Postlethwaite, D.J. Walker, M.E. Strange, J. Howitt, Cdr. R.I. Horton, A.W. Gubbels, and S.W. Ballie. Design and flight testing of an $\mathcal{H}^\infty$ controller for the NRC Bell 205 experimental fly-by-wire helicopter. *AIAA Guidance, Navigation and Control Conference*, 1998.

[69] H. Stalford. Stability conditions for nonlinear control processes using Lyapunov functions with discontinuous derivatives. *Journal of Mathematical Analysis and Applications*, 84:356–371, 1981.

[70] R.F. Stengel. *Optimal Control and Estimation.* Dover, New York, 1994.

[71] A.A. Stoorvogel. *The $\mathcal{H}^\infty$ Control Problem.* Prentice Hall, Englewood Cliffs, 1992.

[72] M.E. Strange and J. Howitt. *Assessment of the Partial Authority Flight Control Augmentation Concept for the Optimisation of Helicopter Flying Qualities.* DERA Report DERA/AS/FDS/CR97107/1.0, Farnborough, U.K., 1997.

[73] M.S. Strange and J. Howitt. The configuring of HELISIM to represent the flight dynamics of the NRC Bell 205 helicopter. *DERA Internal Report*, 1998.

[74] A.R. Teel. Global stabilisation and restricted tracking for multiple integrators with bounded controls. *Systems and Control Letters*, pages 165–171, 1992.

[75] A.R. Teel. Anti-windup for exponentially unstable linear systems. *International Journal of Robust and Nonlinear Control*, 9(10):701–716, 1999.

[76] A.R. Teel and N. Kapoor. The $\mathcal{L}_2$ anti-windup problem: Its definition and solution. *Proceedings of the European Control Conference*, 1997.

[77] M.S. Tombs. *Robust Control System Design with Application to High Performance Helicopters.* PhD thesis, Department of Engineering, University of Oxford, 1987.

[78] M.C. Turner, I. Postlethwaite, and D.J. Walker. Nonlinear tracking control for constrained input multivariable linear systems. *International Journal of Control*, 73(12):1160–1172, 2000.

[79] M.C. Turner, I. Postlethwaite, and D.J. Walker. Nonlinear tracking in constrained input linear systems. *UK Control 2000 Conference*, 2000.

[80] M.C. Turner and D.J. Walker. Modified linear quadratic bumpless transfer. *Proceedings of the American Control Conference*, 4:2285–2289, 1999.

[81] M.C. Turner and D.J. Walker. Linear quadratic bumpless transfer. *Automatica*, 36(8), 2000.

[82] M.C. Turner, D.J. Walker, and A. Alford. Design and Ground-based Simulation of an $\mathcal{H}^\infty$ Limited Authority Controller for a Lynx Helicopter. *submitted for journal publication*, 2000.

[83] F. Tyan and D.S. Bernstein. Anti-windup compensator synthesis for systems with saturating actuators. *International Journal of Robust and Nonlinear Control*, 5(5):521–537, 1995.

[84] A.J. Van der Schaft. *$\mathcal{L}_2$ Gain and Passivity Techniques in Nonlinear Control.* Springer-Verlag, London, 1999.

[85] G. Vinnicombe. Frequency domain uncertainty and the graph topology. *IEEE Transactions on Automatic Control*, 38(9):1371–1383, 1993.

[86] K.S. Walagama and J. Sternby. Inherent observer property in a class of anti-windup compensators. *International Journal of Control*, 52:705–724, 1990.

[87] K.S. Walagama and J. Sternby. Conditioning technique for multiinput multioutput processes with input saturation. *IEE Proceedings, Part D*, 140(4):231–241, 1993.

[88] D.J. Walker and I. Postlethwaite. Full authority active control system design for a high performance helicopter. *16th European Rotorcraft Forum*, pages III.3.2.1–III.3.2.14, 1990.

[89] D.J. Walker and I. Postlethwaite. Advanced helicopter flight control using two-degree-of-freedom $\mathcal{H}^\infty$ optimisation. *AIAA Journal of Guidance, Control and Dynamics*, 19(2):461–468, 1996.

[90] D.J. Walker and M.C. Turner. Robust control of the longitudinal and lateral dynamics of the Bell 205 helicopter. *Proceedings of the American Control Conference*, 4:2742–2746, 1999.

[91] D.J. Walker and M.C. Turner. Recent experiences with the NRC Bell 205 Helicopter. *UK Control 2000 Conference*, 2000.

[92] P.F. Weston and I. Postlethwaite. Analysis and design of linear conditioning schemes for systems containing saturating actuators. *IFAC Nonlinear Control System Design Symposia*, 1998.

[93] P.F. Weston and I. Postlethwaite. Analysis and design of linear conditioning schemes for systems with nonlinear actuators. *Internal Report, Dept. of Engineering, University of Leicester*, 98-6, 1998.

[94] J.C. Willems. Dissipative Dynamical Systems, Part I: General Theory. *Arch. Rational Mech. Anal.*, 45:321–351, 1971.

[95] R.F. Wilson, J.R. Cloutier, and R.K. Yedavalli. Lyapunov-constrained eigenstructure assignment for the design of robust mode-decoupled roll-yaw missile auto-pilots. *Proc. IEEE Conference on Control Applications*, pages 994–999, 1992.

[96] A. Yue. *The Improvement of Helicopter Handling Qualities Using $\mathcal{H}^\infty$ Optimisation.* PhD thesis, Department of Engineering, University of Oxford, 1988.

[97] A. Yue and I. Postlethwaite. Improvement of helicopter handling qualities using $\mathcal{H}^\infty$ optimisation. *IEE Proceedings*, Part D:115–129, 1990.

[98] G. Zames. Feedback and optimal sensitivity: Model reference transformations, multiplicative seminorms and approximate inverses. *IEEE Transactions on Automatic Control*, 26:301–320, 1981.

[99] K. Zhou, J. C. Doyle, and K. Glover. *Robust and Optimal Control.* Prentice Hall, New Jersey, 1996.